INVESTIGATING EXPERIENCE-DEPENDENT PLASTICITY IN THE ACCESSORY OLFACTORY BULB

APPROVED BY SUPERVISORY COMMITTEE

Julian Meeks, Ph.D.

Todd Roberts, Ph.D.

Kimberly Huber, Ph.D.

Lisa Monteggia, Ph.D.

DEDICATION

First and foremost, I would like to thank my advisor Julian, for being an outstanding mentor who is very dedicated to his students. I am so grateful to have had the guidance of such a knowledgeable, patient, and supportive mentor throughout my graduate career.

I would also like to thank my committee members for all of their support and insights through the years.

I would not be where I am today without the enduring support of my family and friends. I'd especially like to thank my parents, David and Lynn, and my sister, Susie, for their love and encouragement, and for not asking too many questions about when I'm going to graduate.

It is hard to imagine what graduate school would have been like without the unwavering support of my fiancé Taylor. I am extremely grateful for his continued, enthusiastic support of my career, and his loving companionship, which has provided me with endless happiness and comfort throughout graduate school and life.

INVESTIGATING EXPERIENCE-DEPENDENT PLASTICITY IN THE ACCESSORY OLFACTORY BULB

by

HILLARY CANSLER

DISSERTATION

Presented to the Faculty of the Graduate School of Biomedical Sciences

The University of Texas Southwestern Medical Center at Dallas

In Partial Fulfillment of the Requirements

For the Degree of

DOCTOR OF PHILOSOPHY

The University of Texas Southwestern Medical Center at Dallas

Dallas, Texas

May, 2018

INVESTIGATING EXPERIENCE-DEPENDENT PLASTICITY IN THE ACCESSORY OLFACTORY BULB

Publication No. _____

Hillary Cansler, Ph.D.

The University of Texas Southwestern Medical Center at Dallas, 2018

Supervising Professor: Julian Meeks, Ph.D.

Chemosensory information processing in the mouse accessory olfactory system (AOS) guides the expression of social behavior. After salient chemosensory encounters, the accessory olfactory bulb (AOB) experiences changes in the balance of excitation and inhibition at reciprocal synapses between mitral cells (MCs) and local interneurons. The mechanisms underlying these changes remain controversial. Moreover, it remains unclear whether MC-interneuron plasticity is unique to specific behaviors, such as mating, or whether it is a more general feature of the AOB circuit. Here, we describe a population of AOB internal granule cells (IGCs) that upregulate expression of the immediate early gene *Arc* following the resident-intruder paradigm in an AOS-dependent manner. Targeted

electrophysiological studies revealed that *Arc*-expressing IGCs in acute AOB slices from resident males displayed stronger excitation than non-expressing neighbors when sensory inputs are stimulated. The increased excitability of *Arc*-expressing IGCs was not correlated with changes in the strength or number of excitatory synapses with MCs, but was instead associated with increased intrinsic excitability and decreased HCN channel-mediated I_H currents. Consistent with increased inhibition by IGCs, MCs responded to sensory input stimulation with decreased depolarization and spiking following resident-intruder encounters. Different populations of IGCs are activated following exposure to males and females, suggesting they are activated in an input-specific fashion. We also describe multiple behavioral paradigms that have been designed to assay social recognition following resident-intruder behavior in conjunction with *in vivo* manipulation of *Arc*-expressing IGCs. Together, these results reveal that non-mating behaviors drive AOB inhibitory plasticity, and indicate that increased MC inhibition involves intrinsic excitability changes in *Arc*-expressing interneurons.

TABLE OF CONTENTS

PRIOR PUBLICATIONS

Cansler HL, Maksimova MA, Meeks JP. 2017. Experience dependent plasticity in accessory olfactory bulb interneurons following male-male social interaction. *J Neurosci **37**: 7240-7252.*

Doyle WI, Dinser JA, **Cansler HL**, Zhang X, Dinh DD, Browder NS, Riddington IM, Meeks JP. 2016. Faecal bile acids are natural ligands of the mouse accessory olfactory system. *Nature Communications* 7:11936.

LIST OF FIGURES

LIST OF TABLES

LIST OF DEFINITIONS

4-OHT – 4 hydroxytamoxifen
AAV – Adeno-associated virus
ACSF – artificial cerebrospinal fluid
AMPAR - α-amino-3-hydroxy-5-methyl-4-isoxazolepropionic acid receptor
ANOVA – Analysis of variance
AOB – Accessory olfactory bulb
AOS – Accessory olfactory system
BAC – Bacterial artificial chromosome
BNST – Bed nucleus of the stria terminalis
ChR2 – Channelrhodopsin 2
CNO – Clozapine N-oxide
d2EGFP – destabilized enhanced green fluorescent protein with a 2 hour half-life
d4EGFP – destabilized enhanced green fluorescent protein with a 4 hour half-life
DREADDs – Designer receptors exclusively activated by designer drugs
ECL – External cellular layer
EGC – External granule cell
EPSP – Excitatory postsynaptic potential
EYFP – Enhanced yellow fluorescent protein
FITC – Fluorescein isothiocyanate
GABA – γ-Aminobutyric acid
GFP – Green fluorescent protein
GL – Glomerular layer
GPCR – G-protein coupled receptor
HCN – Hyperpolarization-activated cyclic nucleotide-gated
Hz - Hertz
ICL – Internal cellular layer
IEG – Immediate early gene
IGC – Internal granule cell
IPSC – Inhibitory postsynaptic current
JGC – Juxtaglomerular cell
KO – knock-out
LOT – Lateral olfactory tract
LTD – Long-term depression
LTP – Long-term potentiation
MC – Mitral cell
MeA – Medial amygdala
mEPSC – Miniature excitatory postsynaptic current
MHC – Major histocompatibility complex
MOB – Main olfactory bulb
MOE – Main olfactory epithelium
MOS – Main olfactory system
mGluR – metabotropic glutamate receptor

MUP – Major urinary protein
mV – millivolt
NA - noradrenaline
NMDAR – N-methyl-D-aspartate receptor
OR – Olfactory receptor
OSN – Olfactory sensory neuron
PBS – Phosphate buffered saline
sEPSC – Spontaneous excitatory postsynaptic current
TRAP – Targeted recombination in active populations
TTL – Transistor-transistor logic
TTX – Tetrodotoxin
VMH – Ventromedial hypothalamus
VNO – Vomeronasal organ
VSN – Vomeronasal sensory neuron
WT – Wild type

CHAPTER ONE
Introduction and Literature Review

A central, overarching goal in neuroscience is to understand how the central nervous system is able to perceive and integrate information from multiple sensory systems to ultimately guide behavior conducive to survival and reproduction. Rodents in particular rely heavily on olfaction to make sense of their world, and they have evolved multiple olfactory systems to accomplish this task. The main and accessory olfactory systems are the two most prominent, and they offer both distinct and overlapping capabilities. Broadly, the main olfactory system is best suited for the detection and processing of a vast array of volatile odorants, while the accessory olfactory system (AOS) specializes in non-volatile social odorants found in the excretions of both conspecifics and heterospecifics. As such, rodents depend on their AOS to navigate many different types of social behavior, including mating, parental behavior, territorial aggression, and predator avoidance. As scientists, we rely on rodent models to help improve our understanding of complex psychiatric disorders, which can involve behavioral phenotypes that are difficult to quantify, including profound changes to social behavior (Huckins et al., 2013). It is therefore critically important that we continue to develop our understanding of how rodents navigate their social world via their olfactory systems.

We currently have a basic understanding of the organization of the AOS, some types of odorants it detects, and some behaviors that depend on it. Still, much remains to be elucidated about how information processing occurs at each stage of the AOS. In particular, the accessory olfactory bulb (AOB) – the first dedicated neural circuit to processing sensory

information from the periphery, is somewhat mysterious. While many AOS-mediated behaviors are considered innate, behavioral and physiological evidence suggests that the AOB is a site of experience-dependent plasticity. This has been best studied in the context of pregnancy block, in which a female forms a chemosensory memory of her recent mate, but remains unexplored in the context of other AOS-mediated social behaviors (Bruce, 1959; Brennan et al., 1990).

There is still much to learn about how the AOB contributes to plasticity in social behaviors. In pregnancy block, one hypothesis proposes that inhibitory gain limits activation of AOB projection neurons, called mitral cells (MCs) to the chemosensory cues of a recent mate (reviewed in Brennan, 2009). This increased inhibition involves changes at reciprocal dendro-dendritic synapses between MCs and AOB interneurons, but the precise cellular and synaptic mechanisms are unknown (Brennan et al., 1990; Araneda and Firestein, 2006; Larriva-Sahd, 2008; Brennan, 2009; Smith et al., 2009a). Further, it remains unclear whether such inhibition is induced in the context of other AOS-mediated behaviors, and the specific neuronal populations and molecular mechanisms that contribute to these effects are not yet clear.

Here, we investigate experience-dependent plasticity in the context of another AOS-mediated behavior: territorial aggression. We show that the immediate early gene *Arc* is induced in a select population of AOB interneurons called internal granule cells (IGCs) following the resident-intruder territorial aggression assay. *Arc* upregulation in these interneurons required intact vomeronasal signaling, indicating that centrifugal inputs were not sufficient to induce *Arc* in this behavioral paradigm. Following resident-intruder

behavior, *Arc*-expressing IGCs in resident males showed enhanced network excitation compared to non-expressing IGCs, while MC activity was suppressed. We investigated the IGC physiological features that underlie their enhanced activity and found no evidence for an increase in excitatory synapse strength or number. Instead, we found that *Arc*-expressing IGCs display a robust increase in intrinsic excitability compared to other IGCs. Further, we explore genetic tools that can aid in future study of *Arc*-expressing IGCs and propose multiple behavioral paradigms that may be used to assess the importance of *Arc*-expressing IGCs in social recognition memory. Together, our results show that AOB inhibitory plasticity occurs after non-mating behaviors, and reveal cellular mechanisms underlying MC inhibition after chemosensory social encounters.

Overview of mammalian olfactory systems

Rodents have evolved multiple olfactory subsystems, upon which they rely heavily to navigate and survive in their complex environments (Fig 1.1A, reviewed in Munger et al., 2009). Each of these systems involves distinct sensory tissues, partially overlapping behavioral significance, and specific trajectories through the brain.

In the main olfactory system (MOS), odorants are detected by olfactory sensory neurons (OSNs) at the main olfactory epithelium (MOE). Each OSN expresses just one of around 1,000 G-protein coupled receptor (GPCR) odorant receptors (ORs), and project to the main olfactory bulb (MOB), where they coalesce with other OSNs expressing the same OR in glomeruli (Firestein, 2001). MOB MCs receive sensory information from OSNs at these glomeruli, and project downstream to multiple higher cortical areas, including the piriform

cortex, olfactory tubercle, and anterior olfactory nucleus (Castro et al., 2007). OSNs respond primarily to volatile chemicals of many varieties, which can provide information to the animal about the safety and quality of their food, nearby predators, or potential mates (Munger et al., 2009).

Within the MOE, a subset of OSNs express trace amine-associated receptors (TAARS) rather than canonical ORs, which are responsive to biogenic amines and male urine (Liberles and Buck, 2006). Another subset of OSNs, found exclusively in the "cul-de-sacs" of the MOE, express multiple receptors from the MS4A family, and are responsive to carbon dioxide, carbon disulfide, urinary peptides, fatty acids, and steroids (Hu et al., 2007; Leinders-Zufall et al., 2007; Greer et al., 2016). These OSNs project to the necklace glomeruli, found along the border of the main and accessory olfactory bulbs. Although OSNs in the necklace system respond to many ethologically relevant cues, the specific behavioral importance of the necklace is not yet clear. Some evidence suggests that may be involved in food-related social learning, as the OSNs in this system respond to carbon disulfide (in rodent breath) as well as food odorants, and are required for social transmission of food preference (Munger et al., 2010).

In addition to the MOS and AOS (discussed below), rodents possess multiple other small sensory tissues. The septal organ of Masera is found at the base of the nasal septum, and contains OSNs that express a subset of the ORs that are also expressed in the MOE (Tian and Ma, 2004). These OSNs respond to volatile odorants much like MOE OSNs, and project to a small subset of MOB glomeruli (Ma et al., 2003). The importance of this system remains mysterious. Additionally, the Grueneberg ganglion, found at the dorsal tip of the nasal cavity,

contains cells that project to the same region where the necklace glomeruli are found (Storan and Key, 2006). The cells of the Grueneberg ganglion don't access the nasal cavity lumen, suggesting they may not respond to odors in the classical way, though they do express olfactory receptors (Fleischer et al., 2006; Fleischer et al., 2007). Some evidence suggests these cells can respond to dimethylpyrazine and cool ambient temperatures (Mamasuew et al., 2011), but the precise importance of this sensory system is not understood.

The accessory olfactory system

From sensation to higher order processing

The AOS begins in the nose, where ligands are detected by vomeronasal sensory neurons (VSNs) in the vomeronasal organ (VNO). The VNO is a mucous-filled, blind-ended tube, equipped with a pumping mechanism that is activated during periods of active investigation (Meredith, 1994). This pumping facilitates the transport of primarily non-volatile ligands from the environment to the receptors on VSNs. VSNs can be divided into two main classes by virtue of the types of receptors they express, although a few exceptions exist. V1R-expressing VSNs are found in the apical layer of the VNO, and project specifically to the anterior AOB, while V2R-expressing VSNs are found in the basal layer of the VNO, and project specifically to the posterior AOB (Munger et al., 2009). These two sensory neuron classes are involved in the detection of different types of ligands. V1R-expressing VSNs (and thus their downstream principal neurons in the anterior AOB) are highly responsive to non-volatile small molecules, like sulfated steroids and bile acids, while V2R-expressing VSNs (and posterior AOB neurons) are responsive to larger protein ligands,

like major urinary proteins (MUPs) and major histocompatibility complex (MHC) peptides (Leinders-Zufall et al., 2004; Chamero et al., 2007; Meeks et al., 2010; Doyle et al., 2016). While over 200 VRs have been identified, very few have known ligands, and even fewer have known ligands with known, stereotyped behavioral effects. However, broadly speaking, we know that the VNO is strongly activated by naturalistic odor blends from conspecifics and heterospecifics, including predators, and some VRs show specificity for male, female, or predator cues. (Isogai et al., 2011).

Sensory neurons from the VNO project directly to the AOB, which is the first neural circuit to process information from the sensory periphery. Within this organization, the AOB is located at a position in the processing stream where sensory information can be modified before it reaches downstream circuits, which are crucial for guiding behavior. AOB projection neurons, called mitral cells, directly receive input from VSNs, and target their axons to the medial amygdala (MeA), bed nucleus of the stria terminalis (BNST) and the posteromedial cortical amygdala (PMCo) (Dulac and Torello, 2003). From the MeA, third order projections target the hypothalamus, including multiple subdivisions of the ventromedial hypothalamus (VMH). All of these downstream regions are critical in guiding behaviors that are necessary for survival and reproduction, including mating, aggression, parental behavior, and predator avoidance (Newman, 1999; Choi et al., 2005; Keshavarzi et al., 2014; Ishii et al., 2017).

The role of the AOS in rodent behavior

Information flowing through the AOS enjoys privileged access to limbic circuits that are crucial for guiding behavior, as described above. Therefore, it should come as no surprise that animals with disruption to sensation in the VNO exhibit profound deficits in many behaviors. Surgical ablations of the VNO found that males exhibit deficits in many sex-typical behaviors, including territorial marking, intermale aggression, and ultrasonic vocalizations (Wysocki and Lepri, 1991). In females, reproductive responses to male odors (i.e. increase in uterine weight), lordosis behavior, and maternal aggression were severely diminished (Wysocki and Lepri, 1991; Keller et al., 2006). Many of these findings have been corroborated in genetic lesioning studies; deletion of Trpc2, an ion channel required for sensory transduction in VSNs, recapitulates many of the same phenotypes observed with vomeronasalectomy (Stowers et al., 2002; Papes et al., 2010).

In addition to the role of the AOS in behavior towards conspecifics, the AOS is critical for interspecies behavior like predator avoidance (Papes et al., 2010). Urine from predators like bobcats, foxes, and rats evokes robust responses in both the VNO and the AOB, indicating that this olfactory subsystem is tuned to compounds present in these naturalistic stimuli (Ben-Shaul et al., 2010; Papes et al., 2010). Further, *Trpc2-/-* animals show a dramatic decrease in predator avoidance behavior compared to wildtype littermates, driven by their lack of ability to detect specific MUP homologs at the VNO (Papes et al., 2010).

The accessory olfactory system is also involved in mate recognition in females. This is demonstrated by a well-studied phenomenon called the Bruce Effect, also known as

pregnancy block. When a recently mated female is exposed a novel male, a hormonal response is initiated which results in the termination of her pregnancy (Bruce, 1959; Reynolds and Keverne, 1979). However, if she is exposed to her mate, she recognizes his scent and her pregnancy is maintained (Bruce, 1959). Pregnancy block is reduced in females with lesioned VNOs, demonstrating the requirement for an intact AOS (Bellringer et al., 1980). Further, infusions of lidocaine to the AOB prevents olfactory memory formation, and prevents pregnancy block, demonstrating the crucial importance of the AOB in this phenomenon (Kaba et al., 1989). In contrast, genetic ablation of the main olfactory epithelium does not interfere with pregnancy block, underlining the importance of the AOS in this effect (Ma et al., 2002).

Urine alone from a novel male is sufficient to induce pregnancy block, and urine from a familiar mate does not, suggesting that urine must contain some signature of individual identity (Leinders-Zufall et al., 2004). However, it is not completely clear what that signature is. It is believed that this signal depends on testosterone, as castrated males do not cause pregnancy block (Bruce, 1965). One candidate family of molecules is MUPs, which can activate VSNs, bind to testosterone-dependent molecules, and are polymorphic in wild mice (Robertson et al., 1997; Chamero et al., 2007). The high molecular weight fraction of urine alone (which contains MUPs) is not sufficient to block pregnancy, but is restored to effectiveness after adding back the low molecular weight fraction, suggesting that MUPs alone cannot confer identity, but may enhance the effectiveness of testosterone-dependent low molecular weight compounds (Peele et al., 2003). Another candidate for conveying identity is the MHC, which is also involved in self-recognition in the immune system.

Congenic male mice differing only in their MHC genotype are capable of producing the pregnancy block effect, suggesting a role for MHC in individual recognition. MHC peptides are short in length and bind to MHC class 1 proteins (Boehm and Zufall, 2006). These peptides differ at key residues between different inbred mouse strains, and cause activity at VSNs that depends on these specific residues (Leinders-Zufall et al., 2004; Chamero et al., 2007). C57BL/6J MHC peptides added to BALB/cJ urine can increase the rates of pregnancy block in a BALB/cJ-mated female (Leinders-Zufall et al., 2004). However, some groups have not observed VSN responses to MHC peptides, and they haven't been observed naturalistically in urine, calling into question their roles as individuality signals and VSN activators (Nodari et al., 2008).

The AOS is required for territorial aggression

Early studies of vomeronasalectomized rodents demonstrated the importance of an intact AOS for the expression of territorial intermale aggression (Wysocki and Lepri, 1991). These findings were later corroborated using genetic ablation of the VNO. Loss of Trpc2, which is required for normal signal transduction in VSNs, results in a complete loss of intermale aggression in the resident-intruder territorial aggression assay (Stowers et al., 2002). More specifically, genetic ablation of $G_{\alpha o}$, a critical second messenger in V2R-expressing VSNs, also results in a significant decrease in territorial aggression, providing a clue about the specific compounds that may drive this particular behavior (Chamero et al., 2011). Similarly, loss of Kirrel3 during development, which is required for coalescence of posterior (but not anterior) AOB glomeruli, also results in a loss of territorial aggression,

further suggesting the importance of odorants detected at V2Rs (Prince et al., 2013). MUPs, which are detected by V2R-expressing VSNs, appear to play a major role in eliciting aggressive behavior: recombinant MUPs painted on the back of a castrated male are sufficient to induce an aggressive response from a resident male (Chamero et al., 2007). Later, it was demonstrated that only a subset of MUPs are capable of eliciting aggressive behavior, and that additional sensory context from a target animal is required to initiate the aggression motor program (Kaur et al., 2014). Interestingly, the same MUPs that can elicit aggressive behavior can also elicit countermarking behavior, in which a male mouse will spread his urine in response to a stimulus (Kaur et al., 2014). Because territorial aggression is a stereotyped behavioral response that can be induced in response to specific odor cues, it provides an attractive paradigm within which to study the way that sensory processing guides behavior in mammals.

The accessory olfactory bulb

AOB microcircuit organization

VSNS project their axons into the glomerular layer (GL) of the AOB where they contact projecting mitral cells (MCs) in glomeruli (Fig. 1.1B). Unlike the main olfactory system, where MCs project one apical dendrite into one glomerulus, AOB MCs sample from multiple glomeruli, which confers the capacity to integrate information (Del Punta et al., 2002; Wagner et al., 2006; Meeks et al., 2010). MCs then project directly to limbic circuits, like the MeA posteromedial cortical amygdala, and BNST (Dulac and Wagner, 2006). MC output is modified by several types of interneurons in the AOB, the most numerous of which

can be divided into categories based on their anatomical location. Juxtaglomerular cells (JGCs) are found in the glomerular layer, and may send dendrites into multiple glomeruli (Larriva-Sahd, 2008). External granule cells (EGCs) are found in the external cellular layer (ECL), where MC cell bodies are found. Internal granule cells, discussed in more detail below, are found ventral to the lateral olfactory tract (LOT) in the internal cellular layer (ICL). AOB interneurons are axonless, and they communicate with MCs at reciprocal, or dendro-dendritic synapses (Jia et al., 1999; Taniguchi and Kaba, 2001). This means that both sides of the synapse contain pre- and post-synaptic components. In this configuration, these interneurons are well positioned to be able to modify or gate information as it leaves the AOB, as is hypothesized to occur in the Bruce effect (Brennan et al., 1990). While most of these interneurons are believed to be GABA-ergic, there is some evidence for AOB interneurons that release neuromodulators (Takami et al., 1992; Jia et al., 1999; Taniguchi and Kaba, 2001; Marking et al., 2017). In addition to neuromodulator-releasing cells within the AOB, the olfactory bulb receives dense neuromodulatory centrifugal inputs, including the noradrenaline (NA) from the locus coeruleus, serotonin from the raphae nucleus, and acetylcholine from the horizontal limb of the diagonal band of Broca (Shipley et al., 1985; McLean et al., 1989; Matsutani and Yamamoto, 2008; Smith et al., 2015; Huang et al., 2017). Within the AOB, neuromodulators can act on both MCs and interneurons, and are believed to play an important role in neural plasticity (Araneda and Firestein, 2006; Smith et al., 2015).

AOB internal granule cells

AOB IGCs are found in the internal cellular layer (ICL) and are more numerous than other cell type found in the AOB (Larriva-Sahd, 2008). IGCs have small ovoid cell bodies, around 15 μm in diameter, which are arranged in compact rows, as "beads on a string" (Larriva-Sahd, 2008). Like other interneurons in the OB, IGCs lack an identifiable axon. They typically have one thick, spiny dendrite that extends into the ECL, where they synapse at distal MC dendrites, as well as a couple of smaller basal dendrites that project locally within the ICL (Larriva-Sahd, 2008). IGCs are GABA-ergic, and inhibit MCs at dendro-dendritic synapses (Jia et al., 1999; Taniguchi and Kaba, 2001). Interestingly, IGCs experience significant cellular turnover in adulthood, and are replenished by adult-born neurons that migrate via the rostral migratory stream (Alvarez-Buylla and Garcia-Verdugo, 2002). IGCs are key drivers of plasticity in the AOB; changes in communication at the synapses between MCs and IGCs are believed to be underlie olfactory memory (Brennan, 2009).

Plasticity in the AOB

Plasticity in the AOB has been most-studied in the context of the Bruce Effect, in which a recently-mated female forms an olfactory memory of her mate (Bruce, 1959; Brennan et al., 1990). As discussed above, when a recently mated female is exposed to the scent of novel male, a hormonal response is initiated through the accessory olfactory pathway that results in termination of the pregnancy (Brennan et al., 1990). However, this response is prevented when she is exposed to the scent of her mate, which is hypothesized to be due to

limited activation of the neural representations of his scent. Historically, the proposed neural substrate for this phenomenon is that after mating, a population of IGCs selectively provides enhanced inhibition to the specific MCs activated by the mate's scent, thus effectively "gating" the transmission of this information before it reaches downstream circuits (Brennan, 2009). This hypothesis is supported by multiple lines of evidence. Microdialysis experiments have demonstrated increased GABA release in the AOB following mating, as well as increased GABA to glutamate ratios upon exposure to the mated male, but not a novel male (Brennan et al., 1995). Similarly, blocking GABA-ergic signaling in the AOB induces pregnancy block (Kaba and Keverne, 1988). Local field potential recordings in the AOB suggest differential activation in response to urine of a novel male compared to that of a recent mate (Binns and Brennan, 2005). Similarly, decreased responsiveness to the mated male's urine was observed downstream in the medial amygdala (Binns and Brennan, 2005). Increased GABA release in the AOB, which limits downstream activation, is hypothesized to be due to changes in the strength of the synapses between MCs and IGCs. Electron microscopy indicates increased post-synaptic density in IGCs in mated but not unmated females (Matsuoka et al., 2004). The pregnancy block effect also depends on NA release in the AOB (Rosser and Keverne, 1985). Infusion of the NA antagonist phentolamine into the AOB after mating prevents olfactory memory formation (Kaba and Keverne, 1988). Other studies have attempted to study synaptic plasticity in the AOB by mimicking the pharmacological conditions present during mating. These studies found that bath-applied NA decreased MC activity through increased GABA release, as well as long-lasting depolarization of IGCs (Araneda and Firestein, 2006; Smith et al., 2009b).

Still, there is a deficit of studies on functionally-defined populations of neurons in the AOB. That is, the specific AOB neurons that are activated by the mated male's scent have not been targeted physiologically. One way to identify these neurons is via immediate early genes (IEGs), which are expressed in recently active neurons. The IEG *Arc* as a marker is especially intriguing, due to its integral role in diverse forms of synaptic plasticity (reviewed in Shepherd and Bear, 2011). Previous studies have shown that the IEG *Arc* is upregulated specifically in IGCs in the rodent AOB after mating, suggesting that it could be used as a marker to identify functionally-defined populations of IGCs (Matsuoka et al., 2002b; Matsuoka et al., 2002a; Matsuoka et al., 2003). One very recent study did just that, using transgenic mice expressing GFP under the control of the *Arc* promoter (Gao et al., 2017). They found that randomly-selected IGCs from mated females showed increased excitatory postsynaptic potential (EPSP) frequency and amplitude compared to non-mated females, and randomly-selected MCs from mated females showed increased inhibitory postsynaptic current (IPSC) frequency compared to non-mated females, in line with current hypotheses about synaptic plasticity in the AOB (Brennan et al., 1990; Gao et al., 2017). However, the same effect was not seen in *Arc* positive compared to *Arc* negative IGCs in mated females, or in *Fos* positive compared to *Fos* negative MCs, suggesting that these are global effects that occur in the AOB after mating, rather than only in functionally defined groups of neurons (Gao et al., 2017). This result was somewhat surprising, given *Arc's* role in synaptic plasticity. They also found that randomly selected IGCs exhibited increased intrinsic excitability after mating, while MCs showed decreased responsiveness, suggesting there may be other mechanisms involved in olfactory memory aside from synaptic changes (Gao et al.,

2017). Still, it is not known whether similar processes occur in the context of other salient, AOS-dependent behaviors.

Activity-regulated cytoskeletal-associated (Arc) protein

Arc as an immediate early gene

Immediate early genes (IEGs) are rapidly transcribed and translated following neural activity, and thus make powerful tools for identifying and characterizing neural circuits that are activated in response to a stimulus or behavior of interest. While may IEGs encode transcription factors, the IEG *Arc* is unique in that it encodes a postsynaptic cytosolic protein (Shepherd and Bear, 2011). This protein is found almost exclusively in the brain, where its expression is mostly confined to principal, CaMKII positive, glutamatergic neurons in the hippocampus and cortex (Vazdarjanova et al., 2006). There are a few exceptions to this rule-of-thumb, including cerebellar Purkinje cells (which are inhibitory), and GABA-ergic medium spiny neurons of the striatum (Vazdarjanova et al., 2006; Mikuni et al., 2013). Additionally, in both the AOB and MOB, *Arc* expression is exclusively seen in inhibitory interneurons, including AOB IGCs (Guthrie et al., 2000; Matsuoka et al., 2002b; Matsuoka et al., 2002a; Matsuoka et al., 2003; Vazdarjanova et al., 2006; Shakhawat et al., 2014).

Transcription of *Arc* is tightly coupled to neural activity, both *in vivo* and *ex vivo*. *Arc* expression can be seen in hippocampal neurons 1-2 hours after exploration of a novel environment, and returns to baseline within another hour, highlighting the stimulus-locked nature of this effect (Guzowski et al., 1999; Ramirez-Amaya et al., 2005). In line with Arc induction after periods of high activity, large amounts of Arc expression can also be seen

shortly following seizure activity (Vazdarjanova et al., 2006). Further, *Arc* expression appears confined to behaviorally-relevant, selective populations of neurons: compartment analysis of Arc protein and *Arc* mRNA expression indicates that *Arc* expression occurs in largely the same population of neurons following exposure to the same environment, while it is seen in relatively distinct populations following exploration of two different environments (Ramirez-Amaya et al., 2005).

Arc transcription can be induced by multiple signaling mechanisms, including PKA and MAPK cascades, calcium influx through voltage-sensitive calcium channels, and activation of group 1 mGluRs (Waltereit et al., 2001; Park et al., 2008; Adams et al., 2009). *Arc* mRNA is rapidly transported to the dendrites, specifically to active synapses, where it is then translated locally and subsequently degraded through the nonsense-mediated decay pathway, limiting the translation that arises from each transcript (Steward et al., 1998; Giorgi et al., 2007). At the synapse, Arc protein complexes with endophilin and dynamin, which are involved in AMPAR endocytosis (Chowdhury et al., 2006). Arc is also involved in F-actin elongation, which is associated with LTP stabilization (Messaoudi et al., 2007). Arc also interacts with the PSD95, a scaffolding protein found in the postsynaptic density that is required for Arc's recruitment to active synapses (Fernández et al., 2017). Structural studies have identified CaMKII as a binding partner of Arc, as well as TARPγ2, which is involved in AMPAR trafficking (Jackson and Nicoll, 2011; Zhang et al., 2015). Although the relationships between and the precise mechanisms of these functions remain unclear, they all suggest that Arc expression is very carefully-orchestrated, and that it may play an important role in synaptic plasticity.

The importance of Arc in neural plasticity and behavior

There is a wealth of evidence implicating *Arc* in diverse forms of neural plasticity, including long-term potentiation (LTP), long-term depression (LTD), and homeostatic scaling (Bramham et al., 2008; Shepherd and Bear, 2011). High frequency stimulation, which induces LTP, induces *Arc* transcription, and *Arc-/-* mice exhibit enhanced early phase, but decreased late phase LTP in the dentate gyrus and CA1 (Plath et al., 2006). Hippocampal infusion of antisense oligodeoxynucleotides for *Arc* prior to LTP induction prevents LTP maintenance but not induction (Guzowski et al., 2000). Interestingly, antisense infusion can also disrupt LTP maintenance when applied 2 hours post-induction, suggesting that *Arc* expression must be sustained in order for LTP to be maintained (Messaoudi et al., 2007). This classical LTP is NMDAR-dependent, but mGluR-dependent LTP was recently discovered to also depend on Arc expression (Wang et al., 2016). In accordance with a role for Arc in LTP, *Arc-/-* mice exhibit deficits in numerous hippocampus-dependent learning and memory paradigms (Guzowski et al., 2000; Plath et al., 2006). Arc appears to also be crucial in non-hippocampal learning, as Pavlovian fear conditioning depends on Arc expression in the amygdala (Ploski et al., 2008; Nakayama et al., 2016). Despite the clear necessity for Arc in LTP, the molecular mechanisms underlying its role are still not entirely clear, though some evidence suggests that its role in f-actin polymerization may be important (Messaoudi et al., 2007).

Arc is also instrumental in mGluR-dependent LTD and synapse elimination (Waung et al., 2008; reviewed in Wilkerson et al., 2017). DHPG, a selective agonist for group 1 mGluRs, rapidly induces *Arc* expression and results in mGluR-LTD (Lüscher and Huber,

2010). *Arc-/-* mice exhibit severely diminished mGluR-mediated LTD, but not NMDAR-dependent LTD, and *Arc* knockdown recapitulates these same results (Plath et al., 2006; Park et al., 2008; Waung et al., 2008; Jakkamsetti et al., 2013). *Arc* mRNA can be induced in the hippocampus by very brief exploration of a novel environment, and primes active synapses for mGluR-triggered LTD upon a second exposure (Jakkamsetti et al., 2013). This function of Arc appears to be conserved across brain regions, as it is also required for mGluR-dependent LTD in the cerebellum (Smith-Hicks et al., 2010). Further evidence for Arc's role in LTD comes from studies of *Fmr1-/-* mice, a model of Fragile X syndrome in which fragile X mental retardation protein (FMRP) is lost. FMRP negatively regulates Arc translation, and *Fmr1-/-* mice exhibit enhanced mGluR LTD (Park et al., 2008).

Homeostatic scaling is the process by which neurons adapt to periods of high or low activity by decreasing or increasing surface expression of AMPARs (Turrigiano, 2008). Arc participates in this process through its role in AMPAR endocytosis (Shepherd et al., 2006). *In vivo*, AMPAR scaling in the visual cortex occurs in response to different manipulations. For example, visual experience leads to AMPAR downscaling in visual cortex, and this effect is impaired in *Arc-/-* animals (Gao et al., 2010). In the context of monocular deprivation in adolescent animals, responses evoked through the deprived eye are depressed, while responses evoked through the open eye are strengthened in an *Arc*-dependent manner (Smith et al., 2009a; McCurry et al., 2010). *Arc* overexpression extends the window within which this plasticity can occur into adulthood, suggesting that the progressive loss of *Arc* may contribute to decreased plasticity in adulthood (Jenks et al., 2017). In support of this

hypothesis, *Arc* expression in the hippocampus is decreased in aged, memory-impaired mice, but not in memory-preserved mutant mice (Qiu et al., 2016).

Due to Arc's exquisite regulation, and clear role as a "master regulator" of synaptic plasticity, it provides a powerful tool for identifying populations of neurons that are activated by a particular stimulus and may be undergoing plasticity. In this body of work, we take advantage of this tool and use Arc as a marker to identify and study AOB interneurons that are activated during the resident-intruder territorial aggression paradigm.

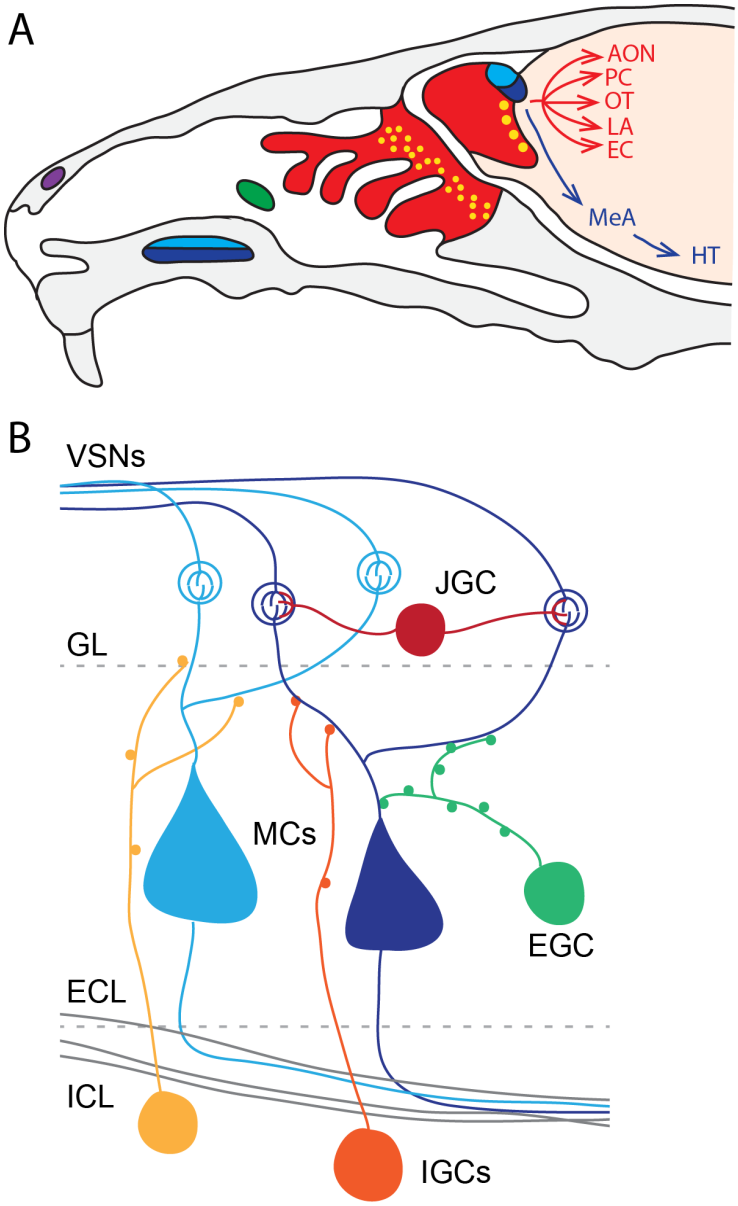

Figure 1.1 ***A,*** Mouse olfactory systems. The main olfactory epithelium and main olfactory bulb are shown in red. The necklace system is shown in yellow. The Grueneberg ganglion is shown in purple. The septal organ of Masera is shown in green. The VNO and AOB are shown in blue, with the apical VNO and anterior AOB in light blue, and the basal VNO and posterior AOB in dark blue. AON anterior olfactory nucleus; PC piriform cortex; OT

olfactory tubercle; LA lateral amygdala; EC entorhinal cortex; MeA medial amygdala; HT hypothalamus. ***B,*** AOB microcircuit organization. VSNs from the vomeronasal organ project to the AOB, where they form synapses with MCs in glomeruli. MCs may sample from multiple glomeruli, and project directly downstream to limbic structures. MC output is modified by multiple classes of interneurons, including JGCs, EGCs, and IGCs, which are the most numerous. AOB accessory olfactory bulb; VSN vomeronasal sensory neurons; JGC juxtaglomerular cell; GL glomerular layer; MC mitral cell; EGC external granule cell; ECL external cellular layer; ICL internal cellular layer; IGC internal granule cell.

CHAPTER TWO
Materials and Methods

Mice

All animal procedures were in compliance with the UT Southwestern Institutional Care and Use Committee. Sexually-naïve adult male mice aged 6-12 weeks were housed on a customized 12/12 light cycle with the lights on from noon until midnight. Food and water were provided *ad libitum*. *Arc-d4EGFP*-BAC (Grinevich et al., 2009) and *Arc*^{tm1St} ("*Arc-/-*" or "Arc-d2EGFP"; Jackson Labs Stock #007665; RRID: IMSR_JAX:007662; Wang et al., 2006) mice were generous gifts from Kimberly Huber. *Trpc2*^{tm1Dlc} ("*Trpc2*-/-" Jackson Labs Stock #021208; RRID: IMSR_JAX:021208; Stowers et al., 2002), *Arc*$^{tm1.1(cre/ERT2)Luo}$/J ("ArcCreER" Jackson Labs Stock #021881; Guenthner et al., 2013), *Gad2*$^{tm2(cre)Zjh}$/J ("Gad2-Cre" Jackson Labs Stock #019022; Taniguchi et al., 2011), *Calb2*$^{tm1(cre)Zjh}$/J ("Calb2-Cre" Jackson Labs Stock #010774; Taniguchi et al., 2011), and *Gt(ROSA)26Sor*$^{tm9(CAG-tdTomato)Hze}$/J ("Ai9" Jackson Labs Stock #007905; RRID:IMSR_JAX:007905; Madisen et al., 2010) mice were obtained from Jackson Laboratory.

Behavior

Resident male mice were individually housed on corn cob bedding, without cage changes, for one week prior to the experiment. All behavior occurred during the dark phase (Zeitgeber time 20-24 h) in a dimly lit room to facilitate video recording. After a 10-minute habituation period, a BALB/cJ male intruder mouse, unless otherwise indicated, was introduced to the resident cage for 10-minute encounter. Following behavior, imaging and

electrophysiological experiments were performed as described below in detail. Behavior videos were scored through a custom MATLAB GUI using a pre-determined behavior ethogram containing aggressive, defensive, olfactory, and exploratory behaviors (Table 1).

Immunofluorescence and imaging

Following behavior (at a time point determined by the specific experiment), animals were briefly anesthetized with inhaled isofluorane, then injected with a ketamine/xylazine cocktail (120 mg/kg ketamine/16 mg/kg xylazine dose) and transcardially perfused with 0.01 M phosphate buffered saline (PBS) followed by 4% paraformaldehyde in PBS. Brains were post-fixed in 4% paraformaldehyde in PBS overnight. Brains were then cryoprotected overnight in PBS containing 25% sucrose, embedded in OCT compound (TissueTek), and flash frozen. 30 μm sections were prepared using a Leica CM3050 S cryostat and processed free-floating. Sections were rinsed 4x in 0.01 M PBS, incubated in 0.1% Triton X in PBS for 2 hours, rinsed 3x, incubated in 10% goat serum in PBS for 2 hours, and incubated in primary antibody in primary block (0.1% Triton X, 10% goat serum in PBS) overnight at 4 °C. Sections were then rinsed 3x in PBS and incubated in secondary antibody in secondary block (0.1% Triton X, 5% goat serum) for 2 hours. Sections were rinsed 3x, incubated in 500 nM DAPI in PBS, and rinsed 3x again. Sections were then mounted on slides in Fluoromount-G mounting medium (SouthernBiotech). Specific antibody information can be found in the methods section of each chapter.

Live slice preparation

Animals were anesthetized with isofluorane and decapitated 3 hours after the resident-intruder paradigm was completed unless otherwise specified. Brains were dissected and 400 μm parasagittal sections of the AOB were prepared using a Leica VT1200 vibrating microtome in ice-cold, oxygenated artificial cerebrospinal fluid (ACSF). ACSF contained (125 mM NaCl, 2.5 mM KCl, 2 mM $CaCl_2$, 1 mM $MgCl_2$, 25 mM $NaHCO_3$, 1.25 mM NaH_2PO_4, 25 mM glucose, 3 mM myo-inositol, 2 mM Na-pyruvate, 0.4 mM Na-ascorbate) with an additional 9 mM $MgCl_2$ in the slicing buffer. After slicing, the slices were kept in a recovery chamber at room temperature (22 °C) containing ACSF with 0.5 mM kynurenic acid to prevent potential glutamate excitotoxicity during the recovery/holding period.

Electrophysiology

Just prior to recordings, slices were transferred to a slice chamber (Warner Instruments) mounted on a fluorescence- and differential interference contrast imaging-equipped upright microscope (FN1 Model, Nikon). Oxygenated ACSF was superfused via a peristaltic pump (Gilson) at a rate of 1-2 mL/min throughout. Slice temperature was maintained at 32-33 °C via inline and chamber heaters (Warner Instruments).

Whole cell patch-clamp recordings were made on d4EGFP+ and d4EGFP– IGCs during a window spanning 4-8 hours following behavior. Thin wall borosilicate glass electrodes with a tip resistance between 4 and 12 MΩ were filled with internal solution containing (in mM) 115 K-gluconate, 20 KCl, 10 HEPES, 2 EGTA, 2 MgATP, 0.3 Na_2GTP, 10 Na phosphocreatine at pH 7.37. All recordings were amplified using a MultiClamp 700B amplifier (Molecular Devices) at 20 kHz and were digitized by a DigiData 1440 analog-

digital converter controlled via pClamp 10.5 software (Molecular Devices, RRID:SCR_011323). Data were analyzed by Clampex 10.5 (Molecular Devices) and custom software written in MATLAB.

2-Photon imaging and analysis

Image stacks up to 200 µm deep were acquired using an excitation wavelength of 890 nm and a 40x (1.0 NA) water-immersion objective (Olympus). Images were denoised using a 3D median filter and deconvolved using a model point spread function in ImageJ (RRID:SCR_003070). Fluorescent cells were counted using a 3D object counting add-on (Bolte and Cordelieres, 2006). Cell counts were normalized to the volume of the cell layer of interest. $I_{Arc}sum$ was computed as follows:

$$I_{Arc}sum = \frac{\sum_{i=1}^{n} I_{Arc(i)}}{x\ \mu m^3}$$

where $I_{Arc(i)}$ is the normalized brightness of each cell ($I_{Arc(i)} = \frac{B_i}{K}$). B_i is the mean pixel intensity within cellular region of interest i, K is the mean pixel intensity within the ICL but outside cellular regions of interest, and x is the total volume within the imaged portion of the ICL. This metric combines relative brightness of all identified cells and is normalized by the imaged volume to facilitate comparisons across experimental preparations.

Stereotaxic injections

For adeno-associated virus (AAV) injections, mice were held under isofluorane anesthesia and given buprenorphine subcutaneously at 0.05 mg/kg for analgesia. Using a

custom-designed stereotaxic apparatus, the mouse's head was rotated back 30º to permit AOB targeting from an anterior direction. Once injection needle was positioned at Bregma, the needle was moved lateral 1000 μm, up 3000 μm, and anterior 4300 μm. A hole was drilled in the skull using a small hand drill. Then, the needle was slowly lowered 3400 μm and virus was injected. After removing the needle slowly, and bathing with sterile saline, the incision was closed using tissue glue. Antibiotic and lidocaine were applied to the incision site, and mice were allowed to recover from surgery for at least 2 weeks prior to any behavior experiment.

4-hydroxytamoxifen (4-OHT) preparation and delivery

4-OHT was used to induce recombination in ArcCreER mice rather than tamoxifen due to its shorter half-life (Guenthner et al., 2013). 4-OHT was dissolved in ethanol at 20 mg/mL by warming to 37 C in a water bath. This solution was sometimes used immediately, or stored at -20 C for up to a week. Corn oil was added to bring the concentration to 10 mg/mL. Then, the ethanol was removed under vacuum centrifugation, giving a final concentration of 20 mg/mL. Resident mice were lightly anesthetized with isofluorane, and 4-OHT was delivered via IP injection at 50 mg/kg. Resident mice were then given 20 minutes to recover and habituate before the intruder mouse was introduced.

Behavior	Frequency/Duration	Category	Description
Attack bite	Frequency	Aggressive	Rapid leap, or darting of head and forebody, towards opponent, ending a bite to the opponent's body.
Aggressive groom	Frequency	Aggressive	Vigorous tugging of opponent's fur, often using the teeth and generally in the back or shoulder region.
Aggressive posture	Duration	Aggressive	Bipedal stance with back hunched. Head and body oriented and leaning towards opponent. Eyes slitted and ears flattened. Body can also be presented laterally to the opponent and rotated away from it. Head oriented towards opponent with eyes slitted and ears flattened.
Attack	Frequency	Aggressive	Rapid approach which is carried out over the back of the opponent. The head comes in contact with the far flank of the opponent, and an attack bite may be given.
Bipedal mount	Duration	Aggressive	Scored when both animals are in the reared position and one of the animals has its forepaws on the back of the other.
Box	Duration	Aggressive	Both animals in upright posture facing each other. Forepaws may touch the other animal.
Chase	Duration	Aggressive	Rapid pursuit of fleeing opponent.
Fight	Duration	Aggressive	Animals roll around biting, kicking, and wrestling, their bodies clasped tightly together.
Mount attempt	Frequency	Aggressive	Any attempt at mounting which falls short of the complete pattern mount in which there are palpitations and pelvic thrusts. Can also be scored when the forepaws of one animal are on the back of the opponent while the opponent is in the prone position.
Mount	Duration	Aggressive	The complete pattern mount in which there are palpitations and pelvic thrusts.
Tail rattle	Frequency	Aggressive	Rapid lashing of tail from side to side. Produces "rattle" when solid object

			(e.g. cage wall) is struck.
Crouch	Duration	Defensive	Body held close to ground with back hunched and legs flexed. Relatively immobile but may show slight scanning movements of the head. Should not be scored if less than 2 seconds.
Defensive attack	Frequency	Defensive	Attack in response to approach.
Defensive posture	Frequency	Defensive	Bipedal stance facing opponent. Eyes open and ears extended. Head oriented forward with tendency to point upwards, especially when opponent is in close proximity. Can also be scored with lateral orientation to opponent. Body rotated away from opponent, head oriented away from opponent especially in close proximity.
Flee	Frequency	Defensive	Runs rapidly and directly away from the opponent. Undirected bouncing movements interspersed with very rapid retreating.
Freeze	Duration	Defensive	Period of immobility except for slight head movements. Should not be scored if less than 5 seconds in duration.
Kick	Frequency	Defensive	Fends off opponent using fore- or hind limbs.
On back	Frequency	Defensive	If an attacked mouse is driven in to a corner or small space, he may roll over on the back and hold all four paws in the air.
Submission	Frequency	Defensive	Rearing up on hind feet, holding out the front paws towards the aggressor, remaining motionless until attacked; it may also squeak and jump.
Withdraw	Frequency	Defensive	Sharp movement of head or front of body away from opponent.
Genital sniff	Duration	Olfactory	Sniffing of the anogenital region of the opponent.
Sniff body	Duration	Olfactory	Sniffing of the body of the opponent.
Sniff head	Duration	Olfactory	Sniffing of the head of the opponent.
Approach	Duration	Other	Ambulation towards the opponent, with attention directed towards the opponent.
Brief	Frequency	Other	Used to code ambiguous contact

contact			behaviors.
Dig	Frequency	Other	Digging in the bedding of the cage. One dig should be coded if the mouse digs in the same location. Another dig should be coded if: the mouse digs in another location, interrupts digging with another behavior, or pauses for more than one second before resuming.
Follow	Duration	Other	Direct movement towards the leaving opponent at a walking pace.
Groom	Frequency	Other	Mouthing and licking of the opponent's fur.
Leave	Frequency	Other	Direct movement away from the opponent at a walking pace.
Rear	Duration	Other	Bipedal stance with scanning movements of the head oriented towards the environment (not the opponent). Forepaws may rest on the cage wall for support.
Straub tail	Frequency	Other	Stiffening of the tail musculature with a 45° angle above the body.

Table 1. Behavior ethogram for resident-intruder videos.

CHAPTER THREE
Arc is expressed in a subset of accessory olfactory bulb internal granule cells following male-male social interaction

Background

Although the AOS is crucial for guiding many innate behaviors, the AOB microcircuit is also plastic. Much of what we know about AOB plasticity comes from studies of pregnancy block, also known as the Bruce effect, in which a female rodent forms a chemosensory memory of her recent mate (Bruce, 1959; Brennan et al., 1990). After this memory is formed, the female will maintain her pregnancy when exposed to odors from her mate, but will abort her pregnancy when exposed to the odors of a novel male. One hypothesis about how this is achieved is that increased inhibition in the AOB circuit limits activation specifically of the cues associated with her mate, resulting in decreased downstream activation. One of the main sources of inhibition in the AOB is IGCs, which vastly outnumber every other cell type in the AOB. IGCs inhibit projecting MCs at dendro-dendritic synapses, and changes at these synapses are hypothesized to play a large role in AOB plasticity (Brennan et al., 1990; Araneda and Firestein, 2006; Larriva-Sahd, 2008; Brennan, 2009; Smith et al., 2009b). Until recently, this plasticity had not been studied in functionally-defined populations of IGCs (that is, IGCs activated by a specific behavior or set of odorants) (Gao et al., 2017). Thus, the cell- and synapse-specific mechanisms involved in inhibitory gain remain obscured.

Immediate early genes (IEGs) are expressed in recently active neurons and can provide extensive information about the cells and networks that participate in sensory and behavioral experiences (Kawashima et al., 2014; Kim et al., 2015; Vousden et al., 2015). The

IEG *Arc* is both an important plasticity-related gene and a useful marker of neuronal populations engaged by experience (Shepherd and Bear, 2011) . Although *Arc* is typically expressed in principal excitatory neurons (*e.g.* cortical and hippocampal pyramidal neurons), studies of *Arc* expression in the AOB show that it is selectively upregulated in subsets of AOB IGCs, but not MCs, in male and female rodents after mating (Matsuoka et al., 2002b; Matsuoka et al., 2002a; Matsuoka et al., 2003). *Arc* expression by interneurons has also been noted in the main olfactory bulb in several studies (Guthrie et al., 2000; Vazdarjanova et al., 2006; Shakhawat et al., 2014). The selective expression of *Arc* by interneurons is atypical (though not unheard of, as it is also seen in cerebellar Purkinje neurons and medium spiny neurons of the striatum), and studying these populations is likely to provide new insights into the role of *Arc* in non-principal neuronal types (Vazdarjanova et al., 2006; Bepari et al., 2012; Mikuni et al., 2013).

Specific materials and methods

Exposure to soiled bedding

To test the response to soiled bedding alone, a small petri dish was filled with bedding from a cage of 4 BALB/cJ males that had gone without cage changes for one week. This petri dish was introduced to the resident's cage for 10 minutes instead of an intruder animal.

BrdU administration

BrdU was dissolved at 15 mg/mL in sterile saline, and administered intraperitoneally at 150 mg/kg. Each *Arc-d4EGFP*-BAC male mouse received 2 injections total, 6 hours apart. Then, mice were made residents and went through the resident-intruder paradigm either 2 or 4 weeks after the BrdU injections. Mice were perfused 90 minutes after behavior was complete and immunofluorescence was completed to assess overlap of Arc and BrdU signals.

Immunofluorescence

Immunofluorescence protocols were followed as described in Chapter 2, with one exception. For BrdU immunofluorescence, all sections were incubated in 2N HCl for 30 minutes prior to the completion of the rest of the protocol. Anti-Arc primary antibody specificity (Synaptic Systems #156003 rabbit polyclonal, RRID: AB_887694) was verified using *Arc-/-* mice and was used at 1:1000. Anti-GFP primary (Abcam #ab13970 chicken polyclonal, RRID: AB_300798) was used at 1:500. Anti-BrdU primary (Accurate Chemical Cat# OBT0030G rat monoclonal) was used at 1:500. Goat anti-rabbit AF633 (Molecular Probes Cat# A21070, RRID: AB_2535731) and goat anti-chicken AF488 (Molecular Probes Cat# A11039, RRID: AB_142924) were both used at 1:2000 dilution.

Results

Arc is expressed specifically in accessory olfactory bulb internal granule cells following resident-intruder behavior

Adult male wild-type C57BL/6J residents were housed individually for one week and then exposed to adult male BALB/cJ intruders for 10 minutes. Arc protein expression was significantly increased 90 minutes after the behavior in AOB IGCs of resident males compared to controls (Wilcoxon-Mann-Whitney test, $p<0.0001$, Fig. 3.1A-D). Previous studies indicated that male-male resident-intruder encounters increase *Fos* expression in the posterior AOB (pAOB), which is selectively innervated by vomeronasal sensory neurons (VSNs) that express members of the V2R subfamily of vomeronasal receptors (Belluscio et al., 1999; Kumar et al., 1999; Rodriguez et al., 1999; Chamero et al., 2007). Consistent with these results, Arc protein expression after the resident-intruder paradigm was selectively upregulated in pAOB IGCs (Wilcoxon-Mann-Whitney test, $p<0.001$, Fig. 3.1E). These initial results show that *Arc* expression in IGCs following resident-intruder behavior is similar to *Arc* expression following mating behavior, and suggest that *Arc* expression occurs in an interneuron population that might increase MC inhibition after resident-intruder encounters.

Arc expression does not depend on aggression

Resident males require 1 week of solo-housing in order to demonstrate the aggressive response when an intruder male is introduced. In one experiment, we solo-housed C57BL/6J residents for one night rather than 1 week prior to the introduction of a BALB/cJ intruder male. This resulted in comparable amounts of olfactory investigation, but no aggression (Fig. 3.2F). Despite the difference in behavior, the 1-night residents still showed robust Arc protein expression in AOB IGCs, indicating that aggressive behavior is not required for this response (Fig 3.2A-E). These results suggest that Arc expression is induced in a sensory-

dependent manner, and doesn't depend on any neuromodulatory or hormonal influence that may accompany aggressive behavior.

Arc expression peaks 90-120 minutes after behavior and returns to baseline by 4 hours

To identify *Arc*-expressing IGCs in live tissue, we utilized *Arc-d4EGFP*-BAC reporter mice (Grinevich et al., 2009). In these mice, a destabilized form of enhanced GFP with a 4-hour half-life (d4EGFP) is expressed under control of the *Arc* promoter on a bacterial artificial chromosome, leaving endogenous *Arc* unperturbed. To assess the *Arc-d4EGFP*-BAC reporter, we used *Arc-d4EGFP*-BAC male mice as residents in the resident-intruder paradigm. We sacrificed animals at various time points following behavior (Fig. 3.3A) and compared Arc protein and d4EGFP immunostaining levels to controls (no intruder, BALB/cJ male soiled bedding only, Fig. 3.3A-D). Arc protein expression began rising by 30 minutes post-behavior, peaked 1-2 hours post-behavior and returned to baseline by 4 hours post-behavior (one-way ANOVA, $F(7,11)=18.64$, $p<0.0001$, n = 1-2 mice and 2-3 sections per condition, 11 mice and 19 sections overall, Fig. 3.3A, C). d4EGFP levels increased significantly by 1 hour post-behavior and remained elevated at 4 hours post-behavior (one-way ANOVA, $F(7,11)=13.07$, $p=0.0002$, Fig. 3.3A, D). We observed strong colocalization between the Arc protein and d4EGFP signals, while some cells showed d4EGFP signal but no Arc protein in the cell soma. This effect could be explained by the fact that Arc protein is often localized to the dendrites (Shepherd and Bear, 2011), and that low levels of d4EGFP expression (indicating low-level *Arc* transcription) were boosted by immunostaining.

Because d4EGFP immunostaining boosts very weak signals, we wanted to test whether d4EGFP expression alone was sufficient to identify *Arc*-expressing cells in living tissue. Live 2-photon imaging of acute AOB slices from *Arc-d4EGFP*-BAC residents revealed robust d4EGFP expression starting at 3 hours post-behavior and remaining strong until 6 hours post-behavior (Fig. 3.3E). Thus, unamplified d4EGFP signals lag behind the immunostaining time course, which is likely due to differences in antibody-amplified versus native d4EGFP signal. Importantly, the time window including the strongest behaviorally-driven d4EGFP expression was well-aligned with the time course of acute slice electrophysiological experiments, making the *Arc-d4EGFP*-BAC mice a strong tool for investigating the physiological properties of *Arc*-expressing IGCs.

Sensory input from the vomeronasal organ is both necessary and sufficient for Arc expression in IGCs

Previous studies of AOB IEG expression indicated that chemosensory stimulation alone (soiled bedding) is sufficient to induce *Arc* expression and that social interaction increases this effect (Matsuoka et al., 2002a). However, our results showed soiled bedding alone was sufficient to induce *Arc* expression to the same level as social interaction with an intruder (Fig. 3.3B-D). One possible explanation for this discrepancy is that we used a much more potent stimulus than that used by Matsuoka et al.: We took soiled bedding from a cage of 4 BALB/cJ males that hadn't been changed in a week while they used "bedding on which an estrous female had been placed for more than 24 hours" (Matsuoka et al., 2002a). The fact

that our stimulus was much more potent could explain the strong response that we saw, and this hypothesis could be tested by using different "dilutions" of soiled bedding.

Before we tested *Arc*-expressing IGC physiology, we wanted to determine whether d4EGFP expression required AOS sensory activation. This was important because different salient behaviors can activate centrifugal input into the entire olfactory bulb (Shipley et al., 1985; Brennan et al., 1990; Nunez-Parra et al., 2013; Rothermel et al., 2014; Oettl et al., 2016). To determine whether sensory activation is required for *Arc* expression, we backcrossed *Arc-d4EGFP*-BAC reporter mice into a *Trpc2*-/- background. *Trpc2*, which is expressed in all vomeronasal sensory neurons and a small percentage of main olfactory sensory neurons, is required for proper chemosensory transduction (Omura and Mombaerts, 2014). Thus, *Trpc2*-/- mice have severely disrupted vomeronasal chemosensory transduction and profound changes to AOS-mediated behaviors while retaining most main olfactory function (Stowers et al., 2002; Kimchi et al., 2007; Papes et al., 2010). We introduced *Arc-d4EGFP*-BAC, *Trpc2*-/- resident males to BALB/cJ male intruders and imaged acutely-prepared live AOB slices using 2-photon microscopy 4 hours post-behavior, a time of robust d4EGFP expression after resident-intruder behaviors (Fig. 3.4). We quantified d4EGFP expression in the posterior ICL for *Trpc2*+/+, *Trpc2*+/-, and *Trpc2*-/- animals exposed to intruders, as well as *Trpc2*+/+ residents that were left alone in an empty cage (no intruder) for 10 minutes (Fig. 3.4 A-F). Compared to the *Trpc2* wild-type, all other groups showed significantly reduced *d4E*GFP expression (one-way ANOVA $F(3,26)=22.75$, $p<0.0001$, Fig. 3F). This reduction occurred despite the fact that Trpc-/- animals do not display deficits in olfactory social investigation (Stowers et al., 2002). Total d4EGFP intensity in *Trpc2*-/-

animals exposed to intruders matched that of *Trpc2*+/+ animals left alone in an empty cage, indicating that sensory input from VSNs is necessary for the elevated *Arc* expression in AOB IGCs (Fig. 3.4F). These results show that *Arc-d4EGFP*-BAC reporter mice label *Arc*-expressing IGCs in living AOB tissue, and show that VSN activation is both necessary and sufficient to induce AOB *Arc* expression after resident-intruder encounters.

Arc is not expressed in Calb2- or Gad2- expressing IGCs

Different molecularly-defined subtypes of interneurons in the AOB have been explored minimally. Our lab has identified two abundant, largely non-overlapping population of interneurons in the AOB defined by their expression of *Calb2* or *Gad2 (*Maksimova & Meeks, in preparation). Together, these two subtypes make up the majority of IGCs found in the AOB, but their specific computational roles remain unclear. We wondered whether *Arc* expression was limited to one subtype of interneurons, which would suggest their specific role in mediating experience-dependent plasticity. In *Calb2*-Cre x Ai9 and *Gad2*-Cre x Ai9 mice, neurons are labeled with tdTomato based on their expression of *Calb2* or *Gad2,* respectively (Taniguchi et al., 2011; Madisen et al., 2012). We used these transgenic animals as residents, then perfused them 90 minutes after resident-intruder behavior and stained for Arc protein expression. Surprisingly, we found that Arc protein did not colocalize with tdTomato expression in either the *Calb2*-Cre or *Gad2*-Cre mice, suggesting that somatic Arc expression is excluded from both of these populations (Fig. 3.5A-B). Our previous experiments showed that somatic Arc protein is found in a subset of *Arc-d4EGFP* expressing cells, leaving open the possibility that *Arc* is transcribed in *Calb2*- or *Gad2*-expressing

neurons, but that somatic Arc protein expression only occurs in other neurons. These results suggest that *Arc* expression is limited to a population of IGCs that does not express *Calb2* or *Gad2*. By virtue of their ability to express Arc, this third, molecularly-undefined population may be particularly important for mediating experience-dependent plasticity in the circuit, while *Calb2*- and *Gad2*-expressing populations may be more important for other aspects of sensory processing.

Arc is not expressed in newborn neurons

The olfactory bulb is one of the few places in the brain where newborn neurons are integrated throughout life (Nunez-Parra et al., 2013). Newborn neurons arriving the accessory olfactory bulb become inhibitory interneurons, including IGCs. Due to the lack of Arc expression in *Calb2*- and *Gad2*-expressing IGCs, we wondered whether Arc expression was limited to recently-integrated newborn neurons. To address this question, we injected resident males with BrdU and assessed colocalization of BrdU signal with Arc expression 2 and 4 weeks post BrdU injections. We found that Arc did not colocalize with the BrdU signal 2 weeks after BrdU injections, suggesting that Arc expression does not occur in immature neurons that have recently arrived in the AOB (Fig 3.5C). At the 4-week time point, almost no BrdU+ neurons were observed, suggesting that BrdU was not adequately taken up in dividing neurons, or BrdU labeled neurons that arrived in the AOB by 2 weeks were no longer present at 4 weeks (data not shown). Taken together, results thus far suggest that Arc expression occurs primarily in a third population of IGCs, with an unknown molecular identity.

Discussion

Experience-dependent plasticity in the AOB has almost exclusively been studied in the female rodent in the context of mating (Binns and Brennan, 2005; Brennan and Kendrick, 2006), but there are many other rodent behaviors that are strongly influenced by the AOS (Maruniak et al., 1986; Wysocki and Lepri, 1991; Stowers et al., 2002; Papes et al., 2010). The principal motivation for this work was a desire to learn more about experience-dependent AOB plasticity in the context of non-mating AOS-mediated behaviors, to determine whether it is a general feature of the AOB circuit, or a specialized response to mating behavior in females. Overall, the results in this chapter characterize the expression of the IEG *Arc* following male-male social interaction, and provides the impetus for future studies concerning plasticity in the AOB following non-mating AOS-mediated behaviors. Findings detailed in this chapter also provide validation of tools that can be used for future functional studies of plasticity in the AOB following male-male social interaction.

We specifically chose to study the resident-intruder territorial aggression paradigm because it is a male-typical AOS-dependent behavior that induces robust IEG activation in the AOB (Maruniak et al., 1986; Wysocki and Lepri, 1991; Kumar et al., 1999; Stowers et al., 2002). *Arc* is upregulated in male and female rodent AOB IGCs following mating (Matsuoka et al., 2002b; Matsuoka et al., 2002a; Matsuoka et al., 2003), suggesting that *Arc*-expressing IGCs may underlie the increased AOB inhibition observed in this context (Kaba and Keverne, 1988; Brennan et al., 1990). Our results show that *Arc* is selectively transcribed and translated in posterior AOB IGCs of male mice following male-male social chemosensory encounters (Figs 3.1-3.3). Previous work has shown that protein pheromones

called major urinary proteins (MUPs) are sufficient to induce aggressive behavior when painted on a castrated male intruder (Chamero et al., 2007). MUPs are detected by VSNs expressing V2Rs, which project selectively to the posterior AOB. Therefore, it was not surprising that we observed primarily posterior expression of Arc. This finding also mirrors previous findings showing c-fos expression occurs mainly in the anterior AOB following exposure to a female, and in the posterior AOB following exposure to a male (Kumar et al., 1999).

In other brain regions, *Arc* expression occurs rapidly following a stimulus, and is tightly temporally regulated, suggesting that it mediates its effects in a carefully orchestrated way. Our study of the time course of *Arc* expression in response to male-male social interaction suggests that the same is true in the AOB. We found that Arc protein begins to appear by 30 minutes after behavior, peaks 90-120 minutes after behavior, and has returned to baseline by 4 hours after behavior (Fig. 3.3A-D). This suggests that Arc expression is time-locked to the stimulus we provided (male-male interaction), rather than continuously present. It also suggests that any effects mediated by Arc itself are set in motion within that 4-hour period. This finding squared nicely with the time course of d4GFP induction in *Arc-d4EGFP*-BAC mice. We found that in acute live slices, sufficient d4EGFP accumulation for targeted physiological studies occurred by around 4 hours after behavior (Fig. 3.3E). Given this finding, we decided to conduct future physiology experiments, detailed in the following chapter, during the 4-8 hours after behavior, a time window following Arc's return to baseline.

In our time course experiments, we found that not every d4EGFP labeled cell had Arc protein expression at the cell soma, and that IGCs with somatic Arc protein also had especially bright d4EGFP expression (Fig 3.3A-B). One explanation for this is that Arc is often localized to the dendrites, rather than the soma (Shepherd and Bear, 2011). However, in some cases, Arc can enter the nucleus and mediate transcriptional changes involved in homeostatic scaling (Korb et al., 2013). It is not clear what might lead to somatic Arc protein in some but not all *Arc*-expressing IGCs. Because nuclear localization can lead to homeostatic scaling, it is possible that this response is only induced following very strong stimulation, while smaller amounts of stimulation lead to Arc expression in dendrites, but not the nucleus. This may result in different physiological consequences for cells that exhibit somatic Arc expression. Unfortunately, the time window of our physiology experiments fell after Arc's return to baseline, prohibiting us from verifying somatic Arc expression after recording.

This work also shows that sensory activation in the absence of aggression is sufficient to induce *Arc* expression in AOB IGCs (Figs. 3.2, 3.3B-D). First, we found that olfactory investigation of a dish of soiled bedding was sufficient to induce robust *Arc* expression at the same level as investigation of another mouse (Fig. 3.3B-D). This was in contrast to previous work showing that exposure to female-soiled bedding induced some Arc expression above baseline in AOB IGCs, but that being allowed to mate increased Arc expression (Matsuoka et al., 2002a). As discussed above, this could be due to differences in the potency of the bedding stimulus used by us and Matsuoka et al. Alternatively, mating in particular might involve a particular neuromodulatory or hormonal influence in the AOB that is not present in

the context of territorial aggression. Second, we showed that one-night residents, who exhibit olfactory investigation, but no aggression, showed Arc induction at the same level as one-week residents, who do exhibit aggression (Figs. 3.1-3.2). Again, this suggests that any hormonal or neuromodulatory influences that may be activated by the salient experience of aggression are not required for this effect. We also show, using *Trpc2*-/- x *Arc-d4EGFP*-BAC residents, that sensory input from the VNO is required for *Arc* expression (Fig 3.4). These results again stress the importance of sensory input for *Arc* expression, rather than the importance of centrifugal inputs to the AOB from higher order brain structures.

In circuits throughout the brain, different molecularly- and morphologically-defined populations of interneurons are important for accomplishing different computational tasks. For example, in the MOB, interneurons in the external plexiform layer are important for MC synchronization, and also broad gain control, while granule cells are more important for contrast enhancement and top-down modulation (reviewed in Burton, 2017). Also in the MOB, CaMKIIα+ granule cells are activated by simple olfactory stimulation, operant conditioning, and long-term associative memory tasks, while CaMKIIα- neurons are activated in perceptual learning tasks (Malvaut et al., 2017). Therefore, I hypothesized that *Arc*-expressing IGCs might be specifically recruited for experience-dependent plasticity from a molecularly-defined subtype of AOB interneurons. Different interneuron types in the AOB are not as well defined as MOB interneurons. Our lab has identified 2 large populations of IGCs defined by their expression of *Gad2* and *Calb2* (Maksimova and Meeks, in preparation). I found that Arc expression did not colocalize with either *Gad2*- or *Calb2*-expressing IGCs, suggesting that Arc expression occurs exclusively in a third, molecular-

undefined population (Fig 3.5). By virtue of its *Arc* expression, this population may be particularly important for mediating experience-dependent plasticity. Because adult-born interneurons are important for plasticity, I wondered whether Arc expression was enriched in adult-born populations. I found that Arc expression did not colocalize with BrdU labeling in 2-week-old neurons, suggesting that Arc is not expressed in immature neurons. Four weeks after BrdU administration, BrdU-labeled IGCs in the AOB were extremely sparse, and also did not colocalize with Arc expression. The extremely sparse nature of the BrdU labeling suggests that larger doses of BrdU, or alternate methods (like labeling neurons as they migrate through the subventricular zone), might be needed to effectively label adult-born neurons. Future work could further investigate whether Arc expression is enriched in adult-born IGCs by using different methods to label adult-born IGCs and examining later time points. Alternatively, perhaps Arc-expressing IGCs simply have a molecular marker that hasn't yet been identified. In the future, RNA-sequencing techniques could be used specifically on IGCs that express *Arc* following male-male interaction to identify a molecular marker, which may help to develop useful genetic tools.

Because *Arc* is an exquisitely regulated gene required for diverse forms of plasticity throughout the brain, its expression in AOB IGCs suggests their importance for AOB plasticity. Interestingly, *Arc* is typically expressed in principal excitatory projection neurons in other parts of the brain, but is conspicuously absent in AOB MCs. This further suggests the specific importance of AOB IGCs as substrates of plasticity, and offers the opportunity for the investigation of the role of Arc in an unusual setting: inhibitory interneurons. Arc is also expressed in AOB IGCs following mating, a behavior known to lead to pheromonal

memory formation in females, further suggesting that Arc-expressing IGCs may play a role in AOB plasticity. Together, the findings and tools detailed in this chapter provided the motivation and means to study the physiological consequences of *Arc* expression following male-male social interaction.

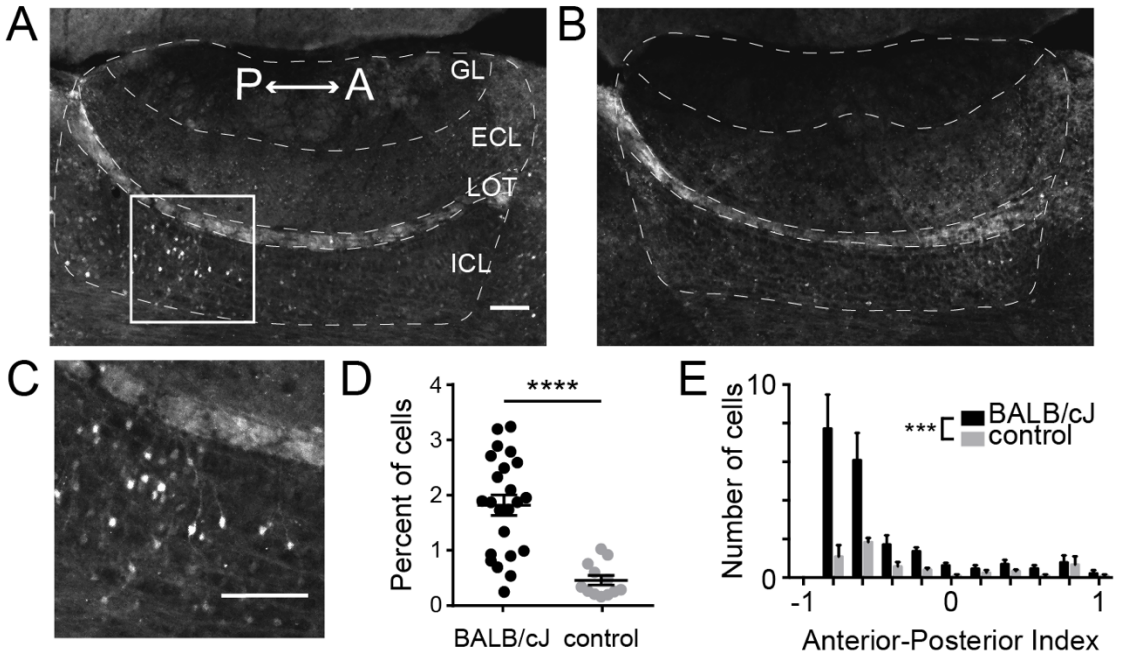

Figure 3.1 Exposing resident males (solo-housed 1 week) to novel male intruders results in upregulation of Arc protein expression in AOB IGCs. ***A,*** Parasagittal section through the AOB of a C57BL/6J male resident 90 minutes after being exposed to a BALB/cJ male intruder. Immunofluorescence indicates Arc protein expression. Scale bar, 100 μm. n=6 animals, 23 sections. ***B,*** AOB section from a control resident that was not exposed to an intruder. n=3 animals, 12 sections. ***C,*** Enhanced view of IGCs in boxed area in ***A***. ***D,*** Percentage of all cells expressing somatic Arc protein. Wilcoxon-Mann-Whitney test, ****$p<0.0001$. Scale bar, 100 μm. ***E,*** Normalized anterior-posterior position of Arc-expressing cells in the ICL. Wilcoxon-Mann-Whitney test, ***$p<0.001$.

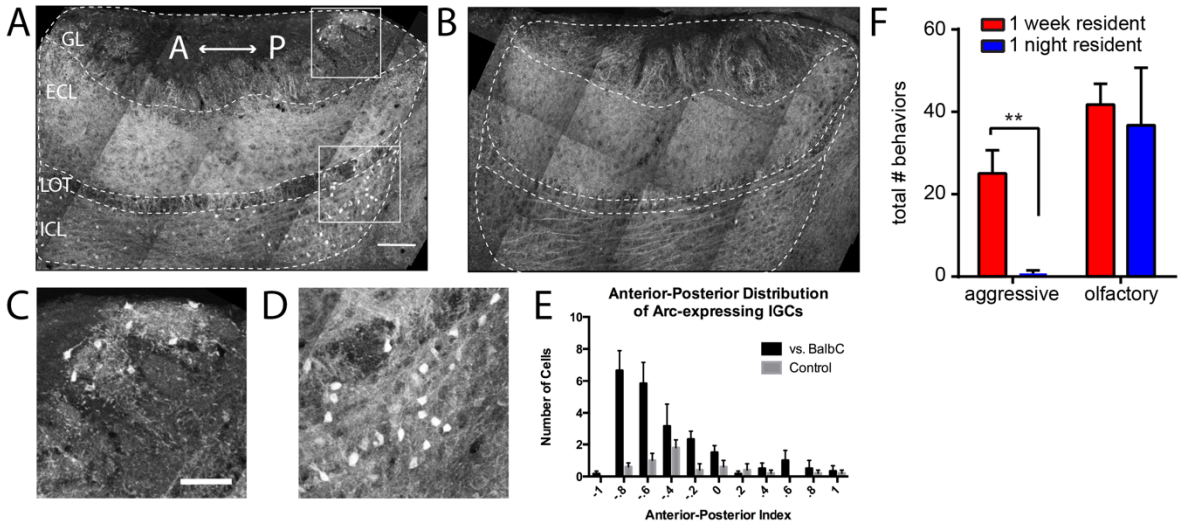

Figure 3.2 Exposing "resident" males (solo-housed 1 night) to novel male intruders results in upregulation of Arc protein expression in AOB IGCs. ***A,*** Parasagittal section through the AOB of a C57BL/6J male "resident" 90 minutes after being exposed to a BALB/cJ male intruder. Immunofluorescence indicates Arc protein expression. Scale bar, 100 μm. n=6 animals, 6 sections. ***B,*** AOB section from a control resident that was not exposed to an intruder. n=5 animals, 5 sections. ***C,*** Enhanced view of JGCs in boxed area in GL ***A***, scale bar, 50 μm. ***D,*** Enhanced view of boxed area in ICL in ***A***. ***E,*** Normalized anterior-posterior position of Arc-expressing cells in the ICL. Wilcoxon-Mann-Whitney test, p=0.16. ***F,*** Number of aggressive and olfactory behaviors exhibited by 1-week (Fig 3.1) and 1-night (Fig. 3.2) residents. Wilcoxon-Mann-Whitney test, **p<0.01.

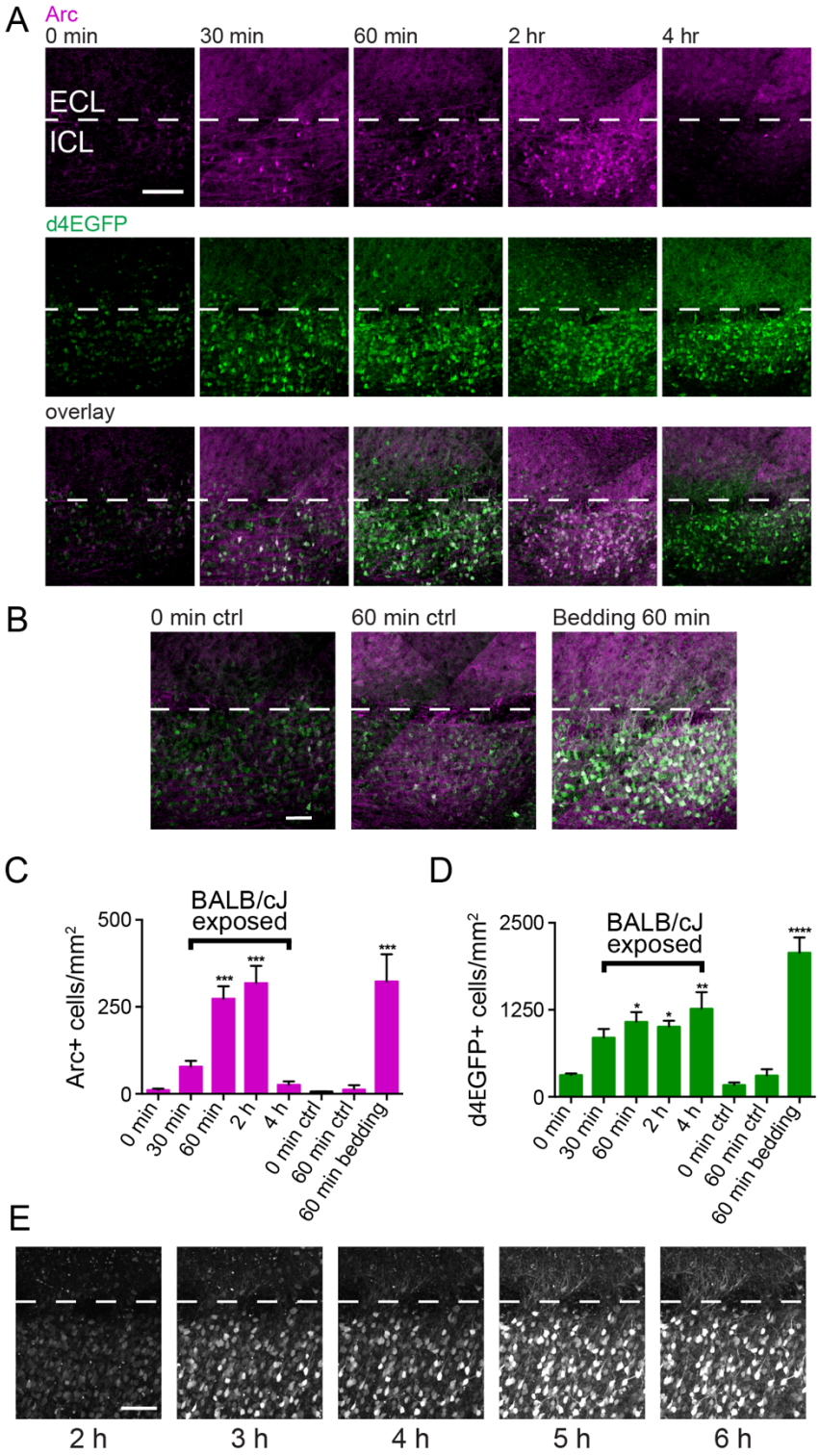

Figure 3.3 Arc protein expression peaks 2 hours after behavior and overlaps with d4EGFP expression in *Arc-d4EGFP*-BAC mice. ***A,*** Parasagittal AOB sections from resident mice

perfused 0, 30, 60, 120, or 240 minutes after behavior, stained for both Arc and d4EGFP. The ICL is indicated by white dotted lines, and posterior AOB is shown. Scale bar, 100 μm. ***B,*** Arc protein and d4EGFP expression in negative control mice that were perfused after 0 or 60 minutes in the behavioral setup but were not exposed to a BALB/cJ intruder (left two panels). Arc protein and d4EGFP expression in a resident mouse that was exposed to soiled BALB/cJ bedding only in the behavioral setup, then was perfused 60 minutes later (right panel). Scale bar, 50 μm. ***C,*** Quantification of Arc immunostaining across conditions. One-way ANOVA, $F(7,11)=18.64$, $p<0.0001$. ***D,*** Quantification of d4EGFP immunostaining across conditions. One-way ANOVA, $F(7,11)=13.07$, $p=0.0002$. For ***C*** and ***D***: *$p<0.05$, **$p<0.01$, ***$p<0.001$, ****$p<0.0001$, compared with the 0 min controls (19 sections across 11 mice; ANOVA corrected for multiple comparisons using Dunnett's method). ***E,*** Time course of d4EGFP expression in a single acute live slice visualized using two-photon microscopy. Each image is a maximum z-projection of a 200 μm slice. Dissection occurred 1 hour after behavior. Scale bar, 100 μm. ctrl, Control.

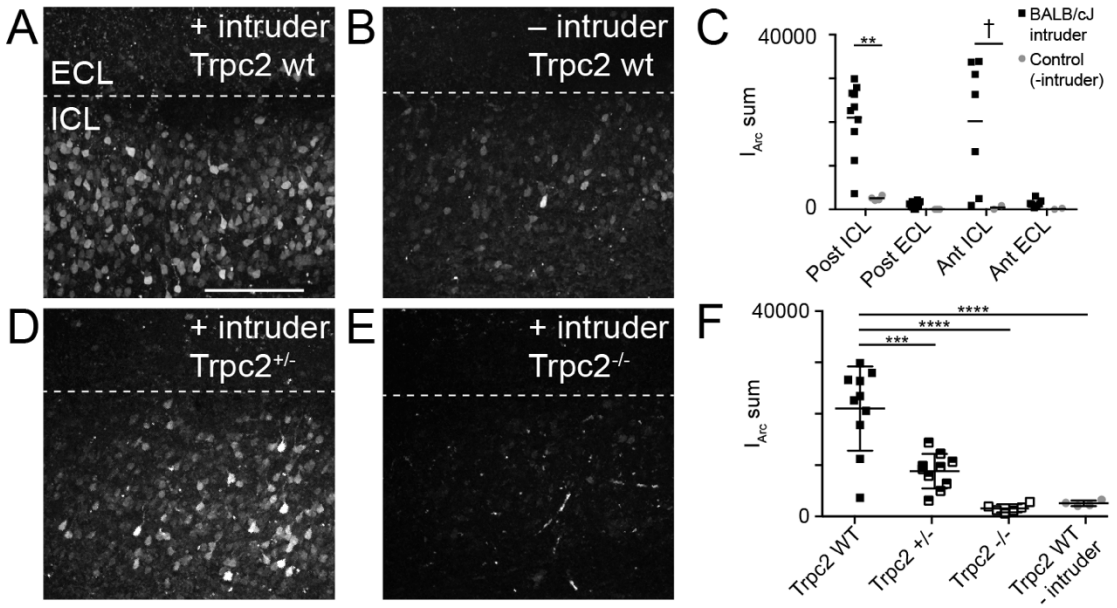

Figure 3.4 *Arc* expression is not upregulated after the resident-intruder assay in *Trpc2*-/- mice. ***A,*** Maximum z-projection of an acute AOB slice taken from an *Arc-d4EGFP*-BAC, *Trpc2*+/+ resident. Posterior AOB is shown. Images were taken 4 hours after exposure to a BALB/cJ intruder. Scale bar, 200 μm. ***B,*** Representative z-projection taken from a control resident that was not exposed to an intruder. ***C,*** Quantification of summed fluorescence across d4EGFP-expressing cells (I_{Arc} sum). Significance in each region was determined using the Wilcoxon-Mann-Whitney test: **p<0.01; †p<0.1. Posterior ICL: n=9 mice, 10 slices (experimental), n=4 mice, 4 slices (control); Posterior ECL: n=9 mice, 10 slices (experimental), n=3 mice, 3 slices (control); Anterior ICL/ECL n=6 mice, 7 slices (experimental) n=2 mice, 2 slices (control). ***D,*** Representative z-projection taken from a *Trpc2*+/- *Arc-d4EGFP*-BAC male resident. ***E,*** Representative z-projection taken from a *Trpc2*-/- *Arc-d4EGFP*-BAC male resident. ***F,*** Quantification of I_{Arc} sum for the posterior ICL of all genotypes. *Trpc2*+/- n=5 mice, 10 slices, *Trpc2*-/- n=3 mice, 6 slices. One way

ANOVA $F(3,26)=22.75$, $p<0.0001$. ***, and **** represent $p<0.001$, and 0.0001, respectively for indicated pairs (corrected for multiple comparisons using Tukey's method).

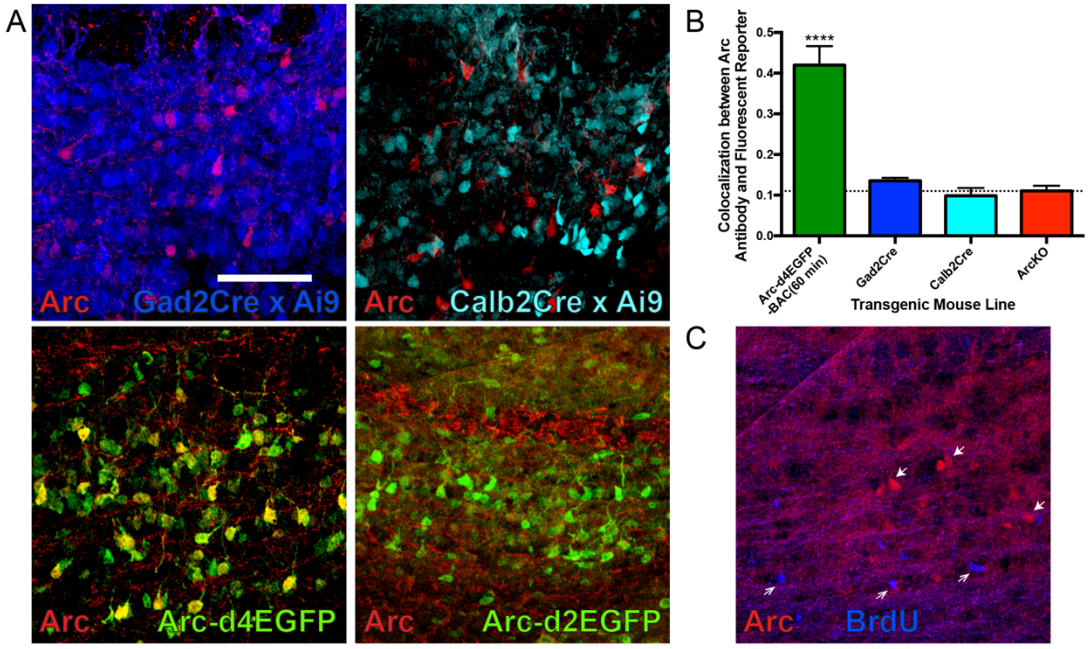

Figure 3.5 Arc is not expressed in *Gad2*- or *Calb2*-expressing IGCs. ***A,*** Parasagittal section through the AOB of residents with genotype *Gad2*-Cre x Ai9 (upper left), *Calb2*-Cre x Ai9 (upper right), *Arc-d4EGFP*-BAC (bottom left), and *Arc*-d2EGFP (bottom right) 90 minutes after being exposed to a BALB/cJ male intruder. Colocalization between Arc and d4EGFP signals provides a positive control, while colocalization between Arc and d2EGFP (which are *Arc-/-*) provides a negative control. Scale bar, 100 μm. ***B,*** Quantification of colocalization between Arc protein and each fluorescent reporter. One-way ANOVA $F(3,17)=2.597$, $p<0.001$. ****$p<0.0001$, compared with the *Arc*-d2EGFP negative control. (n=21 sections across 8 mice, ANOVA corrected for multiple comparisons using Dunnett's method). ***C,*** Representative from a BrdU injected resident, 2 weeks after BrdU injection and 90 minutes after resident-intruder behavior. Filled in arrowheads indicate Arc+ cells, while open arrowheads indicate BrdU-labeled cells. No Arc+/BrdU+ cells were identified in n= 6 sections across 4 mice.

CHAPTER FOUR
Arc-expressing internal granule cells increase their excitability through intrinsic mechanisms following male-male social interaction

Background

Immediate early genes (IEGs) are routinely used to identify neurons and circuits that are activated by a specific behavioral experience (Kawashima et al., 2014; Kim et al., 2015; Vousden et al., 2015). The IEG *Arc* in particular is associated with, and required for, diverse forms of plasticity throughout the brain, and is thus a useful marker for neurons that may be undergoing plasticity (Shepherd and Bear, 2011). *Arc* is most often expressed in principal excitatory neurons, where it mediates many forms of experience-dependent synaptic plasticity (Plath et al., 2006; Vazdarjanova et al., 2006; Jakkamsetti et al., 2013). The previous chapter details our finding that Arc expression is limited to inhibitory interneurons called IGCs in the AOB following male-male social interaction in the resident intruder paradigm. The expression of Arc in this specific cell type suggests that IGCs are instrumental in experience-dependent plasticity in the AOB. Further, by studying the physiology of Arc+ IGCs in comparison to their Arc- neighbors, we can gain a better understanding of the cell-specific mechanisms of plasticity in the AOB.

In principal neuronal types, Arc is essential for many types of plasticity, including long-term potentiation, mGluR-dependent long-term depression, and homeostatic scaling (Plath et al., 2006; Waung et al., 2008). Because the physiological effects of *Arc* expression haven't been studied in non-principal neuronal types, the expected consequences of *Arc* expression in AOB IGCs are unclear. Decades of previous work suggest that increased

inhibitory tone in the AOB accompanies pheromonal memory formation after mating (which induces Arc expression in IGCs). However, much of the previous work in this field has not interrogated functionally-defined populations, but has investigated changes to AOB circuit function as a whole. Additionally, plasticity in the AOB hasn't been investigated in diverse behavioral contexts, and has instead focused on mating behavior, despite the role that the AOS plays in other social behaviors. We hypothesized that *Arc* expression in AOB IGCs would be associated with an increased ability to inhibit their connected MCs. Here, we investigated the network, synaptic, and intrinsic consequences of *Arc* expression in AOB IGCs following male-male social interaction in the resident-intruder paradigm.

Specific materials and methods

Glomerular stimulation

For glomerular stimulation experiments, a theta glass stimulating electrode was placed in the glomerular layer while recordings were made from IGCs. A series of 0.3 ms single pulses was used to construct input-output curves (Stimulus Isolator A365RC, World Precision Instruments), and the stimulation intensity for 20 Hz trains was the highest sub-saturating value from the input-output analysis. One d4EGFP+ and one d4EGFP– neuron were recorded per slice (one at a time). The d4EGFP+ neuron was recorded first in 6/10 pairs. Input-output curves were generated for each neuron, but the stimulation intensity used for both was chosen based on the first neuron recorded. Prior to MC recordings, we confirmed that stimulus conditions effectively recruited IGCs through direct IGC patch clamp recordings (23/24 recordings).

Spontaneous and miniature EPSCs

For mEPSC recordings, 5 minutes of baseline activity was recorded, then 1μM tetrodotoxin (TTX) was washed on for 5 minutes, and 5 minutes of post-drug activity was recorded. Biocytin (3 mg/mL) and/or AlexaFluor568 (166 μM) was added to the internal solution to visualize dendritic arbors and spines. After filling, slices were fixed in 4% PFA in PBS for one hour, and then stored in PBS at 4ºC.

Assessment of intrinsic physiological features

To assess intrinsic electrophysiological features, we subjected patched AOB neurons to a series of current clamp and voltage clamp challenges. Immediately after achieving the whole cell configuration, each cell's resting membrane potential (V_{rest}) was measured in current clamp mode. To standardize measurements across cells with different V_{rest}, we injected steady-state currents to maintain each cell's membrane potential (V_m) between -70 and -75 mV. Based on initial measurements of input resistance (R_{input}), we empirically determined the amplitude of hyperpolarizing current that adjusted V_m by -50 mV (to ~-125 mV). After determining this initial current injection amplitude, we generated a cell-specific 10-sweep Clampex protocol that applied increasingly depolarizing 0.5 s square current pulses, starting with the initial injection amplitude. For example, if the initial current injection was determined to be -100 pA, the 10-sweep protocol would have current injection increments of +20 pA (*i.e.*, -100 pA, -80 pA, -60 pA,…,+80 pA). If the initial depolarization was determined to be -125 pA, the protocol would include increments of +25 pA, etc. This

strategy allowed us to objectively challenge cells with widely varying V_{rest} and R_{input}. In voltage clamp, cells were initially held at -70 mV, and a series of 12 voltage command steps (0.5 s in duration) were applied that spanned -100 mV to +10 mV.

For each cell, both current clamp and voltage clamp protocols were applied up to 4 times, and all reported quantities represent the mean responses across repeated trials. Twenty-six specific intrinsic parameters were extracted from each cell using custom software written in MATLAB. A description of the parameters in Figure 4.3A and the formulas used to calculate them is presented in Table 2. I_H current ratio (Fig. 4.3G) was calculated using the formula

$$\frac{I_{init} - I_{ss}}{I_{init}}$$

where I_{init} is the mean initial current (measured between 10 and 160 ms following the voltage pulse) and I_{ss} is the mean steady-state current (measured between 420 and 470 ms after the voltage pulse) generated by a voltage command step from -70 mV to -100 mV. EPSCs were automatically detected and later separated from noise using a custom computer assisted waveform-based event sorting program written in MATLAB (Hendrickson et al., 2008). EPSC decay was measured by calculating the best fit exponentially-decaying line for the decay period of the EPSC. Initial action potential rising slope was calculated by measuring the peak of the first derivative of voltage with respect to time (dV/dt). Threshold was defined as V_m at the time the dV/dt voltage reached 10% of its peak value (similar to Meeks et al., 2005). Membrane capacitance and input resistance were calculated according to current clamp-based multi-compartmental algorithms (Golowasch et al., 2009). Briefly, the voltage response of each cell to a hyperpolarizing current step was fit with a series of multi-

exponential curves, and the best fit determined by identifying the solution with the lowest value of the Bayesian Information Criterion (to avoid over-fitting).

Immunofluorescence

Biocytin amplification of filled neurons was achieved using streptavidin-Alexa Fluor 568 (ThermoFisher #S11226, RRID: AB2315774). Slices were washed in PBS 3x for 30 minutes each. Slices were then incubated in a blocking solution containing 0.5% TritonX and 10% goat serum in PBS for 2 hours, followed by the same blocking solution containing streptavidin-AF568 at 0.01mg/mL for 4 hours. Slices were then rinsed 3x for 30 min each, and mounted on slides in Fluoromount-G mounting medium. Dendrites were imaged using a 40x (1.3 NA) oil immersion objective on an LSM 510 inverted confocal microscope (Zeiss). Spines were counted and morphological analysis performed using the Simple Neuron Tracer plugin for ImageJ (Longair et al., 2011) by a scorer blinded to the experimental conditions. Spines were counted on the 100 μm of the primary dendrite in the ECL starting at the edge of the LOT.

HCN pharmacology

Blockade of HCN channels was achieved using ZD7288 at 10 μM. Baseline recordings were made, then ZD7288 was washed in for 5 minutes before the next set of recordings were made.

Stereotaxic injections

Two double-transgenic adult males heterozygous for *Arc-CreERT2* and Ai9 alleles were injected bilaterally (as described in chapter 2) with 120 nL of AAV2/9-EF1a-DIO-hChR2(E123T/T159C)-EYFP (titer 8.3 x 10^{12} GC/mL; Mattis et al., 2011). AAVs were purchased from the University of Pennsylvania Vector Core (Catalog #AAV-9-35509).

Optogenetic stimulation

Blue light optogenetic stimulation was applied via the 40x water immersion objective using an installed FITC/GFP filter cube (Nikon). Blue light was filtered from a X-Cite 200DC mercury lamp (Lumen Dynamics). Whole-field illumination was applied at 20 Hz by rapidly shuttering the illumination source via TTL pulses. IGC and MC responses were recorded in both current- and voltage-clamp configuration.

Results

Arc-expressing IGCs respond more strongly than non-expressing IGCs to glomerular stimulation

Previous work showed experience-dependent increases in inhibitory tone in the AOB following salient social behavior, suggesting that IGCs increase their inhibitory influence on MC output (Brennan et al., 1990; Brennan et al., 1995). If the IGCs expressing *Arc* after social chemosensory interactions contribute to AOB experience-dependent plasticity, we hypothesized that *Arc*-expressing IGCs would respond differently to AOB sensory input than non-expressing IGCs. To test this hypothesis, we made targeted whole cell patch clamp

recordings from *Arc*-expressing (d4EGFP+) and non-expressing (d4EGFP–) IGCs in acute slices 4-8 hours after resident-intruder experiments (Fig. 4.1). To simulate sensory activity, we electrically stimulated VSN fibers in the AOB glomerular layer using theta-glass electrodes. Stimulating the glomerular layer induces glutamate release from VSN terminals and activates downstream MCs, which in turn activate IGCs at dendro-dendritic synapses (Fig. 4.1A). Thus, IGC activation resulting from VSN terminal stimulation is a di-synaptic effect. In voltage clamp, *Arc*-expressing IGCs showed increased single pulse EPSC charge transfer and peak current amplitude compared to non-expressing IGCs across stimulus intensities (paired, 2-tailed Student's *t*-test, $p<0.05$, n=10 slices across 7 mice Fig. 4.1B-F). d4EGFP+ IGCs were recorded first in 6/10 experiments, so we investigated possible order effects by comparing these same responses based on the recording order (Fig. 4.1D, F). We found no differences in this comparison (paired, 2-tailed Student's *t*-test, $p>0.05$), indicating that order effects cannot explain the increased excitability of d4EGFP+ IGCs. In order to evaluate the physiological relevance of these responses, we approximated strong MC activation by delivering a 3 s, 20 Hz train of stimuli to glomerular layer (matching MC firing rates measured during direct chemosensory stimulation of the VNO; Meeks et al., 2010). In current clamp, d4EGFP+ IGCS responded to trains with increased peak amplitudes, which were also sustained throughout the 3 second stimulus (repeated measures ANOVA, main effect of group $F(1,18)=4.51$, $p=0.048$, Fig. 4.1G-H). This effect was eliminated when the same data was organized based on recording order (repeated measures ANOVA, no main effect of group $F(1,18)=0.03$, $p=0.87$, Fig. 4.1I). In voltage clamp, the same d4EGFP+ IGCs responded to stimulus trains with significantly greater charge transfer than d4EGFP– IGCs

and sustained this increase throughout the 3 seconds of stimulation (repeated measures ANOVA, main effect of group $F(1,18)=5.52$, $p=0.03$, Fig. 4.1J). As before, this effect was not due to an effect of recording order (repeated measures ANOVA, no main effect of group $F(1,18)=0.07$, $p=0.79$, Fig. 4.1K). These data indicate that *Arc*-expressing IGCs are more engaged by sensory input stimulation, which may reflect enhanced MC-IGC synaptic communication or increased IGC intrinsic excitability. These data also suggest that *Arc*-expressing IGCs may contribute to experience-dependent MC inhibition.

Arc-expressing IGCs do not receive increased excitatory drive

We hypothesized that the increased activation of *Arc*-expressing IGCs was due to a change in the number of MC-IGC synapses or a change in MC-IGC synaptic strength. To test these hypotheses, we recorded spontaneous and miniature EPSCs (sEPSCs and mEPSCs, respectively) from d4EGFP+ and d4EGFP– IGCs (Fig. 4.2). *Arc*-expressing IGCs did not exhibit a significant difference in sEPSC or mEPSC amplitude or frequency (Wilcoxon-Mann-Whitney test, $p>0.05$, Fig. 4.2A-C). In these experiments, biocytin was included in the recording pipette to allow *post hoc* analysis of dendrite morphology and dendritic spine density. Analysis of IGC dendrites showed a trend towards slightly lower spine densities in *Arc*-expressing IGCs compared to non-expressing IGCs (Wilcoxon-Mann-Whitney test, $p=0.0556$, Fig. 4.2D-E). Similarly, there were no differences in average dendritic branch length (d4EGFP+: 485.3 ± 115.7 μm n=6, d4EGFP-: 365.5 ± 57.2 μm n=8, Wilcoxon-Mann-Whitney test, $p=0.57$), maximum dendritic branch length (d4EGFP+: 1813 ± 149.4 μm n=6, d4EGFP-: 1548 ± 231.4 μm n=8, Wilcoxon-Mann-Whitney test, $p=0.41$), or number of

branches (d4EGFP+: 17.5 ± 4.75 branches n=6, d4EGFP-: 14.3 ± 1.89 branches n=8, Wilcoxon-Mann-Whitney test, p=0.59). Taken together, these results indicate that changes in IGC synaptic strength or number cannot explain the increased responses to glomerular stimulation in *Arc*-expressing IGCs.

Arc-expressing IGCs display enhanced intrinsic excitability

Lacking support for our initial hypothesis, we turned to an alternative, which was that *Arc*-expressing IGCs respond more strongly to VSN input stimulation due to changes in intrinsic properties. We utilized a systematic approach in order to assess possible intrinsic physiological differences in an unbiased way. We targeted whole-cell patch-clamp recordings to *Arc*-expressing and non-expressing IGCs 4-8 hours post-behavior and delivered a series of electrophysiological challenges in current and voltage clamp. Using automated algorithms (See specific materials and methods for this chapter), we quantified 26 physiological characteristics covering a variety of intrinsic properties (Table 2). To capture the differences between *Arc*-expressing and non-expressing IGCs, we performed cluster analysis on the 26-dimensional array of characteristics from 100 neurons that had undergone the same electrophysiological challenges (Fig. 4.3A-B). This collection of cells contained 26 d4EGFP+ and 23 d4EGFP– cells, along with 39 control IGCs from mice that had not undergone behavioral challenges and 12 MCs (used as a control population; Fig. 4.3A-B). Four clusters were identified by this analysis. 69.2% of all d4EGFP+ IGCs were assigned to Cluster 3, where neurons exhibited sustained strong spiking activity in response to depolarization and lower levels of spike accommodation. Other intrinsic characteristics,

including input resistance, resting membrane potential and action potential threshold, were highly variable across cells in this cluster, indicating that increased IGC firing frequency was not associated with a systematic change in these other properties.

In assessing individual intrinsic properties, few differed significantly between d4EGFP+ and d4EGFP– IGCs (Fig. 4.3C-H). The most noteworthy individual characteristic was an increase in spiking frequency in response to strong somatic depolarization in *Arc*-expressing IGCs (Wilcoxon-Mann-Whitney test, $p<0.0001$, Fig. 4.3D). d4EGFP+ IGCs demonstrated an increase in the maximal slope of initial action potentials (Wilcoxon-Mann-Whitney test, $p<0.05$, Fig. 4.3E), which was not a result of increased sodium current peak amplitudes (d4EGFP+: 2.33 ± 0.22 nA, d4EGFP–: 2.02 ± 0.14 nA, Wilcoxon-Mann-Whitney test, $p=0.49$) or spike threshold (d4EGFP+: -23.5 ± 1.5 mV, d4EGFP–: -23.0 ± 1.3 mV, Wilcoxon-Mann-Whitney test, $p=0.53$). These results indicate that *Arc*-expressing IGCs are intrinsically more excitable following resident-intruder behavior, which could explain their enhanced responses to glomerular stimulation.

Arc-expressing IGCs exhibit decreased HCN-channel mediated currents

Arc-expressing IGCs also exhibited a slight decrease in hyperpolarization-activated cation (I_H) currents (Fig. 4.3G), which we confirmed by measuring the currents blocked by the HCN channel antagonist ZD7288 (10 μM; Wilcoxon-Mann-Whitney test, $p<0.05$, Fig. 4.3H). Because IGCs have high input resistance (1.0 ± 0.17 GΩ, n = 54 IGCs), small amplitude I_H currents resulted in prominent depolarization ("sag" potential) measured at the soma (d4EGFP+: 5.81 ± 0.62 mV, d4EGFP-: 8.37 ± 0.90 mV, Wilcoxon-Mann-Whitney test,

p=0.11). These basic I_H measurements were made after step hyperpolarization from a steady-state membrane potential near -70 mV, which may have obscured I_H conductances open near IGC resting potential. To measure the contributions of such conductances, we subtracted I_H sag potentials (reflecting conductances activated by the transition from ~-70 to ~-125 mV) from rebound depolarizations that occurred after the hyperpolarizing pulses (reflecting all I_H conductances). This analysis revealed a larger relative contribution of I_H conductances near resting potential in d4EGFP+ IGCs compared to d4EGFP– IGCs, suggesting a slight shift in the voltage-dependence of activation of HCN channels (d4EGFP+: 1.33 ± 0.57 mV, d4EGFP-: 0.23 ± 0.47 mV; Mann-Whitney-Wilcoxon test, p=0.059). At face value, these I_H results were somewhat surprising. However, modulation of I_H has been reported in Arc-dependent plasticity elsewhere in the brain (reviewed in Shah, 2014). In many cases downregulation of I_H has been associated with increased neuronal excitability (Poolos et al., 2002; Brager and Johnston, 2007; Campanac et al., 2008; Yi et al., 2016). These results suggest that downregulation of I_H in *Arc*-expressing IGCs may contribute to the increase in intrinsic excitability that we observed.

Pharmacological blockade of HCN-channel mediated currents does not result in increased activation of IGCs from glomerular stimulation

While our results show that increased intrinsic excitability and decreased I_H are associated, it is not clear whether the decreased in I_H is the direct cause of the increase in intrinsic excitability. A causal relationship between decreased I_H and increased excitability has been shown previously in other forms of short term plasticity (Brager and Johnston,

2007). We hypothesized that if decreased I_H directly causes the increase in excitability, pharmacologically blocking HCN channels should result in increased excitability. Using adult C57BL/6J males, without any behavioral manipulation, we patched IGCs and recorded their responses to glomerular stimulation before and after pharmacological blockade of HCN channels. In this configuration, we found that blockade of HCN channels did not increase the magnitude of the responses of the patched IGCs, suggesting that the decrease in I_H may not be directly causing the observed increase in intrinsic excitability (Fig 4.4A-B). Alternatively, perhaps a decrease in I_H in concert with changes to other voltage-gated channels might lead to the observed increase in excitability, but decreased I_H alone is not sufficient. It is also possible that this manipulation was so extreme that it did not provide meaningful information about the true biological process, and thus does not completely rule out the causation hypothesis. Future experiments could aim to more closely mimic naturalistic downregulation of I_H.

Arc knockout eliminates intrinsic excitability and I_H phenotypes

It may be possible that *Arc* is required for the expression of experience-dependent increases in IGC excitability. To investigate this hypothesis, we utilized *Arc*-d2EGFP knock-in/knock-out animals (Wang et al., 2006). In *Arc*-/- animals, d2EGFP (which has a 2-hour half-life) is knocked-in to the endogenous *Arc* locus and is thus expressed in neurons that would normally express *Arc.* We repeated our intrinsic electrophysiological assay in acute slices taken from *Arc*+/- and *Arc*-/- male residents. d2EGFP+ IGCs in *Arc*-/- mice showed no differences in maximum spiking frequency, I_H sag potential, or I_H currents compared to

d2EGFP– IGCs from the same slices (Fig. 4.5A-C). These results suggest that *Arc* may be required for the observed differences in excitability between *Arc*-expressing and non-expressing IGCs following male-male social interaction. However, interpretation of these results is complicated by the findings from *Arc*+/- mice. Surprisingly, we did not observe the same excitability phenotype in *Arc*+/- mice as we did in *Arc-d4EGFP*-BAC mice (Fig 4.5A). On the other hand, we found that d2EGFP+ cells in *Arc*+/- mice did show a trend towards decreased I_H sag potential compared to d2EGFP- cells, recapitulating the result from *Arc-d4EGFP*-BAC mice (though we didn't test this further with ZD7288) (Fig. 4.5C).

One possible explanation for these inconsistent results is that both copies of the endogenous *Arc* gene are required to induce the specific experience-dependent effects that we observed in the *Arc-d4EGFP*-BAC mice. Because the *Arc*-d2EGFP line is a knock-in, one copy of the *Arc* gene must be lost in order to get any d2EGFP expression. Another caveat that comes with comparing results from *Arc-d4EGFP*-BAC mice and *Arc*-d2EGFP mice is that the d2EGFP has a shorter half-life, which does not lend itself well to the time course of our physiology experiments (4-8 hours after behavior).

Previously we found that *Arc-d4EGFP*-BAC mice do not exhibit any differences in spontaneous or mini EPSCs. As part of our assay of intrinsic features of *Arc*+/- and *Arc*-/- mice, we were able to measure spontaneous EPSCs (sEPSCs) from these neurons. We found no significant differences in sEPSC frequency or amplitude between d2EGFP+ and d2EGFP- IGCs in either *Arc*-/- or *Arc*+/- mice (Fig 4.5D-E). In the *Arc*+/- mice, we did observe a trend towards decreased sEPSC amplitude in d2EGFP+ cells compared to d2EGFP- cells, which was not seen in *Arc-d4EGFP*-BAC mice (Fig 4.2B, 4.5D-E). Because Arc can mediate

endocytosis of AMPA receptors, it is not surprising that d2EGFP+ neurons might show decreased sEPSC amplitude compared to d2EGFP- neurons in *Arc*+/- mice. However, it is not clear how to interpret this result in light of the fact that IGCs from *Arc*-/- mice have similar sEPSC amplitudes to those in d2EGFP+ *Arc*+/- IGCs (Fig. 4.5E). These sEPSC results came from the several seconds of baseline activity following voltage command steps in our intrinsic assay (same as used in Fig. 4.3F), while the results from *Arc-d4EGFP*-BAC mice came from 5-minute long recordings without any type of stimulation. The voltage step paradigm could may have influenced the sEPSC results obtained from *Arc*+/- and *Arc*-/- mice, and should be considered in the interpretation of these results.

Arc-expressing IGCs directly inhibit mitral cells

Prior to investigating the effects of male-male social interaction on MC activity, we wanted to first confirm that *Arc*-expressing IGCs directly inhibit MCs. The primary target of IGCs in the AOB is MCs, and the vast majority of these interneurons are GABA-ergic. However, some interneurons in the AOB may express neuromodulators (Marking et al., 2017). To confirm that *Arc*-expressing IGCs inhibit MCs, we injected a Cre-dependent AAV in the AOBs of ArcCreER+/- x Ai9+/- male residents to drive expression of ChR2 specifically in *Arc*-expressing IGCs. Two weeks after injection, ArcCreER+/- x Ai9 +/- residents were administered 4-OHT and exposed to a novel BALBc/J male intruder. After 7 days, which was necessary for *Arc*-expressing IGCs to accumulate ChR2-EYFP, we prepared acute live slices and tested the effects of blue light stimulation. Under 2-photon microscopy, we found that 43.6% of IGCs expressing tdTomato (from the Ai9 transgene) also expressed

ChR2-EYFP, and that 78.1% of Chr2-EYFP cells also expressed tdTomato (Fig. 4.6A). 20 Hz blue light stimulation resulted in strong inward currents in ChR2+ IGCs in voltage-clamp, as well as action potential firing in current clamp (Fig. 4.6B-C). When we patched (non-fluorescent) MCs, we observed that blue light stimulation induced outward inhibitory postsynaptic currents when the MC was held at -50 mV (Fig 4.6D). We tested MC responses at a variety of holding potentials to elucidate the I-V relationship between MC holding potential and the amplitude of blue light-induced currents (Fig. 4.6E). Linear regression analysis of this data revealed that the reversal potential of these currents was around -60 mV, consistent with a Cl^- conductance. To test whether inhibition from *Arc*-expressing IGCs was sufficient to suppress MC activity, we elicited tonic action potential firing in MCs by depolarizing them to -35 mV using steady-state current injection (Fig 4.6F). Under these conditions, 20 Hz blue light stimulation resulted in immediate and reversible action potential suppression (Fig. 4.6F). These results indicate that *Arc*-IGCs directly inhibit MCs, likely via GABA mediated inhibitory Cl^- conductances. Additionally, they show that *Arc*-expressing IGCs remain capable of strongly suppressing MCs for at least one week following social chemosensory events, consistent with a role for *Arc*-expressing IGCs in experience-dependent chemosensory plasticity after non-mating behaviors.

Male-male social interaction leads to suppressed activation of mitral cells

The increased excitability of *Arc*-expressing IGCs suggests that AOB MCs may experience stimulus-associated suppression following resident-intruder encounters. To test this hypothesis, we measured the responses of posterior AOB MCs to glomerular layer

stimulation during the same 4-8 hour post-behavior time window used in IGC recordings (Fig. 4.7). MCs in current clamp were depolarized via steady-state current injections to -55 mV (just below action potential threshold), and exposed to 3 second, 20 Hz glomerular layer stimulation (Fig. 4.7B-C). We observed less evoked spiking activity in MCs in AOB slices taken from post-behavior resident males than no-intruder controls (repeated measures ANOVA, interaction between group and stimulus, $F(59,1298)=2.45$, $p<0.0001$, n=13 cells, 4 mice for "intruder" group; n=9 cells, 4 mice for "no intruder" group, Fig. 4.7B-C). Voltage clamp experiments from these same cells held at -40 mV revealed suppressed net inward current during the stimulus trains (repeated measures ANOVA, main effect of group, $F(1,22)=8.49$, $p=0.008$, Fig. 4.7D). We observed no differences in net inward current when cells were held at -50 mV (nearer Cl^- reversal potential), indicating that the results at -40 mV reflect the influence of increased outward currents (repeated measures ANOVA, no main effect of group $F(1,22)=0.07$, $p=0.80$). We did not observe increased MC intrinsic excitability post-behavior (MC max spiking frequency: 48.1 ± 2.5 Hz post-behavior, 40.2 ± 2.1 Hz control, Wilcoxon-Mann-Whitney test, $p=0.13$), but did see a small decrease in I_H currents (normalized I_H current ratio 0.0342 ± 0.003 post-behavior, 0.047 ± 0.005, Wilcoxon-Mann-Whitney test, $p=0.035$). Importantly, these currents are much smaller than those observed in IGCs, consistent with recent observations in mitral cells (Gorin et al., 2016). These results confirm that male-male social chemosensory encounters are associated with subsequent MC suppression, consistent with an experience-dependent increase in IGC-MC inhibition.

Discussion

Previously, we characterized the expression of the IEG *Arc* in the AOB following male-male social interaction in the resident-intruder paradigm. Here, we investigate the physiological properties associated with *Arc* expression in IGCs following the same behavior. We demonstrate that *Arc*-expressing IGCs respond more strongly to sensory stimulation than *Arc* negative neighbors. This response is driven by an increase in intrinsic excitability rather than increased excitatory synaptic drive. Increased intrinsic excitability of specific IGCs is accompanied by suppressed activation of MCs, suggesting that *Arc*-expressing IGCs may participate in increased suppression of MC output following salient male-male social interaction.

The specific neurophysiological changes reported in Arc-expressing neurons in other brain regions vary widely and are often subtle (Wang et al., 2006; Ploski et al., 2008; Shepherd and Bear, 2011; Jakkamsetti et al., 2013). For example, *Arc*-deficient pyramidal neurons in visual cortex have an overall reduction in their orientation selectivity, but retain experience-dependent refinement of this selectivity (Wang et al., 2006). In the context of novel environment exploration, *Arc*-expressing hippocampal pyramidal neurons do not show outright synaptic depression, but instead are primed for mGluR-dependent LTD (Jakkamsetti et al., 2013). In the AOB, *Arc* upregulation is conspicuously absent in projecting MCs (Figs. 3.1-3.4). IGCs are physiologically and morphologically different than most of the principal cell types in which *Arc* has been studied. Specifically, IGCs are axonless and use reciprocal dendro-dendritic synapses to communicate with MCs (Jia et al., 1999; Taniguchi and Kaba, 2001). IGCs also experience significant cellular turnover in adulthood, and are replenished

by adult-born neurons that migrate via the rostral migratory stream (Alvarez-Buylla and Garcia-Verdugo, 2002). The selective capacity of IGCs to upregulate *Arc* in response to social chemosensory experience suggests these interneurons may be primary drivers of AOB experience-dependent plasticity.

There are several genetic tools for labeling and manipulating *Arc*-expressing cells in living mouse brain tissue (Wang et al., 2006; Grinevich et al., 2009; Guenthner et al., 2013; Kawashima et al., 2014). We specifically chose *Arc-d4EGFP*-BAC reporter mice for our initial physiological experiments for two reasons. Firstly, endogenous *Arc* expression in these mice is unperturbed. Secondly, the half-life of the d4EGFP reporter allowed us to visualize *Arc*-expressing cells in acute slices for several hours following behavior. *Arc*-d2EGFP knock-in/knock-out mice remain a helpful tool for exploring the *Arc*-dependence of various forms of neuronal plasticity. However, experiments involving these mice use *Arc*-positive controls that are haploinsufficient for *Arc* and limit targeted physiology experiments to shorter time windows.

Previous studies of AOB IGC function used pharmacology to approximate the conditions present during salient social events (Araneda and Firestein, 2006; Smith et al., 2009b; Taniguchi et al., 2013; Smith et al., 2015). These studies revealed important features of IGC neuromodulation, but did not investigate the cellular and synaptic changes that occur in IGCs activated by *bona fide* social behaviors. In *Arc-d4EGFP*-BAC mice, *Arc* expression in IGCs after resident-intruder encounters correlates with increased activation by sensory input (Fig. 4.1) and increased intrinsic excitability (Fig. 4.3). *Arc* expression has been associated with glutamate receptor trafficking in other contexts (Chowdhury et al., 2006; Shepherd et al.,

2006; Waung et al., 2008). However, our data show that the increased network excitability of *Arc*-expressing IGCs is not related to an increase in EPSC frequency or amplitude, nor is there evidence of significant upregulation in the number of dendritic spines (Fig. 4.2). These results were somewhat surprising in light of previous work showing increased size of the postsynaptic density on IGC dendrites in female mice one day after mating, suggesting increased excitatory drive on IGCs (Matsuoka et al., 2004). However, our experiments took place both in a different behavioral context and at an earlier time point, which could indicate that different mechanisms or time courses are present following male-male social encounters. It is also possible that increased excitatory drive occurs across all IGCs following a salient encounter, rather than *Arc*-expressing IGCs alone. If this were the case, we might expect to see synaptic changes following behavior compared to a no-behavior animal, but not between *Arc*-expressing and non-expressing IGCs. There is some evidence to suggest that this may be the case: concurrent with our study, another group investigated mechanisms of plasticity in the female AOB after mating using a similar approach (Gao et al., 2017). Like our study, they used *Arc* expression to identify IGCs that may be undergoing plasticity in the female AOB after mating. They found that mating did induce synaptic plasticity in the bulb: randomly selected IGCs showed increased sEPSC frequency compared to randomly selected IGCs from non-mated females. However, this effect was not seen specifically in *Arc*-expressing IGCs. Additionally, much like our study, they found that IGCs showed increases in intrinsic excitability after mating. The correlations between our findings further support the notion that this form of AOB plasticity occurs across social contexts as a general feature of the AOB circuit rather than only in specific behavioral situations.

IGCs do not receive direct excitation from VSN terminals in the AOB glomerular layer, but are instead activated by glutamate release from MCs at reciprocal dendro-dendritic synapses (Jia et al., 1999; Taniguchi and Kaba, 2001). We did not observe experience-dependent increases in intrinsic excitability in MCs following resident-intruder encounters, suggesting that the increased IGC activation is specific to the IGC postsynaptic response. However, it is also possible that a change in presynaptic function in the MCs providing input to *Arc*-expressing IGCs contributes to this effect. To approach this question will require tools that label both *Arc*-expressing IGCs and their connected MCs in living tissue.

In our investigation of the intrinsic differences between *Arc*-expressing and non-expressing cells, we employed methods aimed at objectively classifying cells based on the expression of 26 specific characteristics. *Arc*-expressing and non-expressing cells were segregated into clusters that differed in their capacity to sustain high frequency spiking (Fig. 4.3). While many studies of Arc-dependent plasticity focus on synaptic plasticity, some work has also addressed the association between *Arc* expression and changes in neuronal firing patterns. In motor cortex, motor training induces *Arc* expression as well as persistent firing patterns specifically in *Arc*-expressing neurons (Ren et al., 2014). This change in firing patterns is due to changes in NMDAR function, which is unexpected given Arc's well-known role in AMPAR trafficking (Ren et al., 2014). While we did not observe any macroscopic changes in sEPSC or mEPSC amplitude or frequency associated with increased excitability, it is possible that we missed subtle shifts in AMPAR or NMDAR currents, as we didn't assess the specific contributions of each.

The increase in excitability was not a result of changes to voltage gated sodium channel threshold, sodium current amplitudes, or macroscopic changes to voltage gated potassium currents. However, this analysis did reveal a trend for Arc-expressing IGCs to possess smaller I_H currents, which we confirmed pharmacologically (Fig. 4.3). HCN channel expression has been noted in the AOB, and in IGCs, but their specific role in AOB circuit function has not yet been determined (Hu et al., 2016). I_H is active at resting membrane potential and gives rise to rebound depolarization after relief from transient hyperpolarization (Robinson and Siegelbaum, 2003; Biel et al., 2009). At face value, the observed decrease in I_H is at odds with the increase in intrinsic excitability seen in *Arc*-expressing IGCs. However, several other studies have shown that plasticity-induced decreases in I_H are associated with increases in excitability (Poolos et al., 2002; Brager and Johnston, 2007; Campanac et al., 2008; Yi et al., 2016). Often, this is due to increases in input resistance that arise from downregulation of HCN channels, though our data didn't indicate an increase in input resistance in *Arc*-expressing IGCs (Brager and Johnston, 2007). This could be explained by dendrite-specific changes in input resistance, which we were unable to detect at the soma. Another possibility is the apparent excitatory influence of decreased I_H could be a shift in the voltage dependence of HCN channel activation, leading to an increased number of HCN channels open at rest. Overall, our results suggest that experience-dependent plasticity modulates IGC I_H currents, perhaps selectively in postsynaptic/dendritic structures (Lorincz et al., 2002; Yi et al., 2016).

To investigate the *Arc*-dependence of the excitability and I_H phenotypes, we also performed recordings from *Arc*-/- and *Arc*+/- mice. The increased excitability that we

observed in *Arc*-expressing cells in d4EGFP mice was not observed in *Arc-/-* mice from the *Arc*-d2EGFP strain. This suggests that *Arc* may participate in the intrinsic differences in AOB IGCs seen after resident-intruder encounters. However, when we performed the same experiment with *Arc+/-* mice, we didn't observe the same increased intrinsic excitability in d2EGFP+ IGCs. Similarly, the decreased I_H depolarization observed in *Arc*-expressing cells in the d4EGFP mice was not seen in *Arc-/-* mice. However, we did see a trend towards decreased I_H depolarization in d2EGFP+ cells in *Arc+/-* mice. This constellation of results is difficult to interpret. One possible explanation is that both endogenous copies of the *Arc* gene are required to mediate the effects we observed to their full extent. Thus, *Arc+/-* d2EGFP mice show some, but not all, of the effects we observed in Arc+/+ d4EGFP mice. Another possibility is that the shorter half-life of the d2EGFP reporter is not well-suited to the experimental timeline we previously established with the *Arc-d4EGFP*-BAC mice. Because we performed recordings during the 4-8 hours after behavior, the d4EGFP signal was well-aligned with this timeline, but the d2EGFP signal was less ideal – by this time point it would already be faded from some cells. This means we likely lumped some cells that should have been considered Arc+ into the d2EGFP- category. If this were true, we might expect that the mean spiking frequency for *Arc+/-* d2EGFP- cells would be higher than that of Arc+/+ d4EGFP- cells, due to the contribution of miscategorized *Arc*-expressing cells; it is worth noting that this is not the case (Fig. 4.3D, 4.5A). Overall, the difference in the half-lives of the GFP reporters makes it difficult to directly compare results from the *Arc-d4EGFP*-BAC mice and the *Arc*-d2EGFP mice. While these data suggest that Arc itself may be important

for the increased intrinsic capacity to respond to sensory input, further investigation will be required to determine the full extent of Arc's participation in the plastic effects we observed.

We confirmed that posterior MC activity is suppressed in AOB slices from resident mice following the resident-intruder assay (Fig. 4.7). This observation supports the hypothesis that experience-dependent upregulation of IGC excitability in *Arc*-expressing cells contributes to MC suppression. The effects were relatively modest, but were achieved despite lacking an experience-dependent marker to select for MCs that were active during the resident-intruder encounter. It is possible that this limitation precluded us from identifying other physiological changes in MCs that are induced following male-male social interaction.

The observed increases in IGC intrinsic excitability and MC suppression are present for at least 8 hours following behavior. This suggests that MC activation upon re-exposure to the same male during this time window would be decreased, which may result in a change in male-male social interactions. In the context of the Bruce Effect, pheromonal learning is AOB-dependent and can persist for many weeks (Brennan and Keverne, 1997). It may be the case that the AOS refines male-male social interactions over similar time courses, but the specific behavioral impacts and time courses of any effects remain to be elucidated. In sum, these data reveal that AOB experience-dependent plasticity involves *Arc* upregulation in IGCs, which results in increased MC inhibition through upregulation of IGC intrinsic excitability. Furthermore, our data show that inhibitory plasticity in the AOB occurs across social contexts and is a general feature of the AOS.

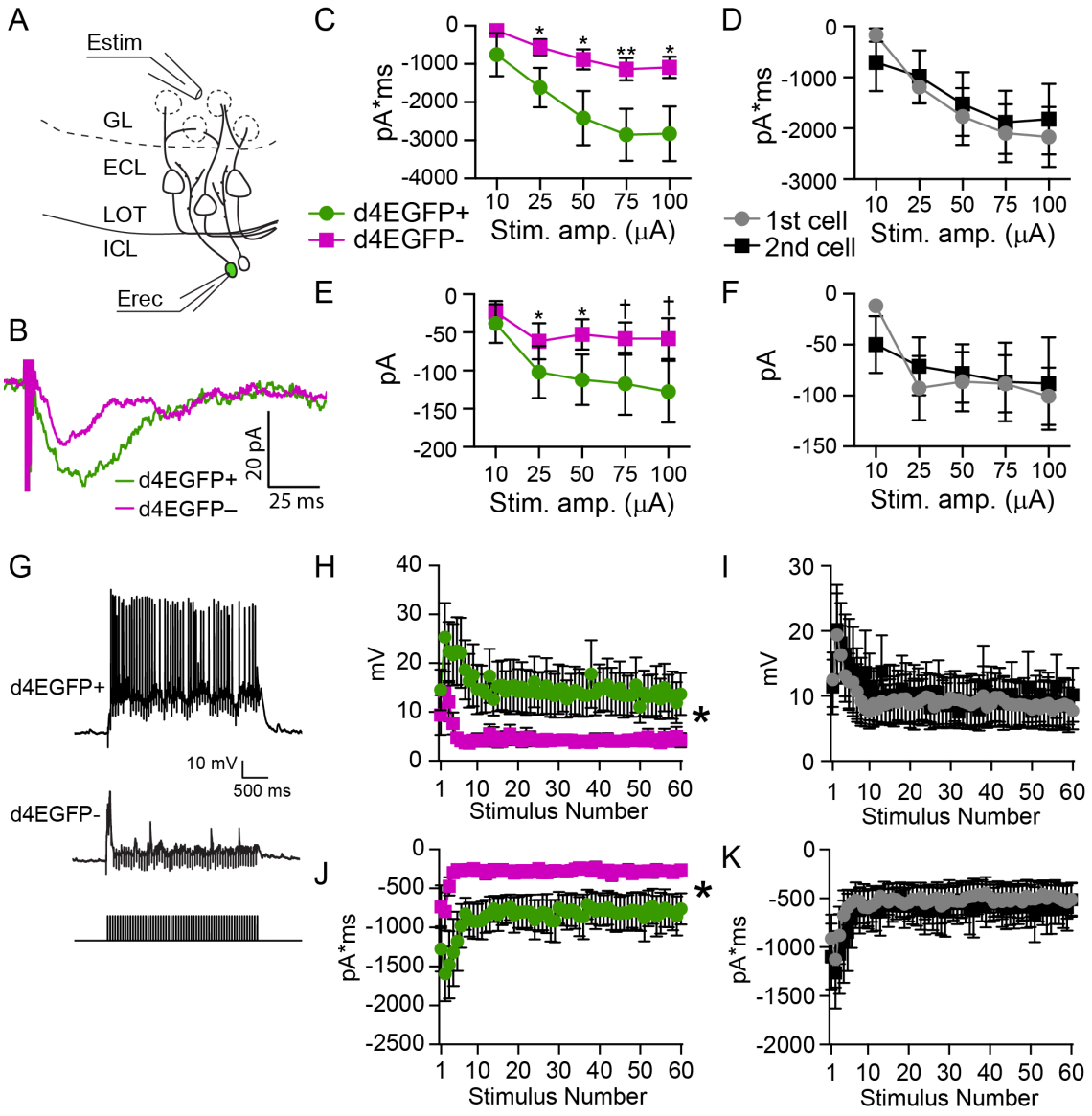

Figure 4.1 *Arc*-expressing IGCs show increased excitation by glomerular layer stimulation. ***A,*** Diagram illustrating experimental setup. Estim: theta glass stimulating electrode. Erec: recording electrode. ***B,*** Sample responses from a single, equal amplitude electrical stimulus from a d4EGFP+ cell and a nearby d4EGFP– cell from the same slice. ***C,*** Input-output curves showing charge transfer in response to a single stimulus pulse for d4EGFP+ and d4EGFP– cells. Paired, 2-tailed Student's *t*-test. * $p < 0.05$, ** $p < 0.01$. ***D,*** Same data from panel C,

grouped by the order in which the cells were recorded rather than d4EGFP expression. ***E,*** Input-output curves showing EPSC amplitude in response to a single pulse; data grouped by d4EGFP expression. Paired, 2-tailed Student's *t*-test. † $p<0.1$ * $p<0.05$. ***F,*** Same data from panel E, grouped by the order in which cells were recorded. ***G,*** Sample traces from d4EGFP+ and d4EGFP– IGCs responding to 3 s, 20 Hz stimulation. ***H,*** Peak amplitude reached in response to each pulse of a 3 s, 20 Hz stimulus train. Repeated measures ANOVA, main effect of group ($F(1,18)=4.51$, $p=0.048$). ***I,*** Same data from panel H, grouped by the recording order. Repeated measures ANOVA, no main effect of group ($F(1,18)=0.03$, $p=0.87$) ***J,*** Total charge transfer in response to each pulse of the 3 s, 20 Hz stimulus train. Repeated measures ANOVA, main effect of group ($F(1,18)=5.52$, $p=0.03$). ***K,*** Same data from panel J, grouped by recording order. Repeated measures ANOVA, no main effect of group ($F(1,18)=0.07$, $p=0.79$). For all panels n = 7 mice, 10 slices, 10 pairs.

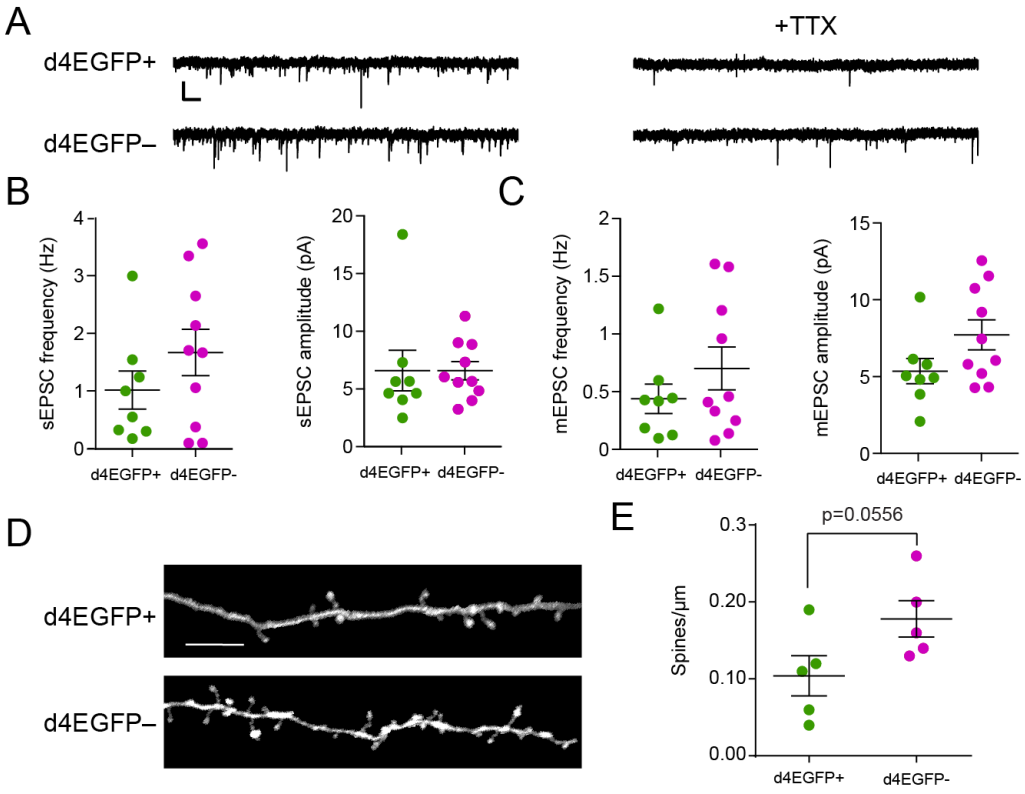

Figure 4.2 *Arc*-expressing IGCs do not display enhanced synaptic strength or number compared to non-expressing IGCs. ***A,*** Sample sEPSC and mEPSC traces from d4EGFP+ and d4EGFP– neurons. Scale bar: 10 pA, 500 ms. ***B,*** Spontaneous frequency and amplitude in d4EGFP+ IGCs. Significance determined using Wilcoxon-Mann-Whitney test (n.s., p>0.05). d4EGFP+ n=8, d4EGFP– n=10, n mice=10. ***C,*** Mini frequency and amplitude of d4EGFP+ and d4EGFP– IGCs. Significance determined using Wilcoxon-Mann-Whitney test (n.s., p>0.05). d4EGFP+ n=8, d4EGFP– n=10, n mice=10. ***D,*** Representative images showing dendritic spines on d4EGFP+ and d4EGFP– IGCs. Scale bar: 10 µm. ***E,*** Spines/um for d4EGFP+ and d4EGFP– neurons. Significance determined using Wilcoxon-Mann-Whitney test. n d4EGFP+ cells=5, n d4EGFP–cells=5, n mice=5.

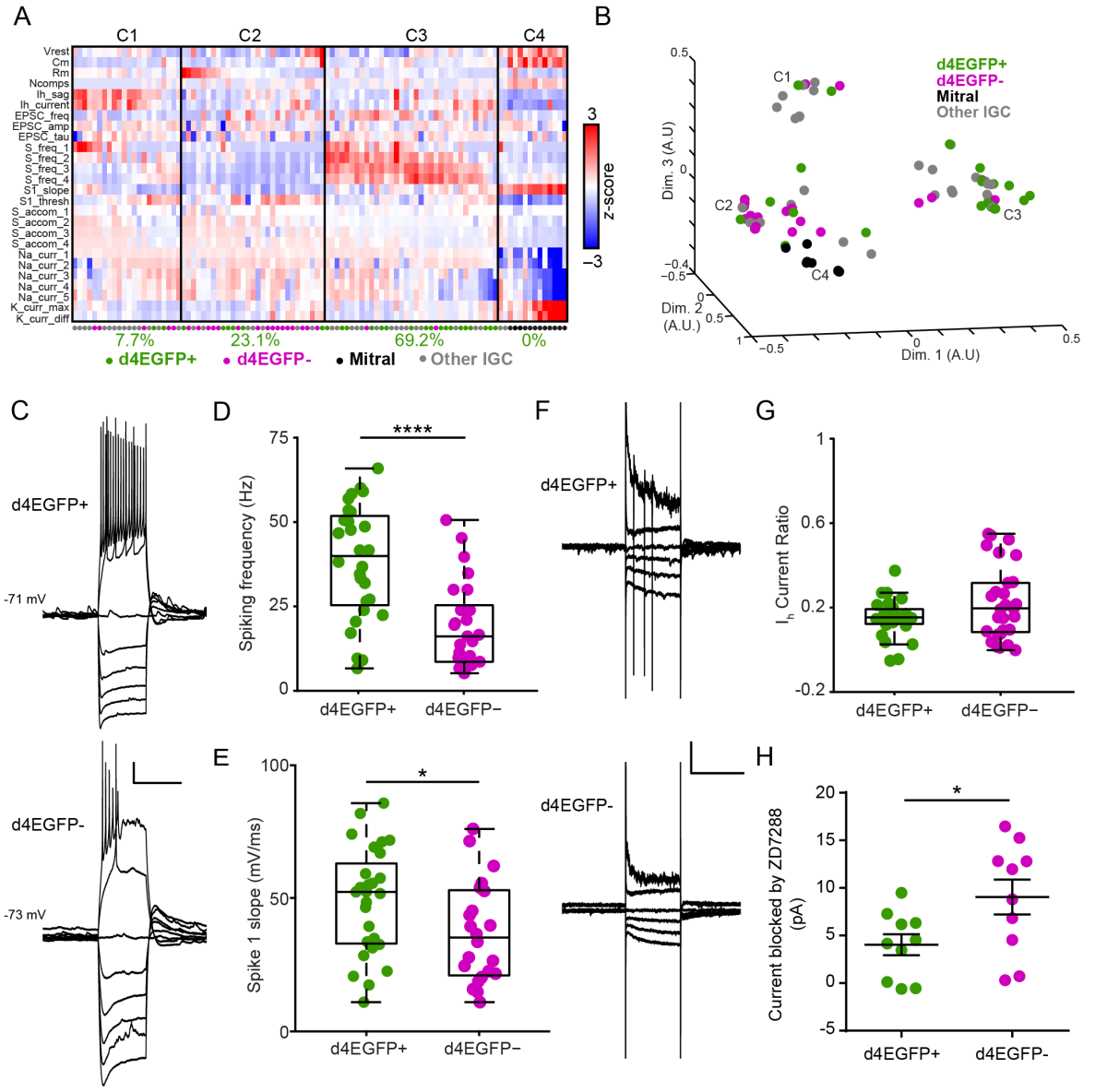

Figure 4.3 *Arc*-expressing IGCs are intrinsically more excitable than non-expressing IGCs. ***A,*** Colorized heat map representation of 26 intrinsic descriptors (rows) across 100 AOB neurons (columns) that were subjected to current- and voltage-clamp challenges. Solid vertical lines indicate divisions between identified clusters. Below each cluster is the percentage of all d4EGFP+ IGCs within that cluster. ***B,*** Multidimensional scaling of relative

differences across all 26 dimensions from (A) into 3 dimensions. Each individual colored point indicates a cell, and C1-C4 refer to the cluster definitions in (A). For A and B, d4EGFP+ IGC n=26, d4EGFP– IGC n=23, n animals=15, other IGC n=39, mitral n=12, n animals=37. ***C,*** Sample traces for d4EGFP+ and d4EGFP– IGCs for current clamp ramp challenges. Scale bar: 10 mV, 500 ms. ***D,*** d4EGFP+ IGCs exhibit significantly increased spiking frequency when depolarized by a current injection (d4EGFP+ n=26, d4EGFP– n=23, Wilcoxon-Mann-Whitney test, $p<0.0001$). ***E,*** d4EGFP+ and d4EGFP– IGCs demonstrate increased maximal action potential slope (d4EGFP+ n=26, d4EGFP– n=23, Wilcoxon-Mann-Whitney test, $p<0.05$). ***F,*** Sample traces for d4EGFP+ and d4EGFP- IGCs for voltage clamp ramp challenges. Traces displayed show responses to being held at -100, -90, -80, -70, -40, and -20 mV. Scale bar: 50 pA, 500 ms. ***G,*** I_H current ratio for d4EGFP+ and d4EGFP– cells (d4EGFP+ n=26, d4EGFP– n=23, Wilcoxon-Mann-Whitney test, $p=0.24$). ***H,*** I_H subtracted currents following 10 μM ZD7288 application for d4EGFP+ and d4EGFP– IGCs (d4EGFP+ cells n=10, d4EGFP–cells n=10, n mice=9, Wilcoxon-Mann-Whitney test, $p<0.05$).

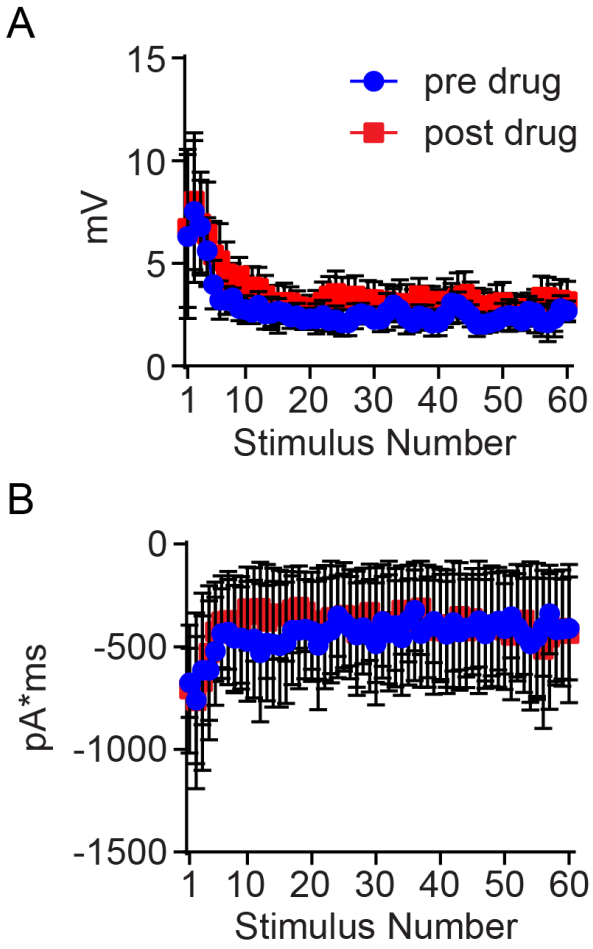

Figure 4.4 HCN channel blockade alone does not increase responsiveness of IGCs to glomerular stimulation. ***A,*** Peak amplitude reached in response to each pulse of a 3 s, 20 Hz stimulus train, pre- and post- application of 10 μM ZD7288. Repeated measures ANOVA, no main effect of group ($F(1,4)=0.3056$, $p=0.61$) n=5 cells, 2 mice. ***B,*** Total charge transfer in response to each pulse of the 3 s, 20 Hz stimulus train, pre- and post- application of 10 μM ZD7288. Repeated measures ANOVA, main effect of group ($F(1,8)=0.01072$, $p=0.92$) n= cells, 2 mice.

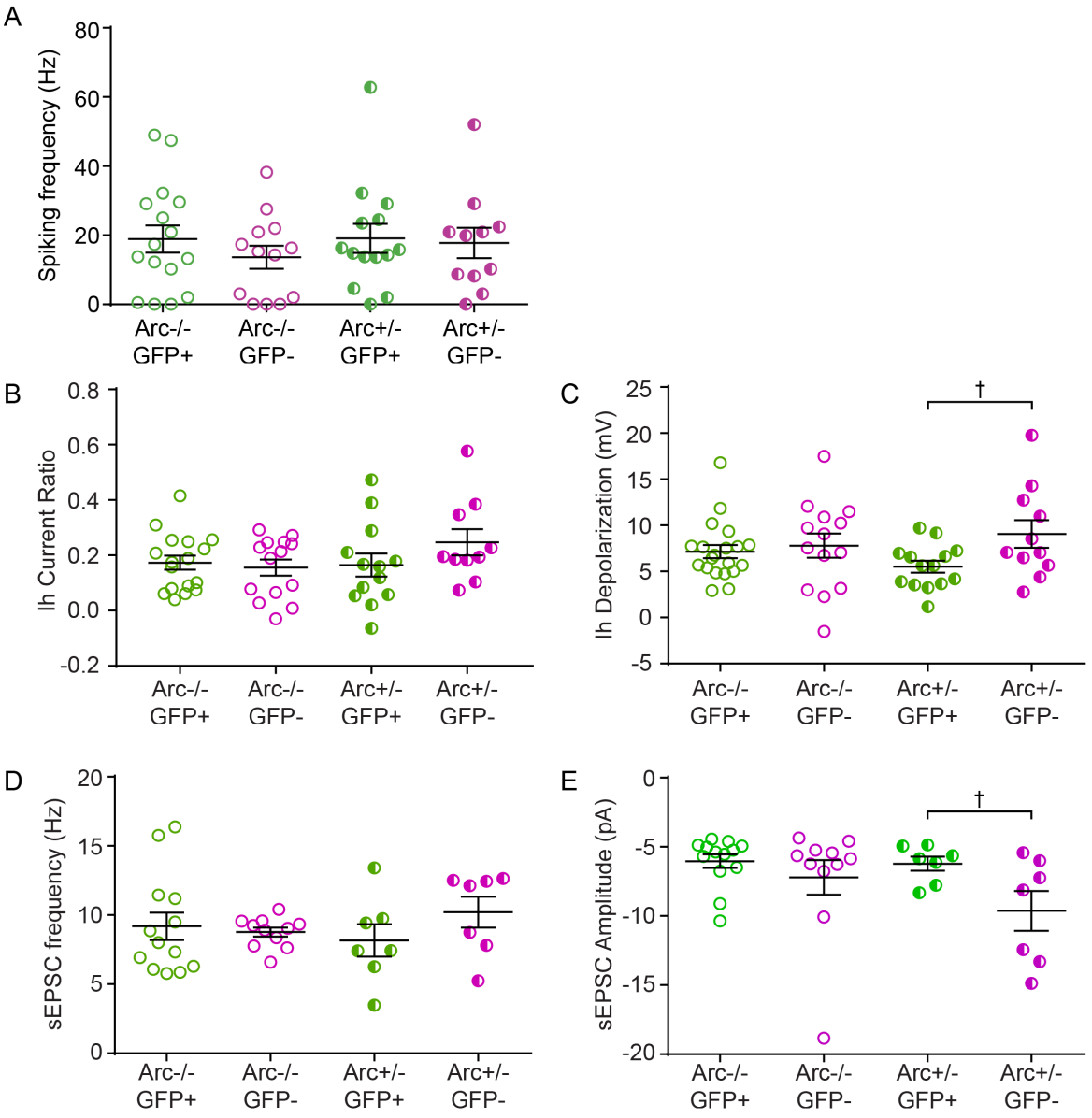

Figure 4.5 Spiking frequency and I_H phenotypes are not recapitulated in *Arc-/-* mice. ***A,*** No difference in spiking frequency was observed between d2EGFP+ and d2EGFP- IGCs in *Arc-/-* or *Arc+/-* mice (*Arc-/-*: d2EGFP+ n=16, d2EGFP- n=13, Wilcoxon-Mann-Whitney test, p=0.3; *Arc+/-*: d2EGFP+ n=14, d2EGFP- n=11, Wilcoxon-Mann-Whitney test, p=0.8). ***B,*** No difference in I_H current ratio was observed between d2EGFP+ and d2EGFP- IGCs in *Arc-*

/- or *Arc*+/- mice (*Arc*-/-: d2EGFP+ n=17, d2EGFP- n=14, Wilcoxon-Mann-Whitney test, p=0.8; *Arc*+/-: d2EGFP+ n=13, d2EGFP- n=10, Wilcoxon-Mann-Whitney test, p=0.13). ***C,*** No difference in I_H sag potential was observed between d2EGFP+ and d2EGFP- IGCs in *Arc*-/- or *Arc*+/- mice (*Arc*-/-: d2EGFP+ n=20, d2EGFP- n=14, Wilcoxon-Mann-Whitney test, p=0.45; *Arc*+/-: d2EGFP+ n=14, d2EGFP- n=11, Wilcoxon-Mann-Whitney test, p=0.0507). ***D,*** No difference in sEPSC frequency was observed between d2EGFP+ and d2EGFP- IGCs in *Arc*-/- or *Arc*+/- mice (*Arc*-/-: d2EGFP+ n=13, d2EGFP- n=11, Wilcoxon-Mann-Whitney test, p=0.57; *Arc*+/-: d2EGFP+ n=7, d2EGFP- n=7, Wilcoxon-Mann-Whitney test, p=0.32). ***E,*** No difference in sEPSC amplitude was observed between d2EGFP+ and d2EGFP- IGCs in *Arc*-/- or *Arc*+/- mice (*Arc*-/-*:* d2EGFP+ n=13, d2EGFP- n=11, Wilcoxon-Mann-Whitney test, p=0.5; *Arc*+/-: d2EGFP+ n=7, d2EGFP- n=7, Wilcoxon-Mann-Whitney test, p=0.0973).

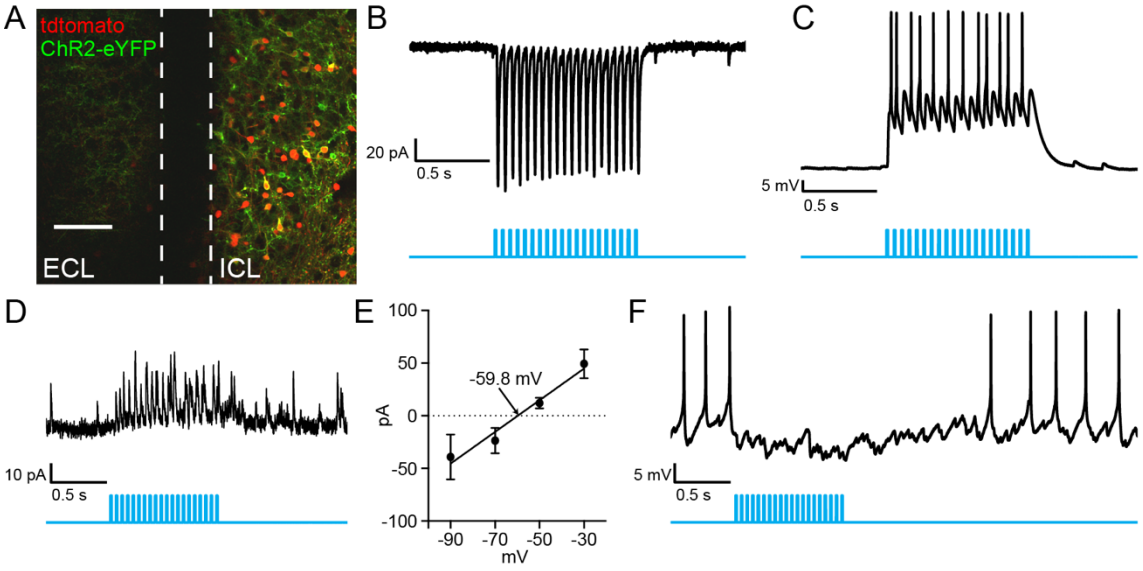

Figure. 4.6 *Arc*-expressing IGCs directly inhibit mitral cells. ***A,*** 2-photon image of an acute live slice illustrating Arc-Cre mediated expression of tdTomato (via the ROSA26 locus) and ChR2-GFP (via viral infection). ***B,*** 20 Hz blue light stimulation of Arc/ChR2-expressing IGCs leads to strong inward currents. ***C,*** IGC current clamp recording demonstrating light-induced action potentials. ***D,*** Mitral cell held at -50 mV during 20 Hz stimulation of Arc-expressing IGCs. ***E,*** I-V relationship between mitral cell holding potential and IGC induced currents. n=2 mice. ***F,*** Mitral cell at -35 mV fires spontaneous action potentials, which are inhibited by optical activation of Arc-expressing IGCs.

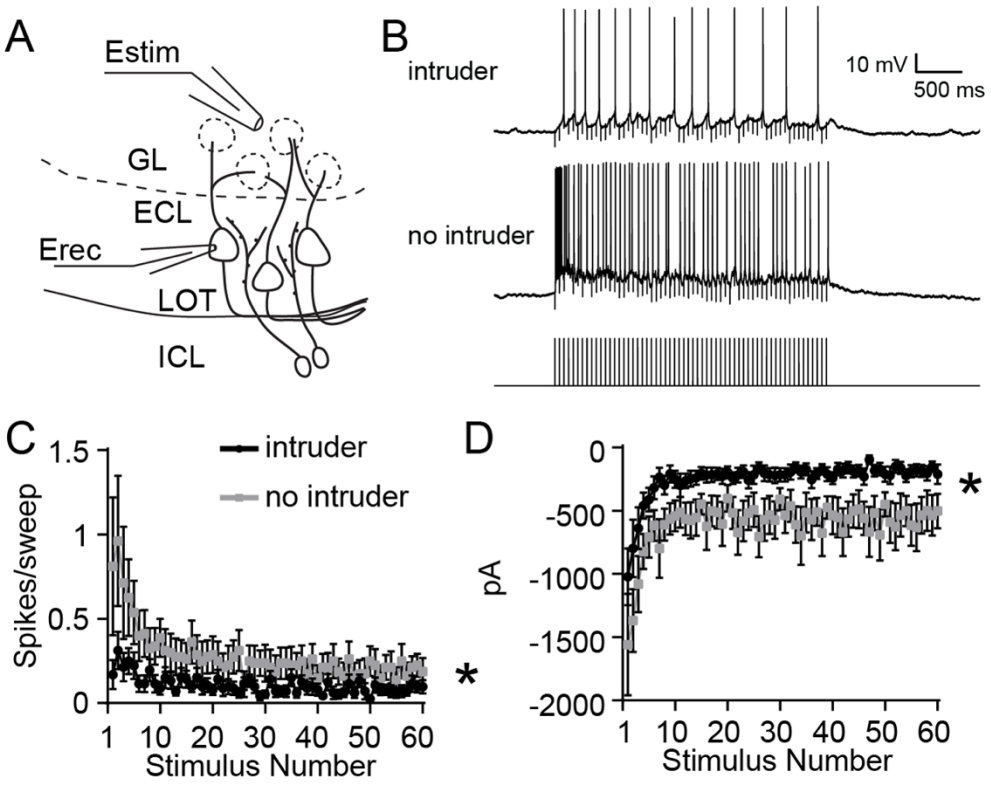

Figure 4.7 MCs show decreased excitation by glomerular stimulation following resident-intruder behavior. ***A,*** Diagram illustrating experimental setup. Estim: theta glass stimulating electrode. Erec: recording electrode. ***B,*** Sample MC responses to 3 s, 20 Hz GL stimulation from residents that interacted with an intruder and control residents (no intruder). ***C,*** Per-stimulus spike probability in response to each pulse of 3 s, 20 Hz stimulation while cell was artificially brought to the subthreshold potential of -55 mV. Repeated measures ANOVA, interaction between group and stimulus ($F(59,1298)=2.45$, $p<.0001$) Behavior: n cells=14, n mice=4. No behavior: n cells=10, n mice=4. ***D,*** Peak current amplitude in response to 3 s, 20 Hz stimulation while cell was held at -40 mV. Repeated measures ANOVA, main effect of group ($F(1,22)=8.49$, $p=0.008$). Behavior: n cells=13, n mice=4. No behavior: n cells=9, n mice=4.

Shorthand	Description	Mode	Method	Reference
Vrest	resting membrane potential	I Clamp	direct measurement	N/A
Cm	membrane capacitance			
Rm	input resistance			
Ncomps	number of model compartments	I Clamp	see reference	Golowasch, et al, 2009
Ih_sag	hyperpolarization-induced depolarizing potential	I Clamp	$I_{H,sag} = V_{init} - V_{ss}$	N/A
Ih_current	hyperpolarization-induced depolarizing current	V Clamp	$I_{H,curr} = I_{init} - I_{ss}$	N/A
EPSC_freq	mean spontaneous EPSC frequency	V Clamp	direct measurement after waveform sorting	
EPSC_amp	mean spontaneous EPSC amplitude	V Clamp		Hendrickson, et al, 2008
EPSC_tau	mean spontaneous EPSC decay constant	V Clamp	least-squares exponential decay	N/A
S_freq_1	Spiking frequency - Lv. 1	I Clamp	direct measurement	N/A
S_freq_2	Spiking frequency - Lv. 2	I Clamp	direct measurement	N/A
S_freq_3	Spiking frequency - Lv. 3	I Clamp	direct measurement	N/A
S_freq_4	Spiking frequency - Lv. 4	I Clamp	direct measurement	N/A
S1_slope	Initial action potential rising slope	I Clamp	initial spike derivative peak	
S1_thresh	Initial action potential threshold	I Clamp	Vm @ 10% of initial spike derivative	Meeks, et al, 2005
S_accom_1	Spike rate accomodation - Lv. 1	I Clamp		
S_accom_2	Spike rate accomodation - Lv. 2	I Clamp	$\frac{S_{init} - S_{final}}{S_{init} + S_{final}}$	
S_accom_3	Spike rate accomodation - Lv. 3	I Clamp		
S_accom_4	Spike rate accomodation - Lv. 4	I Clamp		N/A
Na_curr_1	Voltage-gated sodium current amplitude - Lv. 1	V Clamp	direct measurement	N/A
Na_curr_2	Voltage-gated sodium current amplitude - Lv. 2	V Clamp	direct measurement	N/A
Na_curr_3	Voltage-gated sodium current amplitude - Lv. 3	V Clamp	direct measurement	N/A
Na_curr_4	Voltage-gated sodium current amplitude - Lv. 4	V Clamp	direct measurement	N/A
Na_curr_5	Voltage-gated sodium current amplitude - Lv. 5	V Clamp	direct measurement	N/A
K_curr_max	Voltage-gated potassium current - maximum	V Clamp	direct measurement	N/A
K_curr_diff	Non-inactivating voltage-gated potassium current	V Clamp	direct measurement	N/A

Table 2. Parameters used for multidimensional analysis of intrinsic features.

CHAPTER FIVE
Potential role for AOB plasticity in male-male social behavior

Background

So far, we have shown that a specific population of AOB IGCs upregulate *Arc* in response to resident-intruder behavior. These IGCs undergo plasticity resulting in increased intrinsic excitability, and thus increased inhibition of MCs. One large remaining question is: what does this olfactory memory mean for the mouse's future behavior? The most similar phenomenon to this olfactory memory is the Bruce effect in female rodents. In this context, females learn the specific odor of her mate, and are able to distinguish between her mate's scent and that of other males. When she smells her mate, her pregnancy is maintained, but when she smells the scent of a different male, a physiological response is induced which results in termination of her pregnancy (Brennan, 2009). Thus, this memory confers an ability for her to distinguish between individuals. With our work and that of Gao et al., it seems that similar memory formation processes may occur following male-male social interaction and female-male mating. For example, in both contexts, *Arc* expression occurs in IGCs on a similar time course, and changes to IGC excitability are observed. Therefore, we might hypothesize that other aspects of these phenomena are similar as well; perhaps the resident male is learning to recognize the individual with whom he has fought, and would be able to distinguish between two different males in the future.

If the plasticity we have studied aids in individual recognition, we might expect different populations of IGCs to be activated by different individuals. If this is true, it would confirm that these IGC populations have the capacity to confer individual recognition in the

AOB. But how much of a role does this olfactory memory play in the resident's future behavior? We already know that mice will typically engage in less olfactory investigation with a familiar animal, compared to a novel animal, but it is unclear whether this finding holds up when the animals become familiar with each other in an aggressive context. Here we explore transgenic, behavioral, and physiological tools that will allow us to determine the importance of olfactory memory in the AOB in social memory and individual recognition. Our primary purpose was to develop behavioral paradigms that assess social recognition, which may be used in the future alongside perturbations of *Arc*-expressing IGCs to determine the importance of first-order sensory processing in social memory.

Specific materials and methods

Repeated resident-intruder with triple transgenic mice

The resident-intruder paradigm was used as described in chapter 2. The resident mice were ArcCreER+/- x Ai9+/- *Arc-d4EGFP*-BAC+. The intruder mice (male BALB/cJ) were socially housed prior to the first encounter. Repeated encounters were conducted with the same intruder mouse on consecutive days. Following the first encounter, the intruder mice were solo-housed (rather than ear-tagged) for identification purposes. For some experiments, a novel male of the DBA/2J strain was used on the final day.

Repeated resident-intruder with cohousing

On day 1, a C57BL/6J female "intruder" was introduced to the resident's home cage for 10 minutes (Fig 5.3A). This female intruder was ovariectomized and was given β-

estradiol 48 hours prior to behavior, as described below. On day 2, an adult male BALB/cJ intruder was introduced to the resident's home cage for 10 minutes. Then, on the morning of day 3, the same BALB/cJ intruder from day 2 was introduced into the resident's home cage for a brief cohousing period. On the evening of day 4, the BALB/cJ intruder was removed from the resident's cage. Then, on day 5, the resident-intruder assay was repeated using the same BALB/cJ intruder. Behavior was scored for both day 2 and day 5 to assess differences following the cohousing period.

Social novelty test

A modified social novelty test was used to assess familiarity with another male mouse. The paradigm is outlined in Fig. 5.4A. Resident mice were first exposed to a C57BL/6J female for a 10-minute encounter on day 1. These females were ovariectomized and had received an injection of β-estradiol 48 hours prior to the encounter in order to simulate estrus, as described below. Residents were then exposed to the same BALB/cJ male intruder for three consecutive days (days 2-4) or 10 minutes each. Depending on the experiment, [residents] may have been given an additional 30 minutes to interact with the intruder on day 3. On day 5, the social novelty test was used to assess interaction with the familiar intruder and a novel male of a different strain. This test was carried out in a 61 cm x 44.5 cm x 23 cm plexiglass box divided into three equally sized chambers. The center chamber was empty while the left and right chambers each held a mesh pencil cup containing a mouse (either the familiar or novel mouse). This mesh cup had openings large enough to allow the mice to physically touch each other, but small enough to prevent escaping the cup. Residents

were given 10 minutes to habituate to the center chamber, 10 minutes to habituate to the whole arena (including empty cups), and 10 minutes to explore while the cups contained the mice. The side of the arena containing the novel mouse was alternated to balance any potential side bias. Cup mice were habituated to the cups for 20 minutes each on the 3 consecutive days (one hour total) before the social novelty test. Time in each chamber was scored, as well as time interacting with each cup.

β-estradiol administration

β-estradiol was dissolved in ethanol at 1mg/mL and stored at -20° C until use. 10 uL of 1 mg/mL β-estradiol in ethanol was then mixed with 10 mL corn oil to make a 0.001 mg/mL solution. 100 ng β-estradiol was then administered subcutaneously by injecting 100 uL corn oil.

Stereotaxic injections

Two double-transgenic adult males heterozygous for *Arc-CreERT2* a were injected bilaterally (as described in chapter 2) with 300 nL of AAV5-EF1a-DIO-hM4D(i) (titer 1 x 10^{12} – 1 x 10^{13} GC/mL; Mattis et al., 2011).

DREADD inactivation of IGCs

To test the usefulness of $hM4D_i$-DREADDs in acute live slices, ACSF contained, in μM: 2.5 Gabazine, 10 AP5, 1 NBQX to block baseline synaptic activity. This way, changes in the resting membrane potential of patched IGCs could not be attributed to network effects

of CNO application. Then, CNO was applied at 10 μM. Baseline activity was recorded throughout the duration of wash-in.

Results

Arc is expressed in the same IGCs upon re-exposure to the same intruder animal

To further investigate whether *Arc*-expressing IGCs are activated in an input-specific manner, we decided to test whether different strains of mice (with different odor-profiles) would activate different populations of IGCs. To accomplish this, we crossed ArcCreER x Ai9 mice with *Arc-d4EGFP*-BAC mice to make "triple transgenic" animals. This genetic strategy permitted permanent labeling of Arc-expressing IGCs on day 1, via CreER recombination and tdTomato expression, and transient labeling of Arc-expressing neurons on day 4, via the *Arc-d4EGFP*-BAC transgene. On day 1, we exposed triple transgenic residents to a novel male BALB/cJ intruder 20 minutes after an injection of 4-OHT (Fig. 5.1A). On days 2-4, the resident was exposed to the same BALB/cJ intruder in the resident-intruder paradigm (Fig. 5.1A). On day 4, 3 hours after behavior was complete, we prepared acute live slices and imaged the AOB under 2-photon microscopy (Fig. 5.1B-C). As expected, we found that IGCs activated on the first day (labeled with tdTomato) largely overlapped with IGCs from the fourth day (labeled with d4EGFP) (Fig. 5.1C). This result was expected; if these IGCs are activated in an input-specific manner, it follows that two sensory experiences with the same intruder would activate the same population of neurons.

Arc is expressed in the same IGCs upon exposure to two novel males of different laboratory strains

We hypothesized that different laboratory strains, which have different MHC peptides and MUP profiles, would activate different populations of IGCs (Leinders-Zufall et al., 2004; Kaur et al., 2014). To investigate this, we repeated the same experiment described above, but introduced a novel male of the DBA/2J strain on the fourth day. Surprisingly we found that IGCs activated by the BALB/cJ male on day 1 (labeled with tdTomato) largely overlapped with those activated by the DBA/2J mouse (labeled with d4EGFP), closely mirroring the result from the previous experiment (Fig. 5.1C). This result could indicate 1) that the BALB/cJ and DBA/2J strains are not sufficiently divergent in their odor profiles to activate distinct populations of IGCs, 2) that our tools are insufficient to demonstrate subtle differences in IGC activation during these two encounters, or 3) *Arc*-expressing IGCs are not activated in an input-specific manner, but are instead bulk-activated in response to a salient encounter.

Option three seems unlikely, given that previous experiments showed that loss of *Trpc2* results in no *Arc* expression in IGCs, suggesting it is not due to centrifugal neuromodulatory inputs activated during a particular behavioral state. A strong possibility is that our tools are not robust enough. We have observed that the *d4EGFP* signal in the *Arc-d4EGFP*-BAC line has gotten significantly dimmer through the generations. Therefore, it is possible that we are only able to (barely) visualize the very brightest d4EGFP+ cells in these experiments, while the tdTomato labeled cells are brighter and more numerous. In this case, it would make sense that any d4EGFP+ cell has a high likelihood of colocalizing with a

tdTomato cell. This does not exclude the possibility that males from the BALB/cJ and DBA/2J strains are not significantly different in their odor profiles. BALB/cJ and DBA/2J strains are both from the Castle lineage of laboratory strains, and thus may not differ significantly in their MUP or MHC repertoires, which may result in strongly overlapping populations of *Arc*-expressing IGCs (Cheetham et al., 2009). We could further investigate this possibility by testing additional laboratory strains, genetically diverse wild mice, or females.

Arc is expressed in largely non-overlapping IGCs following exposure to males and females of the same laboratory strain

If *Arc*-expressing IGCs are activated in an input-specific manner, we would expect that two significantly different stimuli would induce *Arc* expression in distinct populations of IGCs. To test this idea in a more extreme way than we had done previously, we exposed a triple transgenic resident to a BALB/cJ male on days 1-3, but then introduced a BALB/cJ female on the fourth day prior to imaging (Fig. 5.1B). We found that exposure to a BALB/cJ male and BALB/cJ female activated largely distinct populations of IGCs, which was particularly noticeable in the anterior AOB (Fig. 5.1C). These results provide further evidence that IGCs are induced to express *Arc* in an input-specific manner, rather than being the result of bulk-activation during a behavioral stimulus. Additionally, this population of female-activated *Arc*-expressing IGCs could be used as a control population in future perturbation experiments; perturbing these specific IGCs should not interfere with the resident's memory of a male.

Assessing familiarity in the repeated resident-intruder paradigm

The behavioral paradigm used in the previous experiment (Fig. 5.1A) permitted analysis of behavior across repeated resident-intruder encounters (Fig. 5.2A). Behavior videos from each day were scored using a pre-determined behavior ethogram containing aggressive, defensive, and olfactory behaviors (Table 1). Previous literature indicates that as a mouse becomes more familiar with another mouse, he will engage in less olfactory investigation towards that mouse (Kogan et al., 2000; Hitti and Siegelbaum, 2014). In our hands, with this cohort of mice, we found that this wasn't the case. When we examined total olfactory duration through the full 10-minute encounter, we saw a slight (though statistically insignificant) decline in olfactory investigation across repeated encounters for residents exposed to the same BALB/cJ intruder over 4 days (Fig. 5.2B). Surprising, among the residents exposed to the same BALB/cJ intruder over the first 3 days, this pattern was not replicated, and they instead increased their investigation on days 2 and 3 (Fig. 5.2B). Upon introduction of the novel DBA/2J intruder on day 4, they decreased their investigation back down to what was previously observed on day 1 (Fig. 4.2B). Because of the large variance in behavior in these types of assays, it is common to look specifically at behavior during a brief time window at the beginning of the assay. We looked at olfactory investigation during the first 30 (Fig. 5.2C) and 60 (Fig. 5.2D) seconds of each resident-intruder encounter. While this analysis did not reveal a significant decline in olfactory investigation among resident exposed to the same BALB/cJ intruder for 4 days, it did show increased investigation on day 4 for animals exposed to a novel DBA/2J intruder (Fig. 5.2C-D). We also examined olfactory investigation by the resident over the course of the 10-minute encounter by looking at total

olfactory investigation in 1-minute bins (Fig. 5.2E) and cumulative olfactory investigation (Fig. 5.2F). Combining both groups of mice for day 1 of investigation revealed that resident mice investigate most intensely during the first two minutes of the encounter, declining as the 10-minute period elapses (Fig. 5.2E-F, purple trace). Qualitatively, this same pattern of investigation was replicated by the animals exposed to a novel male on day 4 (Fig. 5.2E-F, blue trace), indicating that this behavior pattern may occur each time the resident is exposed to a novel male. In support of this, the same behavioral pattern is not replicated among the residents exposed to the same familiar intruder on day 4 (Fig. 5.2E-F, red trace), indicating that the time course of olfactory investigation changes when the intruder is familiar.

While simple measurements of olfactory duration across repeated exposures is often used to assess social familiarity, we were unable to robustly replicate these findings in our hands (Fig. 5.2B-D). This could be due to our relatively small sample size (n=5 in each group) or our use of triple transgenic mice, which are heterozygous for *Arc*. If the problem is heterozygous expression of *Arc,* this issue needs to be addressed, as future experiments involving manipulation of *Arc*-expressing IGCs will require use of ArcCreER+/- animals (which are heterozygous for *Arc*). One potential strategy, as demonstrated in Fig. 5.2E-F, is to analyze patterns of olfactory investigation over time, rather than at static time points. Still, high variance, as well as a labor- and time-intensive behavioral scoring process, motivated us to develop additional strategies for reliably assessing social memory.

Cohousing the resident and intruder decreases olfactory investigation time during the second encounter

We hypothesized that 4 10-minute encounters over 4 days was not enough exposure for the resident to treat the intruder as familiar, and that more extended exposure to the intruder might reduce the variance in olfactory investigation that we observed previously. To test this hypothesis, we first exposed C57BL/6J male residents to ovariectomized C57BL/6J female mice (given an injection of β-estradiol 48 hours prior to simulate estrus) (Fig. 5.3A). This was included in the paradigm so that in future experiments, we could "TRAP" female-activated IGCs as a negative control for perturbation experiments (Fig. 5.1C). Next, we exposed residents to a male BALB/cJ intruder in the resident-intruder assay. We then cohoused C57BL/6J male residents and their BALB/cJ male intruders for 2 days, before a second resident-intruder test. We scored behavior in each resident-intruder test as previously, and found that this paradigm was robust at producing decreased olfactory investigation in the second encounter. Olfactory investigation was significantly decreased in the second encounter, looking at the first 60 seconds (Fig. 5.3B) and the first 5 minutes (Fig. 5.3C-E) of each 10-minute encounter. Because the resident-intruder paradigm is primarily used to study aggressive behavior, we wondered whether the cohousing period might increase or decrease aggression. We found that some mice increased and others decreased their aggression during the second encounter, suggesting that the cohousing period had no clear, singular effect on future aggressive behaviors (Fig. 5.3F). Notably, the two mice who were most aggressive in the first encounter either killed, or were killed by, the intruder during the cohousing period (Fig. 5.3F). Interestingly, these two mice were also on the lower end for sniffing time in the

first encounter (Fig. 5.3B-C). The fact that 2 of 12 pairings ended with one animal being killed suggests that this paradigm may not be the best option for future use. However, the strong, statistically significant decrease in olfactory investigation suggest that this behavioral paradigm could be used to reliably and robustly measure familiarity in the future, potentially alongside opto- or chemogenetic perturbations.

Resident males can recognize familiar animals in the social novelty test

We also explored another behavioral strategy for assessing social memory: a modified social novelty test (Fig. 5.4). We used a familiarization protocol similar to what was used previously. The resident was briefly exposed to a female on day 1, then the same male on days 2-4 (Fig. 5.4A). On day 3, we gave the resident and intruder an additional 1 hour to interact with the intruder, in an attempt to provide more investigation time (as with cohousing, but with less opportunity for physical harm). On day 5, after a habituation period, residents were allowed to explore a three-chamber arena, in which one side held the familiar intruder under a cup (designed to permit physical contact), and the other side held a novel DBA/2J male under a cup. Based on previous results, we would expect that the resident mouse would spend more time investigating the novel mouse compared to the familiar mouse. Using this paradigm, we found that residents spent less time in the chamber containing the familiar male than the novel male (Fig. 5.4B-D). Similarly, the spent less time specifically investigating the cup containing the familiar mouse (Fig. 5.4E-G). These results suggest that this paradigm can be used as a robust readout of familiarity and social memory, and could thus be used in future experiments where *Arc*-expressing IGCs are perturbed.

While the extra hour of interaction time provided a greater opportunity for familiarization, it also resulted in several severely injured intruder mice. Therefore, we tweaked this paradigm by eliminating the extra hour of social interaction on day 3, to see whether the same results could be achieved without the injury to the intruders (Fig. 5.5A). To our great surprise, we found that our previous results were completely reversed (Fig. 5.5B-G). Residents spent significantly more time in the chamber containing the familiar mouse (Fig. 5.5B-D) and significantly more time investigating the cup containing the familiar mouse (Fig. 5.5E-G). Though the mechanisms of this behavioral switch are unknown, it is clear that the test mouse can distinguish between the familiar and novel animal. Therefore, this paradigm could still be used in the future to assess social memory, even though this effect is the opposite of what we originally expected. Additionally, future work could investigate the mechanism behind the behavioral switch that occurs here.

Arc-expressing IGCs can be manipulated in slices using opto- and chemogenetic strategies

The behavioral experiments described above lay the groundwork for future experiments in which we will assess the importance of specific populations of *Arc*-expressing IGCs for social memory. In order to accomplish this goal, we need to be able to manipulate these neurons *in vivo* using optogenetic or chemogenetic strategies. Using ArcCreER+/- mice, we can inject Cre-dependent viral vectors encoding opsins or DREADDS into the AOB. Then, we can pair a 4-OHT injection with a resident-intruder encounter to gain permanent access to *Arc*-expressing IGCs activated during that encounter, and manipulate those specific IGCs in the future (i.e. during the social novelty test). To test the feasibility of

this approach, we expressed ChR2 in *Arc*-expressing IGCs in the AOB. We found that ChR2 in expression in these IGCs can induce firing, and can silence MC activity (Fig. 4.6). Optogenetic strategies provide strong temporal precision and reversibility, but require implantation of an optical fiber and tethering during behavior. Therefore, we wanted to also test the feasibility of DREADDs for IGC manipulation. We injected a Cre-dependent AAV expressing a G_i-DREADD into the AOB of a male ArcCreER+/- resident, then induced recombination in *Arc*-expressing IGCs via 4-OHT injection just prior to the resident-intruder paradigm. Two weeks later, we prepared acute live slices and patched fluorescent IGCs (Fig. 5.6A). We found that washing on CNO resulted in strong hyperpolarization, and cessation of tonic firing, in the patched IGC (Fig. 5.6B). These results suggest that G_i-DREADDs can be used to take specific populations of *Arc*-expressing IGCs offline during a behavioral test. While this strategy affords less temporal specificity, and no reversibility, it allows the animals to move freely and avoids any damage that may arise from implantation of an optical fiber.

Aggressive behavior is altered in ArcKO mice

We have demonstrated that *Arc* expression in AOB IGCs is associated with an important function: plasticity. The experiments above outline ways that we could test the importance of this plasticity in social memory, but we also wondered whether Arc itself is required for normal behavior in the resident-intruder paradigm in the first place. To test this hypothesis, we used *Arc-/-* mice as residents in the resident-intruder paradigm and compared their behavior to Arc+/+ 1-week residents (which are aggressive) to Arc+/+ 1-night residents

(which are not aggressive). We found that *Arc-/-* mice show significantly decreased aggressive behavior compared to wild-type mice (Fig. 5.7A). This was not due to lack of olfactory investigation, as *Arc-/-* mice initiated the same number of sniffing bouts, and sniffed for the same amount of time (if not more) than the wild-type mice (Fig. 5.7B-C, E). In addition to decreased aggressive behavior, we also noticed a few other behavioral differences. *Arc-/-* mice approached the intruder less frequently (and therefore also "left" less often), and spent less time rearing against the walls of the cage (an exploratory behavior) (Fig. 5.7D-E). The *Arc-/-* mice also spent significantly more time in a defensive, crouched posture (Fig. 5.7E), suggesting they may experience more anxiety in this social context.

These results are somewhat difficult to interpret because the *Arc-/-* mice are embryonic, whole-brain knockouts, meaning that this effect on behavior could be due to the lack of Arc during development, or in a non-AOS brain region. Nevertheless, these results implicate *Arc* expression in a behavior that depends on a functioning accessory olfactory system.

Discussion

The work detailed in chapters 3 and 4 suggests that plasticity in the AOB occurs as a general feature of the circuit following salient social experiences. But what is the purpose of this olfactory memory for the mouse? After mating, females can recognize the individual with whom she mated, so it follows that a similar form of plasticity in males following aggression may result in an ability to recognize the individual with whom he fought. In females, this individual recognition is achieved by decreased downstream representation of

the learned odors of her mate, which is accomplished through increased inhibition of those signals in the AOB. This limited downstream activation prevents the initiation of a hormonal response that would otherwise lead to termination of her pregnancy. What might be the behavioral result of a similar process of synaptic plasticity in a male mouse? One possibility is that limiting downstream activation of the cues of a familiar male might lead to a decrease in the investigation of that male. Indeed, social recognition memory is often measured by investigation time, with lower investigation times indicating familiarity. To test the hypothesis that plasticity in the AOB is crucial for social recognition memory, we need a robust behavioral test for social recognition. Then, we can use that test alongside perturbations of specific groups of AOB IGCs to determine their importance in social recognition memory.

Many groups use repeated exposure paradigms to induce and assess familiarity. Typically, these paradigms result in decreased olfactory investigation over time. When we exposed residents to the same intruder over 4 days, we had difficulty reproducing these results and observed high behavioral variability (Fig. 5.2A-D). This may be due to a low number of animals, or could be a side effect of the fact that they have multiple transgenes. In the future, this simple repeated exposure paradigm might be tweaked to provide slightly more investigation on each day, or additional days of investigation, to try to increase the robustness of this effect and reduce variability. Additionally, it may be useful to analyze the progression of olfactory investigation over time, rather than at static time points, as it can provide a fuller, more dynamic view of investigation behavior (Fig. 5.2E-F).

We also tried a cohousing strategy (Fig. 5.3) which was very effective at reducing investigation time upon the second exposure, suggesting that utilization of this paradigm in the future could reduce variability, and increase interpretability of outcomes, while reducing the number of animals needed for each experiment. However, an unwanted side-effect of this strategy is that 2/12 pairings resulted in the death of either the resident or the intruder, suggesting this is not the best strategy for the welfare of the animals. One potential solution is cohousing with a divider, so that the animals can be exposed to each other's scents long-term without the ability to fight. Another possibility is attempting to reduce the aggression displayed by the resident by not solo-housing the residents for a week. As we, and others, have observed, not solo-housing residents results in decreased aggressive behavior in the resident-intruder test (Fig. 3.2F). This approach might include the added benefit of simplifying the research question: we would be left with the question of social familiarity without the complicating factor of aggression (which can vary widely from mouse to mouse). It is worth remembering, however, that all of our physiological studies of residents thus far have included territorial aggression as a stimulus. While we have shown that aggression is not necessary for Arc expression, it may still be required for the physiological phenotypes we observed.

While cohousing between two resident-intruder assays was effective at reducing investigation time, we were also interested in identifying behavioral tasks that could indicate familiarity while further reducing behavioral variability between animals. We decided to try a modified social novelty test, where a familiar and novel mouse are housed on either side of three-chamber box (Figs. 5.4-5.5). We hoped that this strategy would reduce behavioral

variability for a number of reasons. First, it provides a more simplified read-out of investigation, in the form of time in each chamber, and time interacting with each cup, rather than requiring quantification and analysis of complex behaviors. Second, the placement of the test mice under cups means that all investigations are initiated and terminated by the "resident," reducing the influence of each individual intruder's behavior. Finally, the availability of two "choices" – one novel and one familiar - may further amplify any disinterest in the familiar cup mouse, while before, the resident had no choice but to investigate the familiar intruder because there was no other option. We found that this behavioral strategy did indeed give us with a robust read-out of familiarity (the "residents" spent significantly less time investigating the familiar cup mouse), while also providing a greatly simplified scoring process.

During our initial trial of this paradigm, we intended to provide an extra hour of investigation on days 3 and 4 in order to increase total investigation time and more strongly induce familiarity (Fig. 5.4). After the first day of this, we found that the residents became extremely aggressive, and worried for the welfare of the intruder mice. Thus, the extra hour on day 4 was eliminated, and future cohorts did not receive the extra hour on day 3 (Fig. 5.5). To our great surprise, the loss of this extra hour of investigation not only eliminated the preference for the novel mouse, but resulted in a strong, statistically-significant preference for the familiar mouse (Fig. 5.5). The mechanisms behind this behavioral switch are unknown. It seems possible that the extra hour of interaction on day 3 may allow for a "defeat" (and subsequent decreased investigation) that cannot be achieved in 10-minute increments. Maybe the 10-minute increments, in which the animals are not allowed to fight

to "defeat," creates a drive in the resident to fully defeat the intruder, resulting in increased interaction in the social novelty test. Further experiments would need to be done to determine when and how this behavioral switch is flipped. In any case, it seems possible that either version of this behavioral paradigm could be used to assess familiarity while manipulating *Arc*-expressing IGCs *in vivo*, as both versions induce robust, statistically-significant outcomes. In fact, these different outcomes may be a feature rather than a bug; perhaps the olfactory memory we have identified in the AOB is only important either prior to or after defeat. If this were the case, we might find that manipulation of *Arc*-expressing IGCs would only affect outcomes in one or the other behavioral paradigm. While this behavioral paradigm may offer a viable strategy for assessing social memory, it is important to note that it remains to be seen whether the behavioral results we have obtained are AOS-dependent. The first step should be to repeat the experiments using *Trpc2*-/- mice to determine the importance of the AOS in this particular behavior.

Given Arc's role in synaptic plasticity and memory, it is not surprising that *Arc*-/- mice exhibit deficiencies in memory related behavioral tasks (Plath et al., 2006). If plasticity of *Arc*-expressing IGCs is important for olfactory memory and social recognition, we might expect that social recognition might be compromised in *Arc*-/- mice. While this question remains to be investigated, we did notice that *Arc*-/- mice behave differently in the resident-intruder paradigm compared with Arc+/+ mice (Fig. 5.7). Specifically, they exhibit less aggression, despite no difference in olfactory investigation, as well as decreased exploration and increased crouching, suggesting they may experience elevated anxiety in this test. While it is noteworthy that aggression in this task depends on a functioning AOS, we cannot

conclude that behavioral deficits of *Arc-/-* mice in this test are due to loss of Arc specifically in the AOB or other AOS circuits. To test this hypothesis, we would need to knock it out specifically in the AOB in an adult animal.

It is also possible that these results from *Arc-/-* mice may reveal a role for plasticity prior to the resident intruder test. In order to observe aggressive behavior, residents must be solo-housed for one week prior to the resident-intruder test (Fig. 5.7A). During this week, residents are deprived of any olfactory cues other than their own. In other sensory modalities, sensory deprivation leads to (Arc-dependent) homeostatic scaling (Wang et al., 2006; Jenks et al., 2017). This leads to enhanced responses when sensory input is restored. It is therefore possible that something similar may occur in the olfactory modality: sensory deprivation during the 1-week solo-housing period may lead to homeostatic downscaling, resulting in increased responses when a stimulus, the intruder, is introduced. If this were the case, the response would be blunted in both 1-night residents, and 1-week *Arc-/-* residents, which is what we observed (Fig. 5.7). This hypothesis could be tested further by introducing intruder-soiled bedding into the resident's cage during the solo-housing period. Then, the importance of Arc in this process could be determined by knocking out Arc specifically in the AOB in adulthood.

Ultimately, these behavioral studies lay the groundwork for future experiments that will determine the specific importance of plasticity in *Arc*-expressing IGCs for social memory. Here, we have outlined a number of behavioral strategies which will allow assessment of social recognition, and provide paradigms in which *Arc*-expressing IGCs can

be “TRAP-ed” and manipulated during behavior using optogenetic (Fig. 4.6) or chemogenetic (Fig. 5.6) strategies.

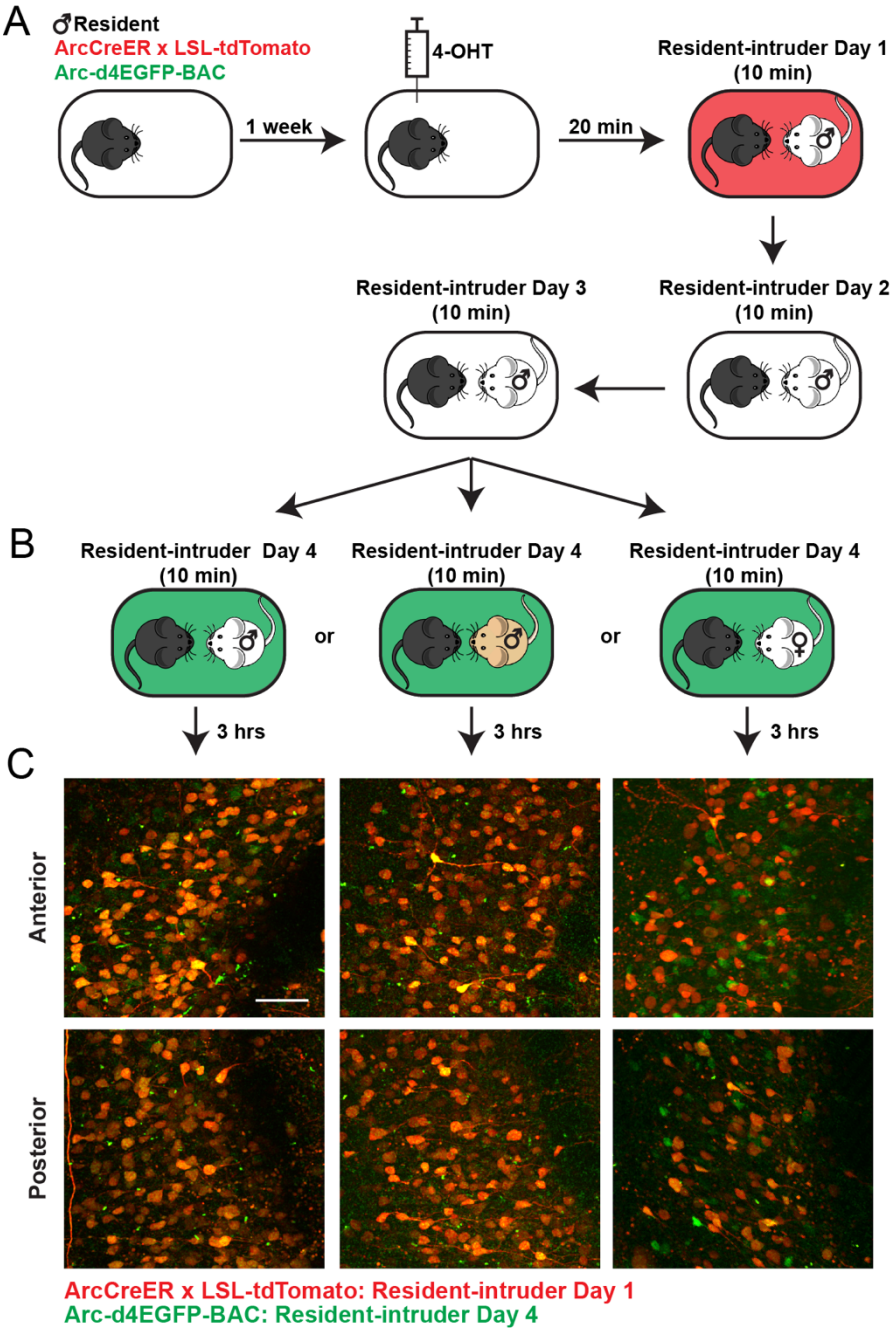

Figure 5.1 Visualizing *Arc* expression in response to two separate behavioral encounters. ***A,*** All residents were ArcCreER+/-, Ai9+/-, and *Arc-d4EGFP*-BAC+. This permitted permanent labeling of *Arc*-expressing IGCs with tdTomato by timing an injection of 4-

hydroxytamoxifen (4-OHT) with the resident-intruder paradigm, and transient labeling of *Arc*-expressing IGCs with d4EGP. Residents were solo-housed for one week, then given 4-OHT at 50 mg/kg 20 minutes before the resident-intruder paradigm. A novel male BALB/cJ intruder was used. The same male BALB/cJ intruder was used for subsequent encounters on days 2 and 3. ***B,*** On the fourth day, residents were exposed to either the same intruder, a novel male DBA/2J intruder, or a novel female BALB/cJ "intruder." ***C,*** Three hours later, acute live slices were prepared and AOB IGCs were imaged under 2 photon microscopy. Under these conditions, tdTomato signal indicates IGCs that were activated on day 1, while d4EGFP signal indicates IGCs that were activated on day 4. Scale bar 100 μm.

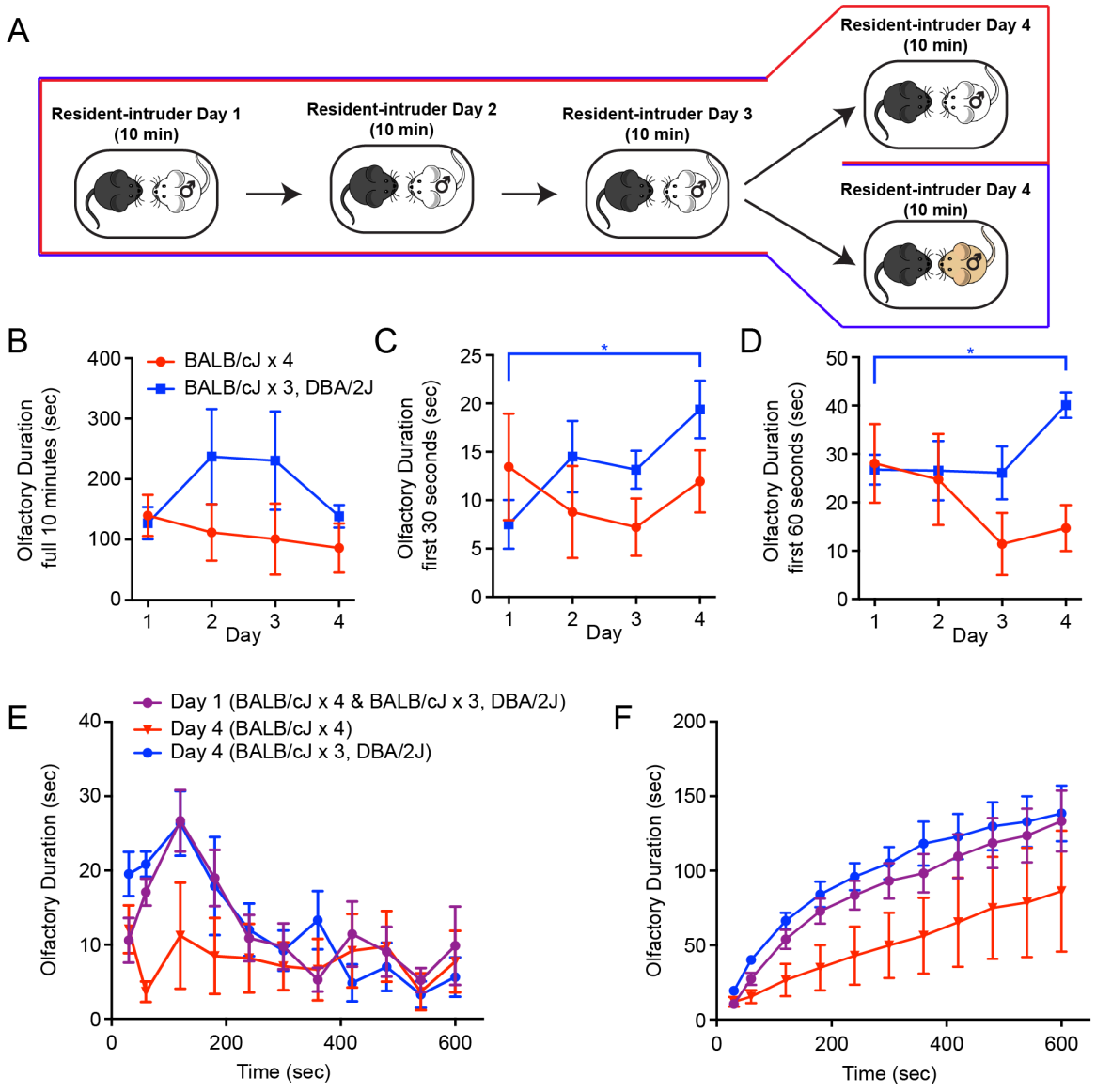

Figure 5.2 Measuring sniffing duration in repeated resident-intruder paradigms to assess familiarity. ***A***, Ten ArcCreER+/- Ai9+/- *Arc-d4EGFP*-BAC resident mice were subjected to four subsequent days in the resident-intruder paradigm. For the first 3 days, both groups saw the same BALB/cJ male intruder each day (red and blue box). On the fourth day, half of the residents saw the same intruder again (red box), and half saw a novel DBA/2J male intruder

(blue box). ***B,*** Olfactory duration for the entire encounter (10 minutes) on each day. Red: t-test between day 1 and 4, n.s.; blue: t-test between day 1 and 4, n.s. ***C,*** Olfactory duration for first 30 seconds of 10-minute encounter on each day. Red: t-test between day 1 and 4, n.s.; blue: t-test between day 1 and 4, p=0.016. ***D,*** Olfactory duration for first 60 seconds of each 10-minute encounter on each day. Red: t-test between day 1 and 4, n.s.; blue: t-test between day 1 and 4, p=0.011. ***E,*** Olfactory duration across the 10-minute encounter in 1 minute bins. Purple plot represents all 10 animals on day 1. Red plot represents the 5 residents who saw the familiar intruder on day 4. Blue plot represents the 5 residents who saw the novel intruder on day 4. ***F,*** Cumulative olfactory duration across 10-minute encounter. *$p<0.05$

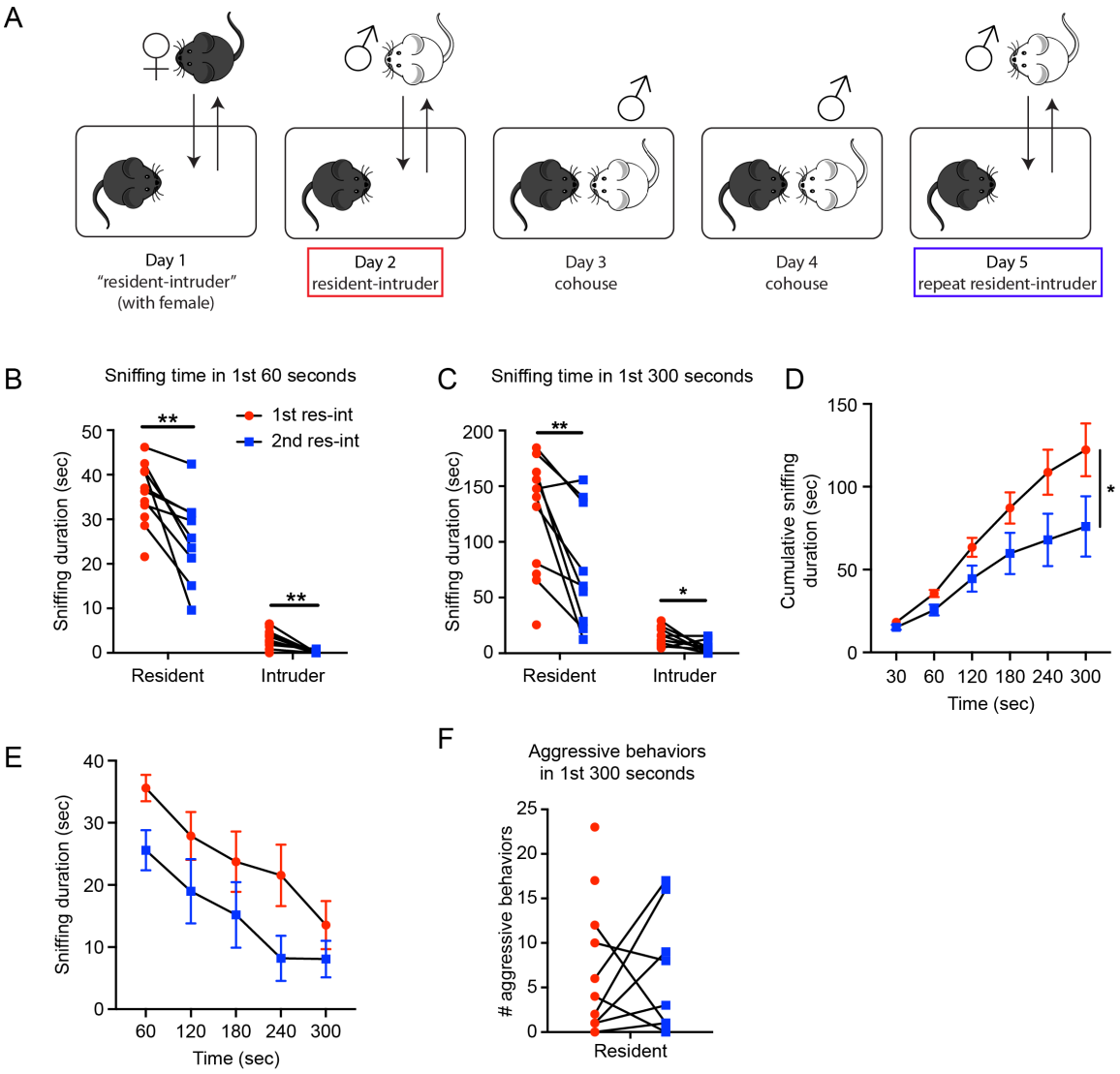

Figure 5.3 Cohousing the resident with the intruder for 2 days reduces olfactory investigation during the second resident-intruder encounter. ***A,*** Outline of the behavioral paradigm used. On day 1, an ovariectomized C57BL/6J female, injected with β-estradiol 48 hours prior, was introduced to the resident C57BL/6J male's home cage for 10 minutes. On day 2, a novel male BALB/cJ intruder was introduced to the resident's home cage for 10 minutes. On the morning of day 3, the same BALB/cJ intruder was placed in the resident's

cage for a brief cohousing period. On the evening of day 4, the BALB/cJ intruder was removed. On day 5, the same BALB/cJ intruder was introduced to the resident's cage for a 10-minute encounter. Behavior videos were scored for days 2 and 5. ***B,*** Sniffing time in first 60 seconds of the 10-minute encounter on days 2 and 5 for both the resident and the intruder. Both residents and intruders sniffed significantly less on the second encounter. Residents: paired two-tailed t-test, p=0.0039; Intruders: paired two-tailed t-test, p=0.0042. ***C,*** Sniffing time in first 5 minutes of 10-minute encounter on days 2 and 5 for both the resident and the intruder. Both residents and intruders sniffed significantly less on the second encounter. Residents: paired two-tailed t-test, p=0.0046; Intruders: paired two-tailed t-test, p=0.027. ***D,*** Cumulative sniffing duration for residents only during first 5 minutes of 10-minute encounter on days 2 and 5. Repeated measures ANOVA, interaction between group and time, $F(5,90)=3.115$, $p=0.012$. ***E,*** Sniffing duration in 1-minute bins through first 5 minutes of 10-minute encounter. Repeated measures ANOVA, no interaction between group and time, $F(4, 72)= 0.5819$, $p=0.68$. ***F,*** Number of aggressive behaviors displayed by the resident during the first 5 minutes of each 10-minute encounter. Paired two-tailed t-test, $p=0.44$. *$p<0.05$ **$p<0.01$

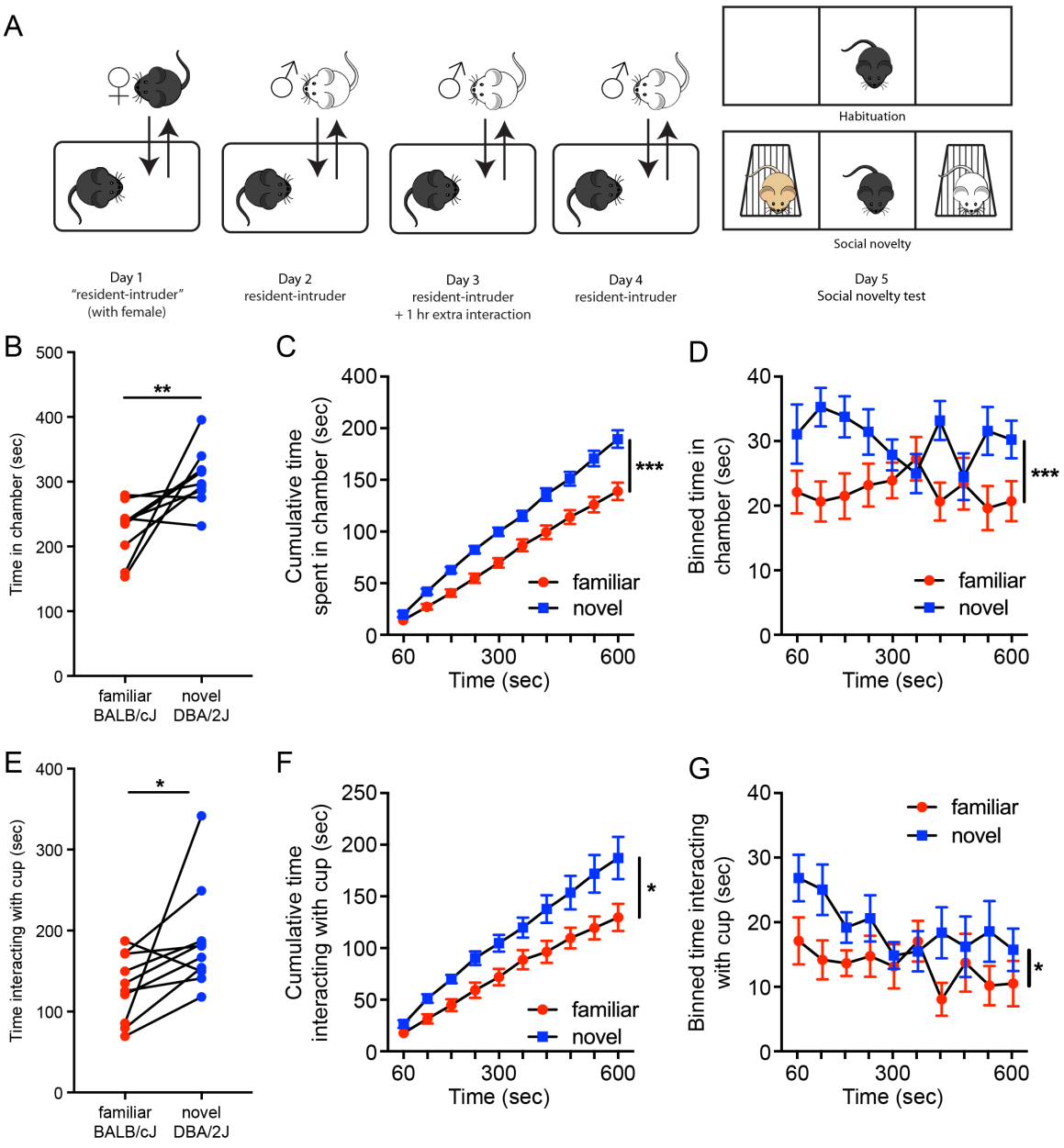

Figure 5.4 A modified social novelty test can be used to assess familiarity. ***A,*** Outline of behavioral paradigm used. On day 1, an ovariectomized C57BL/6J female, injected with β-estradiol 48 hours prior, was introduced to the resident C57BL/6J male's home cage for 10 minutes. On day 2, a novel male BALB/cJ intruder was introduced to the resident's home

cage for a 10-minute encounter. On day 3, the same BALB/cJ intruder was again introduced for a 10-minute encounter, then stayed in the cage for an additional hour before being removed. On day 4, the same BALB/cJ intruder was introduced for a final 10-minute encounter. On day 5 the social novelty test was conducted: after being allowed to habituate to the arena, the resident mouse was allowed 10 minutes to explore the 3-chamber arena in which one side housed the familiar BALB/cJ intruder under a mesh cup, while the other side housed a novel DBA/2J male under a mesh cup. ***B,*** Time each resident spent in each chamber. Paired two-tailed t-test, $p=0.01$. ***C,*** Cumulative time the residents spent in each chamber. Repeated measures ANOVA, main effect of chamber, $F(1,18)=20.44$, $p=0.0003$. ***D,*** Time the residents spent in each chamber, in 1-minute bins. Repeated measures ANOVA, main effect of chamber, $F(1,18)=17.86$, $p=0.0005$. ***E,*** Time each resident spent interacting with each cup. Paired two-tailed t-test, $p=0.043$. ***F,*** Cumulative time the residents spent interacting with each cup. Repeated measures ANOVA, main effect of chamber, $F(1,19)=7.819$, $p=0.012$. ***G,*** Time the residents spent interacting with each cup, in 1-minute bins. Repeated measures ANOVA, main effect of chamber, $F(1,18)=5.849$, $p=0.026$. *$p<0.05$ **$p<0.01$ ***$p<0.001$

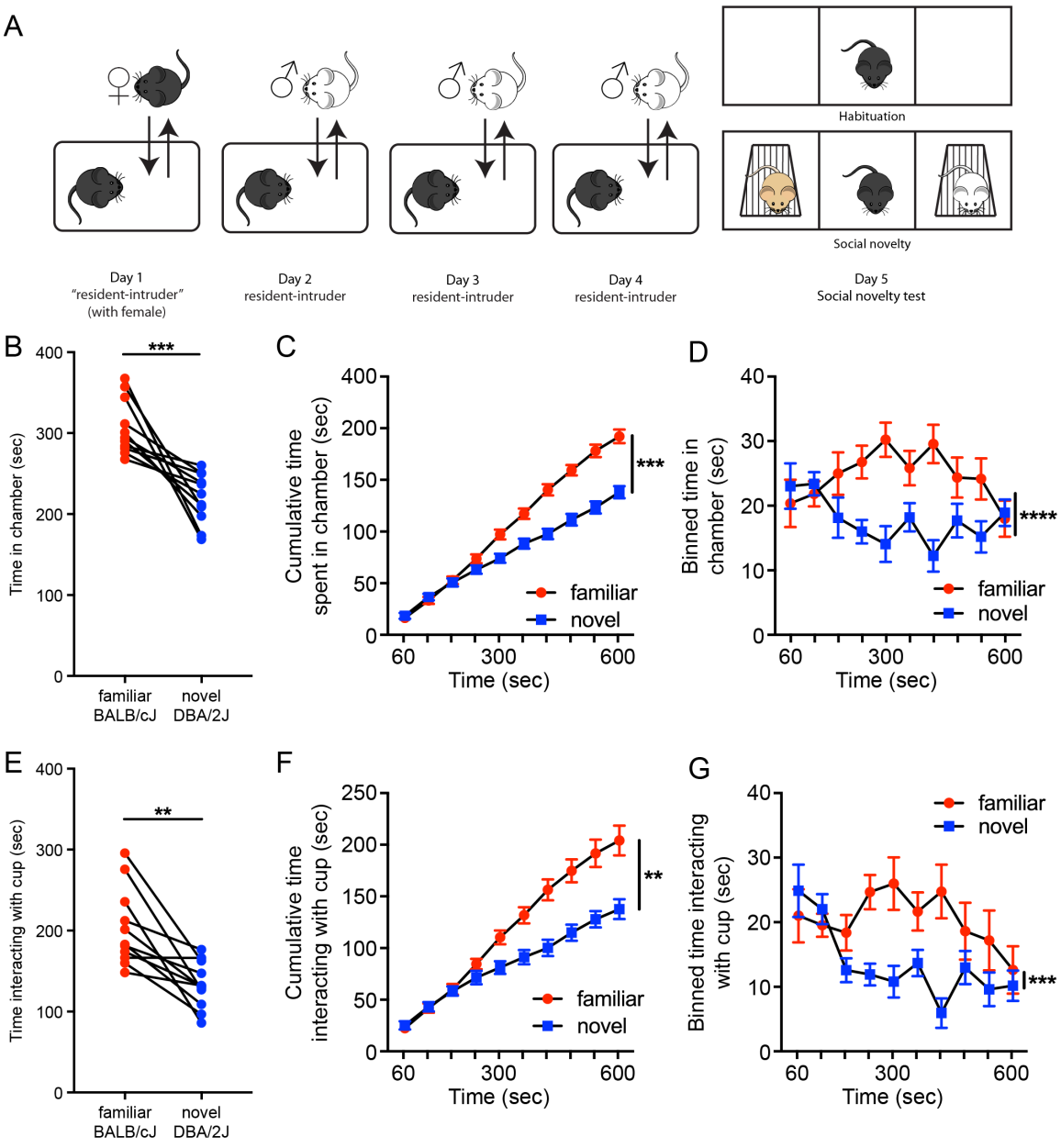

Figure 5.5 A modified social novelty test, lacking an extra hour of interaction on day 3, results in different behavioral outcomes. ***A,*** Outline of behavioral paradigm used. On day 1, an ovariectomized C57BL/6J female, injected with β-estradiol 48 hours prior, was introduced to the resident C57BL/6J male's home cage for 10 minutes. On days 2-4, a novel male BALB/cJ intruder was introduced to the resident's home cage for a 10-minute encounter. On

day 5 the social novelty test was conducted: after being allowed to habituate to the arena, the resident mouse was allowed 10 minutes to explore the 3-chamber arena in which one side housed the familiar BALB/cJ intruder under a mesh cup, while the other side housed a novel DBA/2J male under a mesh cup. ***B,*** Time each resident spent in each chamber. Paired two-tailed t-test, p=0.0008. ***C,*** Cumulative time the residents spent in each chamber. Repeated measures ANOVA, main effect of chamber, $F(1,20)=21.24$, $p=0.0002$. ***D,*** Time the residents spent in each chamber, in 1-minute bins. Repeated measures ANOVA, main effect of chamber, $F(1,20)=38.42$, $p<0.0001$. ***E,*** Time each resident spent interacting with each cup. Paired two-tailed t-test, p=0.0013. ***F,*** Cumulative time the residents spent interacting with each cup. Repeated measures ANOVA, main effect of chamber, $F(1,20)=12.98$, $p=0.0018$. ***G,*** Time the residents spent interacting with each cup, in 1-minute bins. Repeated measures ANOVA, main effect of chamber, $F(1,20)=17.21$, $p=0.0005$. *p<0.05 **p<0.01 ***p<0.001 ****p<0.0001

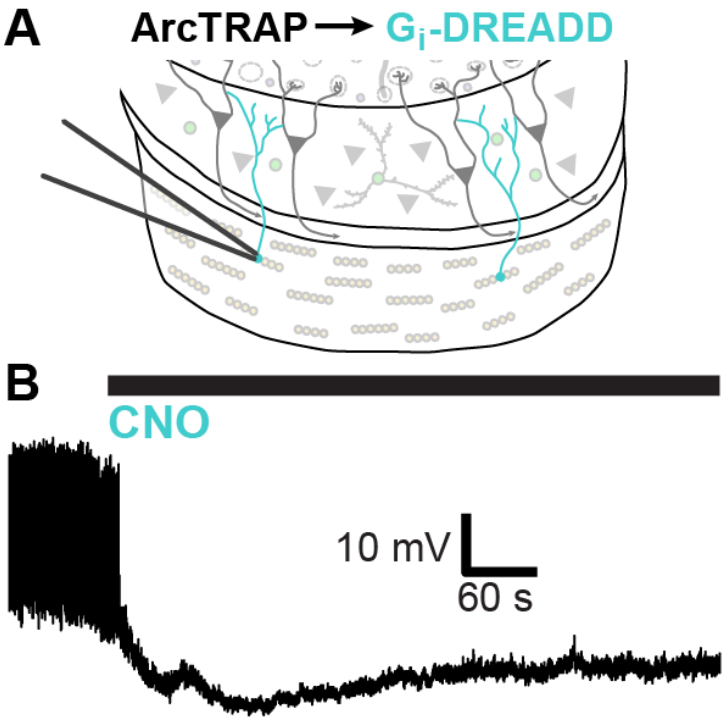

Figure 5.6 *Arc*-expressing IGCs can be controlled chemogenetically using G_i-DREADDs. ***A,*** ArcCreER+/- residents were injected with a Cre-dependent AAV expressing a G_i-DREADD. Residents were injected with 4-hydroxytamoxifen 20 minutes prior to exposure to a novel male BALB/cJ intruder for 10 minutes. Two weeks later, acute lives slices were prepared and G_i-DREADD-expressing IGCs were patched to test effectiveness of CNO application. ***B,*** Current clamp trace from a patched IGC artificially held at a depolarized potential via steady-state current injection to induce tonic firing. Application of 10 μM CNO caused hyperpolarization and cessation of spiking.

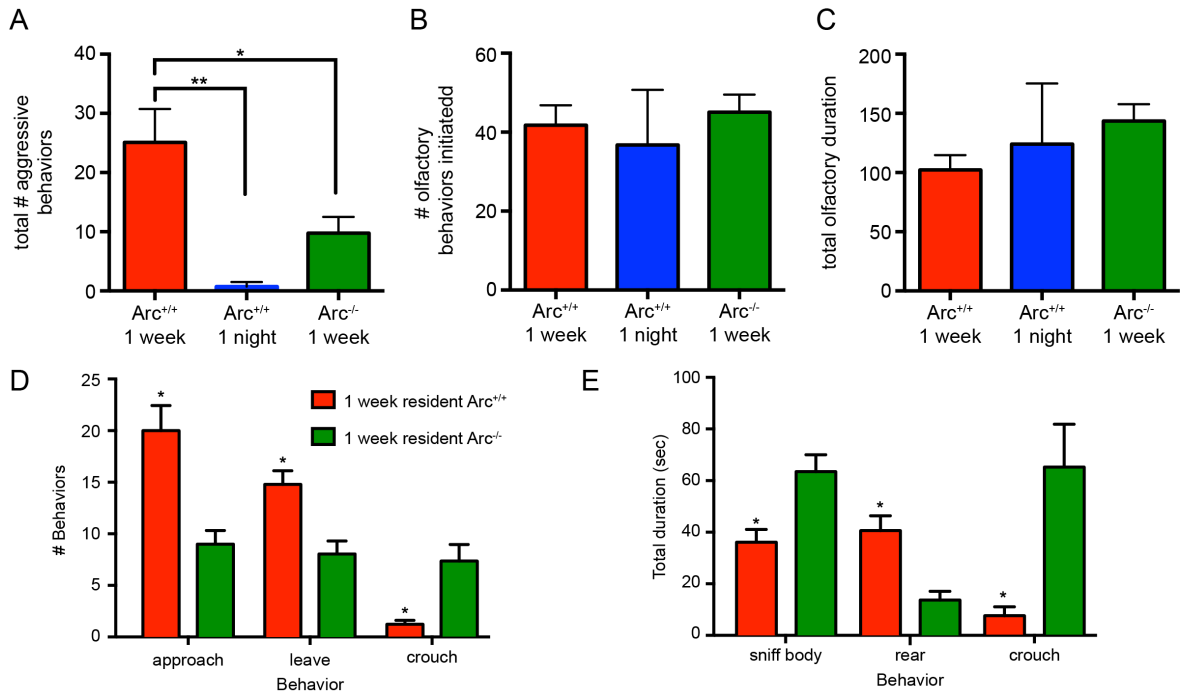

Figure 5.7 Behavior in the resident-intruder paradigm is altered in *Arc-/-* mice. ***A,*** Total number of aggressive behaviors displayed during 10-minute resident-intruder encounters by Arc+/+ residents that were solo housed for 1 week or 1 night, as well as *Arc-/-* residents that were solo-housed for 1 week. Kruskal-Wallis test H(3)=11.12, p=0.0039. Corrected for multiple comparisons using Dunn's test. *p<0.05 **p<0.01 ***B,*** Total number of olfaction investigation bouts initiated by each group. Kruskal-Wallis test H(3)=0.3345, p=0.85. Corrected for multiple comparisons using Dunn's test. ***C,*** Total duration of olfactory investigation for each group. Kruskal-Wallis test H(3)=3.947, p=0.14. Corrected for multiple comparisons using Dunn's test. ***D,*** Of all behaviors scored, each frequency behavior that was statistically different between Arc+/+ and *Arc-/-* residents. Multiple t-tests, corrected for multiple comparisons using the Holm-Sidak method. Approach, p=0.013; leave, p=0.022; crouch, p=0.011. ***E,*** Of all behaviors scored, each duration behavior that was statistically

different between Arc+/+ and *Arc-/-* residents. Multiple t-tests, corrected for multiple comparisons using the Holm-Sidak method. Sniff body, p=0.023; rear, p=0.0056; crouch, p=0.014. *p<0.05 **p<0.01

CHAPTER SIX
Conclusions and Recommendations

Conclusions

Here, we have identified a novel form of AOB plasticity that occurs following male-male social interaction. We determined that *Arc* is expressed specifically in AOB internal granule cells following resident-intruder behavior. Olfactory stimulation is necessary for this effect, as demonstrated with *Trpc2* knockouts, and olfactory stimulation alone is sufficient (Figs. 3.3-3.4). Different populations of IGCs express *Arc* after interaction with a male vs. a female, providing evidence that they are activated in an input-specific fashion (Fig. 5.1). Following *Arc* expression, these IGCs become more responsive to stimulation, while mitral cell activity was suppressed (Figs. 4.1, 4.7). To our surprise, we found that this increased responsiveness was not driven by an increase in excitatory synaptic drive. Instead, *Arc*-expressing IGCs exhibited an increase in intrinsic excitability, along with a decrease in HCN-mediated cation currents (Figs. 4.2-4.3). Preliminary behavior results detailed here provide paradigms that may be used in the future to assess the importance of *Arc*-expressing IGCs in social memory (Figs. 5.3-5.5), as well as an opportunity to investigate the behavioral "switch" that occurs when residents are given extra time to interact prior to the modified social novelty test (Figs. 5.4-5.5). Together, our work provides evidence that AOB plasticity occurs in response to salient social encounters besides mating, which had not been explored in our field. Additionally, our data suggest that this plasticity occurs through a novel mechanism: one that involves changes to intrinsic rather than synaptic physiology. This body

of work opens to the door to further investigation of the specific mechanisms of this type of plasticity, as well as its role in social recognition memory.

Recommendations

Time course of IGC plasticity following male-male social interaction

Our results demonstrate that short-term plasticity occurs in the AOB following male-male social interaction, but the longevity of this memory remains to be determined. Previous work shows that the Bruce effect persists for 30 days, suggesting that the physiological substrates of the pheromonal memory formed at mating persist on the same timescale (Kaba and Keverne, 1988). Electron microscopy work suggests that the nature of this memory in the AOB changes over time, with increased post-synaptic density at the excitatory side of the reciprocal synapse early on, and increased post-synaptic density at the inhibitory side at later stages (Matsuoka et al., 2004). Future work could address the question of the longevity of plasticity that results from male-male social interaction. This could be accomplished by using ArcCreER x Ai9 mice, which permit permanent labeling of all neurons that transiently-express Arc during the resident-intruder paradigm. These labeled neurons could then be subjected to the same experiments that we conducted in chapter 4 to test their physiological properties at various time points. It will be important to know how long this memory persists so that we can correlate the time spans of the physiological changes with the time spans of any behavioral consequences of plasticity. For example, if we attempt to manipulate behavior by manipulating *Arc*-expressing IGCs a week after they are initially induced, it would be

useful to know whether the physiological changes we observed at early time windows (4-8 hours after behavior) are still present at the 1-week time point.

Molecular identity of Arc-expressing IGCs

Previously, we showed that somatic Arc protein does not colocalize with either *Gad2* or *Calb2* (Fig 3.5). Future work could aim to determine the molecular marker expressed by Arc-expressing IGCs. This could be accomplished by conducting a screen using antibodies against common molecular markers for inhibitory interneurons. This would be a straightforward approach but could turn out to be time-consuming without much benefit. Alternatively, single-cell RNA-seq could be used on *Arc-d4EGFP*+ neurons following the resident-intruder paradigm. This approach could be costly and it is possible that the data could be difficult to interpret if no clear molecular marker is identified. However, this experiment could also offer information about transcriptional programs that are activated in IGCs following socially-salient experiences, which could provide further mechanistic insights alongside a molecular marker. Having a known molecular marker for IGCs that are capable of expressing *Arc* could open up potential genetic tools for use in future experiments. For example, it could allow us to gain genetic access to a negative control population of IGCs comparable to Arc-TRAPed IGCs, which would be useful for both *in vivo* and *ex vivo* opto- or chemo-genetic manipulation experiments.

Additionally, such a tool would provide us with another negative control population for physiological studies. Currently, we are able to compare d4EGFP+ IGCs to d4EGFP- IGCs in the same animal, which is a powerful method. However, with these mice, it is only

possible to identify the IGCs capable of expressing Arc once they have been activated. If we could identify a molecular marker for IGCs capable of expressing Arc, we could record from them prior to our behavioral manipulations, and compare their properties to Arc-d4EGFP+ IGCs. This approach could provide us with further evidence that *Arc* expression in IGCs induces plasticity, rather than that *Arc* expression is limited to IGCs that are already intrinsically more excitable.

Role of plasticity in Arc-expressing IGCs for social memory

The behavioral significance of physiological changes in *Arc*-expressing IGCs is one of the largest remaining questions. In the context of pregnancy block, increased inhibitory tone in the AOB has a clear physiological consequence for the female: lack of pregnancy block when exposed to the scent of her recent mate. This memory in the AOB confers on the female the ability to identify and distinguish between individual males (Brennan, 2009). Thus, it is reasonable to hypothesize that if a similar physiological process occurs in the AOB following salient male-male social interaction, the resulting memory may also confer on the male the ability to recognize a specific individual. A powerful way to test this hypothesis would be to specifically manipulate *Arc*-expressing IGCs during a behavioral assay for social memory. Multiple such behavioral assays are outlined in chapter 5. Specifically, the paradigms in Figs. 5.3A and 5.4A were designed with such an experiment in mind. ArcCreER animals could be used as residents, and Cre-dependent viruses expressing a G_i-coupled DREADD could be injected to the AOB prior to the experiment. Then, 4-OHT injections could be paired with behavior on either day 2 (to express DREADDs in IGCs

activated by the male intruder) or day 1 (to express DREADDs in IGCs activated by a female intruder). Thanks to the results illustrated in Fig. 5.1C, we already know that these two populations of IGCs are largely distinct. Then, the TRAP-ed population of IGCs could be inhibited by injecting CNO prior to the final behavioral test on day 5: either a second resident-intruder test after a cohousing period (Fig. 5.3A) or a modified social novelty test (Fig. 5.4A). If these AOB neurons are crucial for recognizing a familiar individual, inactivating them via G_i-DREADDs should disrupt behavioral readouts of social recognition, which would implicate early sensory processing in the complex phenomenon of social recognition memory. As a negative control, inactivation of female-activated IGCs shouldn't disrupt social recognition of a familiar male.

Further investigation of the requirement for Arc in AOB plasticity

Previously, we tested the requirement for Arc in the increased excitability we observed in AOB IGCs following resident intruder behavior by repeating a subset of our physiology experiments in *Arc-/-* mice. While these results indicated that the intrinsic excitability phenotype was lost in *Arc-/-* mice, the experiment was far from perfect. First, the *Arc-/-* mice we used are constitutive knockouts, which prevents us from excluding a developmental effect. Further, the d2EGFP label, which labels neurons that would have expressed *Arc*, has a shorter half-life than the d4EGFP expressed in the mice we used for the majority of our experiments. Thus, we may have been investigating slightly different populations of neurons, as discussed in chapter 4. One way to approach this question would be to cross the *Arc-d4EGFP*-BAC mice with a floxed-Arc line, then inject a Cre-expressing

virus into the AOB prior to resident-intruder experiments. This would permit us to record d4EGFP+ and d4EGFP- neurons (using the same time course as we used previously) in which *Arc* was knocked out recently. Alternatively, cannulas could be implanted in the AOB of *Arc-d4EGFP*-BAC mice and *Arc* antisense oligonucleotides could be infused into the AOB prior to resident-intruder behavior, which would prevent *Arc* mRNAs from being translated. This method would permit a scrambled control within the same brain in the other hemisphere. If we can conclusively determine the importance of Arc itself for the physiological changes we observe, it would provide meaningful context for future studies of the specific requirements for *Arc* induction, discussed below.

If we had a way to specifically knock out *Arc* in the AOB, we could use the same animals in behavior experiments as well. This would allow us to determine if Arc expression in the adult AOB is required for normal aggressive responses in the resident-intruder paradigm. Additionally, these animals could be used in the behavioral paradigms outlined in chapter 5, to determine whether Arc in the adult AOB is necessary for changes in behavior over time.

Specific molecular requirements for Arc induction

In this body of work, we have explored the physiological changes that accompany *Arc* expression in AOB IGCs. However, many questions remain regarding the conditions necessary and sufficient for *Arc* expression in these cells. If Arc is required for the physiological effects that we have observed, having the ability to induce Arc expression in a slice, or prevent Arc expression *in vivo* could provide some useful experimental tools. In the

hippocampus, *Arc* is induced in response to activation of group 1 mGluRs, which are enriched in the AOB (Castro et al., 2007; Park et al., 2008; Jakkamsetti et al., 2013). Whether group 1 mGluR activation is required for *Arc* expression could be tested infusing group 1 mGluR antagonists into the AOB prior to resident-intruder behavior, then assessing Arc expression via transgenic fluorescent reporters or immunohistochemistry. Whether group 1 mGluR activation is sufficient to induce *Arc* expression could be tested in the same way, by infusing group 1 mGluR agonists to the AOB and measuring *Arc* expression. Alternatively, acute live slices could be prepared from *Arc-d4EGFP*-BAC mice, and group 1 mGluR agonists could be washed onto the slice in the bath, while changes in d4EGFP fluorescence are assessed under 2-photon microscopy. If activation of group 1 mGluRs are necessary and sufficient for *Arc* expression (and if Arc itself is required for the physiological changes we observed), we would have access to an expanded toolbox for interfering with olfactory memory formation in future behavioral paradigms. For example, infusion of group 1 mGluR antagonists into the AOB prior to an initial resident-intruder encounter might prevent decreased olfactory investigation on the second encounter.

Work on AOB plasticity following mating has shown that NA release in the AOB during mating is required for pregnancy block (Kaba and Keverne, 1988; Brennan et al., 1995). It is therefore reasonable to hypothesize that a similar requirement may exist for the plasticity we have observed in response to resident-intruder behavior. This hypothesis could be tested by infusing NA antagonists into the AOB of *Arc-d4EGFP*-BAC mice prior to resident-intruder behavior, then assessing IGCs for Arc/d4EGFP expression and physiological properties.

Specific causes of increased intrinsic excitability

Another question that remains open is the direct cause of the increased intrinsic excitability observed in *Arc*-expressing IGCs, although our data offer some clues. Specifically, our data supports, but does not prove, the hypothesis that downregulation of I_H currents are involved in the changes to intrinsic excitability. HCN channels can be regulated on the timescale of short-term plasticity (reviewed in Shah, 2014). In the hippocampus, downregulation of I_H has been causally linked to increased intrinsic excitability in the context of mGluR-dependent LTD (which is Arc dependent), suggesting that such a relationship could also exist in AOB IGCs (Brager and Johnston, 2007). This observed increase in intrinsic excitability is due to increases in membrane resistance that arise from decreased I_H currents, but we didn't observe changes in membrane resistance in *Arc*-expressing IGCs. HCN channels are more densely expressed as distance from the soma increases, which could be a factor in our inability to detect differences in membrane resistance in whole-cell configuration (Shah, 2014). Unfortunately, making more localized recordings at IGC dendrites would be prohibitively difficult, if not impossible. Therefore, it might be worthwhile to try some molecular biology approaches to assess levels of HCN channels. For example, western blot analysis for different HCN channel isoforms on synaptoneurosomes before and after behavior might indicate whether specific isoforms are trafficked away from the membrane following behavior. Quantitative immunofluorescence approaches might also be used to address the same question.

It is also possible that changes to other conductances could be involved in generating the increase in intrinsic excitability observed in *Arc*-expressing IGCs. Our initial results did not suggest any macroscopic changes to voltage-gated sodium or potassium channels in *Arc*-expressing IGCs. However, these results do not rule out the possibility that specific isoforms of these voltage-gated channels are regulated, and there is an opportunity to determine which specific isoforms may be involved. This could be done pharmacologically, using specific antagonists to measure the influence of each channel type in *Arc-d4EGFP*+ and *Arc-d4EGFP*- IGCs after behavior, as we have done previously with HCN channel antagonists. This approach could help to identify candidate channels, which could then be assessed further using genetic approaches (i.e. knockdown and overexpression).

Nature of the behavioral differences in the modified social novelty test

As part of our efforts to develop a behavioral paradigm that could be used to assess social memory while manipulating *Arc*-expressing IGCs, we stumbled upon an interesting behavioral phenomenon. We found that residents given an extra hour to interact with an intruder prior to the modified social novelty test preferred to interact with the novel mouse, while residents not given the extra hour strongly preferred to interact with the familiar intruder (Figs. 5.4-5.5). This result was highly unexpected, given the body of literature demonstrating that mice prefer to interact with a novel mouse over a familiar mouse. This finding opens up the door to further study of what underlies this behavioral phenomenon. This could be approached from multiple angles. One interesting question is whether specific olfactory subsystems are required for either outcome (familiar-preference or novel-

preference). This could be tested by repeating the experiments using *Trpc2-/-* and *Trpc2+/-* animals, or with animals that have selectively had their MOEs ablated using $ZnSO_4$ treatment. If this phenomenon is found to be AOS-dependent, the role of *Arc*-expressing IGCs can be addressed using *in vivo* manipulation strategies described previously. One possibility is that the early sensory memory in the AOB might be important for one outcome but not the other (i.e. for novelty-preference but not familiarity-preference). For example, perhaps the extra hour of interaction results in an increased importance of higher-order structures, while the primary sensory level memory is more important when there has been less interaction.

Another angle is the behavioral one: what is the cause of the behavioral switch? A simple hypothesis is that the extra hour (which triples total interaction time prior to the social novelty test) is what is needed to allow sufficient familiarization for decreased interest in the social novelty test. If this were the case, we might suspect that without the extra hour, the resident might show no preference for either cup mouse. Instead, the resident shows strong preference for the familiar mouse, suggesting that some other process is involved. It could be that the extra hour of interaction allows a sufficient amount of social defeat, which reduces interest on later encounters, while the repeated 10-minute encounters don't allow the resident to adequately "defeat" the intruder, which creates a drive to investigate him further in the modified social novelty test. One way to test this hypothesis would be to eliminate the territorial aggression aspect by not solo-housing the residents prior to the experiment, as previous work indicates that this solo-housing period is required to elicit aggressive behavior (Fig. 3.2F). If lack of social defeat is what drives the preference for the familiar animal,

eliminating aggressive behavior would result in equal preference for either cup mouse or preference for the novel cup mouse.

BIBLIOGRAPHY

Adams PJ, Robinson RA, Hudgins ED, Wissink EM, Dudek SM (2009) NMDA receptor-independent control of transcription factors and gene expression. NeuroReport 20:1429.

Alvarez-Buylla A, Garcia-Verdugo JM (2002) Neurogenesis in adult subventricular zone. The Journal of neuroscience : the official journal of the Society for Neuroscience 22:629-634.

Araneda RC, Firestein S (2006) Adrenergic enhancement of inhibitory transmission in the accessory olfactory bulb. The Journal of neuroscience : the official journal of the Society for Neuroscience 26:3292-3298.

Bellringer JF, Pratt HP, Keverne EB (1980) Involvement of the vomeronasal organ and prolactin in pheromonal induction of delayed implantation in mice. Journal of reproduction and fertility 59:223-228.

Belluscio L, Koentges G, Axel R, Dulac C (1999) A map of pheromone receptor activation in the mammalian brain. Cell 97:209-220.

Ben-Shaul Y, Katz LC, Mooney R, Dulac C (2010) In vivo vomeronasal stimulation reveals sensory encoding of conspecific and allospecific cues by the mouse accessory olfactory bulb. Proceedings of the National Academy of Sciences of the United States of America 107:5172-5177.

Bepari AK, Sano H, Tamamaki N, Nambu A, Tanaka KF, Takebayashi H (2012) Identification of optogenetically activated striatal medium spiny neurons by Npas4 expression. PLoS One 7:e52783.

Biel M, Wahl-Schott C, Michalakis S, Zong X (2009) Hyperpolarization-activated cation channels: from genes to function. Physiological reviews 89:847-885.

Binns KE, Brennan PA (2005) Changes in electrophysiological activity in the accessory olfactory bulb and medial amygdala associated with mate recognition in mice. The European journal of neuroscience 21:2529-2537.

Boehm T, Zufall F (2006) MHC peptides and the sensory evaluation of genotype. Trends in neurosciences 29:100-107.

Bolte S, Cordelieres FP (2006) A guided tour into subcellular colocalization analysis in light microscopy. Journal of microscopy 224:213-232.

Brager DH, Johnston D (2007) Plasticity of intrinsic excitability during long-term depression is mediated through mGluR-dependent changes in I(h) in hippocampal CA1 pyramidal neurons. The Journal of neuroscience : the official journal of the Society for Neuroscience 27:13926-13937.

Bramham CR, Worley PF, Moore MJ, Guzowski JF (2008) The immediate early gene arc/arg3.1: regulation, mechanisms, and function. The Journal of neuroscience : the official journal of the Society for Neuroscience 28:11760-11767.

Brennan P, Kaba H, Keverne EB (1990) Olfactory recognition: a simple memory system. Science (New York, NY) 250:1223-1226.

Brennan PA (2009) Outstanding issues surrounding vomeronasal mechanisms of pregnancy block and individual recognition in mice. Behavioural brain research 200:287-294.

Brennan PA, Keverne EB (1997) Neural mechanisms of mammalian olfactory learning. Progress in neurobiology.
Brennan PA, Kendrick KM (2006) Mammalian social odours: attraction and individual recognition. Philosophical transactions of the Royal Society of London Series B, Biological sciences 361:2061-2078.
Brennan PA, Kendrick KM, Keverne EB (1995) Neurotransmitter release in the accessory olfactory bulb during and after the formation of an olfactory memory in mice. Neuroscience 69:1075-1086.
Bruce HM (1959) An exteroceptive block to pregnancy in the mouse. Nature 184:105.
Bruce HM (1965) EFFECT OF CASTRATION ON THE REPRODUCTIVE PHEROMONES OF MALE MICE. Journal of reproduction and fertility 10:141-143.
Burton SD (2017) Inhibitory circuits of the mammalian main olfactory bulb. Journal of Neurophysiology.
Campanac E, Daoudal G, Ankri N, Debanne D (2008) Downregulation of dendritic I(h) in CA1 pyramidal neurons after LTP. The Journal of neuroscience : the official journal of the Society for Neuroscience 28:8635-8643.
Castro JB, Hovis KR, Urban NN (2007) Recurrent dendrodendritic inhibition of accessory olfactory bulb mitral cells requires activation of group I metabotropic glutamate receptors. The Journal of neuroscience : the official journal of the Society for Neuroscience 27:5664-5671.
Chamero P, Marton TF, Logan DW, Flanagan K, Cruz JR, Saghatelian A, Cravatt BF, Stowers L (2007) Identification of protein pheromones that promote aggressive behaviour. Nature 450:899-902.
Chamero P, Katsoulidou V, Hendrix P, Bufe B, Roberts R, Matsunami H, Abramowitz J, Birnbaumer L, Zufall F, Leinders-Zufall T (2011) G protein Gαo is essential for vomeronasal function and aggressive behavior in mice. Proceedings of the National Academy of Sciences 108:12898-12903.
Cheetham SA, Smith AL, Armstrong SD, Beynon RJ, Hurst JL (2009) Limited variation in the major urinary proteins of laboratory mice. Physiology & behavior 96:253-261.
Choi GB, Dong H-w, Murphy AJ, Valenzuela DM, Yancopoulos GD, Swanson LW, Anderson DJ (2005) Lhx6 Delineates a Pathway Mediating Innate Reproductive Behaviors from the Amygdala to the Hypothalamus. Neuron 46:647-660.
Chowdhury S, Shepherd JD, Okuno H, Lyford G, Petralia RS, Plath N, Kuhl D, Huganir RL, Worley PF (2006) Arc/Arg3.1 interacts with the endocytic machinery to regulate AMPA receptor trafficking. Neuron 52:445-459.
Del Punta K, Puche A, Adams NC, Rodriguez I, Mombaerts P (2002) A divergent pattern of sensory axonal projections is rendered convergent by second-order neurons in the accessory olfactory bulb. Neuron 35:1057-1066.
Doyle WI, Dinser JA, Cansler HL, Zhang X, Dinh DD, Browder NS, Riddington IM, Meeks JP (2016) Faecal bile acids are natural ligands of the mouse accessory olfactory system. Nature Communications 7:11936.

Dulac C, Torello AT (2003) Molecular detection of pheromone signals in mammals: from genes to behaviour. Nature reviews Neuroscience 4:551-562.
Dulac C, Wagner S (2006) Genetic analysis of brain circuits underlying pheromone signaling. Annual review of genetics 40:449-467.
Fernández E et al. (2017) Arc Requires PSD95 for Assembly into Postsynaptic Complexes Involved with Neural Dysfunction and Intelligence. Cell Reports 21:679-691.
Firestein S (2001) How the olfactory system makes sense of scents. Nature 413:35093026.
Fleischer J, Schwarzenbacher K, Breer H (2007) Expression of trace amine-associated receptors in the Grueneberg ganglion. Chemical senses 32:623-631.
Fleischer J, Schwarzenbacher K, Besser S, Hass N, Breer H (2006) Olfactory receptors and signalling elements in the Grueneberg ganglion. Journal of neurochemistry 98:543-554.
Gao M, Sossa K, Song L, Errington L, Cummings L, Hwang H, Kuhl D, Worley P, Lee H-K (2010) A Specific Requirement of Arc/Arg3.1 for Visual Experience-Induced Homeostatic Synaptic Plasticity in Mouse Primary Visual Cortex. The Journal of Neuroscience 30:7168-7178.
Gao Y, Budlong C, Durlacher E, Davison IG (2017) Neural mechanisms of social learning in the female mouse. eLife 6.
Giorgi C, Yeo GW, Stone ME, Katz DB, Burge C, Turrigiano G, Moore MJ (2007) The EJC Factor eIF4AIII Modulates Synaptic Strength and Neuronal Protein Expression. Cell 130:179-191.
Golowasch J, Thomas G, Taylor AL, Patel A, Pineda A, Khalil C, Nadim F (2009) Membrane capacitance measurements revisited: dependence of capacitance value on measurement method in nonisopotential neurons. J Neurophysiol 102:2161-2175.
Gorin M, Tsitoura C, Kahan A, Watznauer K, Drose DR, Arts M, Mathar R, O'Connor S, Hanganu-Opatz IL, Ben-Shaul Y, Spehr M (2016) Interdependent Conductances Drive Infraslow Intrinsic Rhythmogenesis in a Subset of Accessory Olfactory Bulb Projection Neurons. The Journal of neuroscience : the official journal of the Society for Neuroscience 36:3127-3144.
Greer PL, Bear DM, Lassance J-MM, Bloom ML, Tsukahara T, Pashkovski SL, Masuda FK, Nowlan AC, Kirchner R, Hoekstra HE, Datta SR (2016) A Family of non-GPCR Chemosensors Defines an Alternative Logic for Mammalian Olfaction. Cell 165:1734-1748.
Grinevich V, Kolleker A, Eliava M, Takada N, Takuma H, Fukazawa Y, Shigemoto R, Kuhl D, Waters J, Seeburg PH, Osten P (2009) Fluorescent Arc/Arg3.1 indicator mice: a versatile tool to study brain activity changes in vitro and in vivo. J Neurosci Methods 184:25-36.
Guenthner CJ, Miyamichi K, Yang HH, Heller HC, Luo L (2013) Permanent Genetic Access to Transiently Active Neurons via TRAP: Targeted Recombination in Active Populations. Neuron 78:773-784.

Guthrie K, Rayhanabad J, Kuhl D, Gall C (2000) Odors regulate Arc expression in neuronal ensembles engaged in odor processing. Neuroreport 11:1809-1813.
Guzowski JF, McNaughton BL, Barnes CA, Worley PF (1999) Environment-specific expression of the immediate-early gene Arc in hippocampal neuronal ensembles. Nature neuroscience 2:1120-1124.
Guzowski JF, Lyford GL, Stevenson GD, Houston FP, McGaugh JL, Worley PF, Barnes CA (2000) Inhibition of activity-dependent arc protein expression in the rat hippocampus impairs the maintenance of long-term potentiation and the consolidation of long-term memory. The Journal of neuroscience : the official journal of the Society for Neuroscience 20:3993-4001.
Hendrickson RC, Krauthamer S, Essenberg JM, Holy TE (2008) Inhibition shapes sex selectivity in the mouse accessory olfactory bulb. The Journal of neuroscience : the official journal of the Society for Neuroscience 28:12523-12534.
Hitti FL, Siegelbaum SA (2014) The hippocampal CA2 region is essential for social memory. Nature 508:88-92.
Hu J, Zhong C, Ding C, Chi Q, Walz A, Mombaerts P, Matsunami H, Luo M (2007) Detection of Near-Atmospheric Concentrations of CO2 by an Olfactory Subsystem in the Mouse. Science 317:953-957.
Hu R, Ferguson KA, Whiteus CB, Meijer DH, Araneda RC (2016) Hyperpolarization-Activated Currents and Subthreshold Resonance in Granule Cells of the Olfactory Bulb. eNeuro 3.
Huang Z, Thiebaud N, Fadool DA (2017) Differential serotonergic modulation across the main and accessory olfactory bulbs. The Journal of physiology 595:3515-3533.
Huckins LM, Logan DW, Sánchez-Andrade G (2013) Olfaction and olfactory-mediated behaviour in psychiatric disease models. Cell and Tissue Research 354:69-80.
Ishii KK, Osakada T, Mori H, Miyasaka N, Yoshihara Y, Miyamichi K, Touhara K (2017) A Labeled-Line Neural Circuit for Pheromone-Mediated Sexual Behaviors in Mice. Neuron 95:123-815098112.
Isogai Y, Si S, Pont-Lezica L, Tan T, Kapoor V, Murthy VN, Dulac C (2011) Molecular organization of vomeronasal chemoreception. Nature 478:241-245.
Jackson AC, Nicoll RA (2011) Stargazing from a new vantage--TARP modulation of AMPA receptor pharmacology. The Journal of physiology 589:5909-5910.
Jakkamsetti V, Tsai NP, Gross C, Molinaro G, Collins KA, Nicoletti F, Wang KH, Osten P, Bassell GJ, Gibson JR, Huber KM (2013) Experience-induced Arc/Arg3.1 primes CA1 pyramidal neurons for metabotropic glutamate receptor-dependent long-term synaptic depression. Neuron 80:72-79.
Jenks KR, Kim T, Pastuzyn ED, Okuno H, Taibi AV, Bito H, Bear MF, Shepherd JD (2017) Arc restores juvenile plasticity in adult mouse visual cortex. Proceedings of the National Academy of Sciences:201700866.
Jia C, Chen WR, Shepherd GM (1999) Synaptic organization and neurotransmitters in the rat accessory olfactory bulb. Journal of neurophysiology.
Kaba H, Keverne EB (1988) The effect of microinfusions of drugs into the accessory olfactory bulb on the olfactory block to pregnancy. Neuroscience 25:1007-1011.

Kaba H, Rosser A, Keverne B (1989) Neural basis of olfactory memory in the context of pregnancy block. Neuroscience 32:657-662.
Kaur AW, Ackels T, Kuo T-HH, Cichy A, Dey S, Hays C, Kateri M, Logan DW, Marton TF, Spehr M, Stowers L (2014) Murine pheromone proteins constitute a context-dependent combinatorial code governing multiple social behaviors. Cell 157:676-688.
Kawashima T, Okuno H, Bito H (2014) A new era for functional labeling of neurons: activity-dependent promoters have come of age. Front Neural Circuits 8:37.
Keller M, Pierman S, Douhard Q, Baum MJ, Bakker J (2006) The vomeronasal organ is required for the expression of lordosis behaviour, but not sex discrimination in female mice. European Journal of Neuroscience 23:521-530.
Keshavarzi S, Sullivan RK, Ianno DJ, Sah P (2014) Functional properties and projections of neurons in the medial amygdala. The Journal of neuroscience : the official journal of the Society for Neuroscience 34:8699-8715.
Kim Y, Venkataraju KU, Pradhan K, Mende C, Taranda J, Turaga SC, Arganda-Carreras I, Ng L, Hawrylycz MJ, Rockland KS, Seung HS, Osten P (2015) Mapping social behavior-induced brain activation at cellular resolution in the mouse. Cell Rep 10:292-305.
Kimchi T, Xu J, Dulac C (2007) A functional circuit underlying male sexual behaviour in the female mouse brain. Nature 448:1009-1014.
Kogan JH, Franklandand PW, Silva AJ (2000) Long-term memory underlying hippocampus-dependent social recognition in mice. Hippocampus 10:47-56.
Korb E, Wilkinson CL, Delgado RN, Lovero KL, Finkbeiner S (2013) Arc in the nucleus regulates PML-dependent GluA1 transcription and homeostatic plasticity. Nature neuroscience 16:874-883.
Kumar A, Dudley CA, Moss RL (1999) Functional dichotomy within the vomeronasal system: distinct zones of neuronal activity in the accessory olfactory bulb correlate with sex-specific behaviors. The Journal of neuroscience : the official journal of the Society for Neuroscience 19:RC32.
Larriva-Sahd J (2008) The accessory olfactory bulb in the adult rat: a cytological study of its cell types, neuropil, neuronal modules, and interactions with the main olfactory system. The Journal of comparative neurology 510:309-350.
Leinders-Zufall T, Brennan P, … WP (2004) MHC class I peptides as chemosensory signals in the vomeronasal organ. MHC class I peptides as chemosensory signals in the vomeronasal organ.
Leinders-Zufall T, Cockerham RE, Michalakis S, Biel M, Garbers DL, Reed RR, Zufall F, Munger SD (2007) Contribution of the receptor guanylyl cyclase GC-D to chemosensory function in the olfactory epithelium. Proceedings of the National Academy of Sciences of the United States of America 104:14507-14512.
Liberles SD, Buck LB (2006) A second class of chemosensory receptors in the olfactory epithelium. Nature 442:645-650.
Longair MH, Baker DA, Armstrong JD (2011) Simple Neurite Tracer: open source software for reconstruction, visualization and analysis of neuronal processes. Bioinformatics 27:2453-2454.

Lorincz A, Notomi T, Tamas G, Shigemoto R, Nusser Z (2002) Polarized and compartment-dependent distribution of HCN1 in pyramidal cell dendrites. Nature neuroscience 5:1185-1193.
Lüscher C, Huber KM (2010) Group 1 mGluR-dependent synaptic long-term depression: mechanisms and implications for circuitry and disease. Neuron 65:445-459.
Ma D, Allen ND, Bergen YCH, Jones CME, Baum MJ, Keverne BE, Brennan PA (2002) Selective ablation of olfactory receptor neurons without functional impairment of vomeronasal receptor neurons in OMP-ntr transgenic mice. European Journal of Neuroscience 16:2317-2323.
Ma M, Grosmaitre X, Iwema CL, Baker H, Greer CA, Shepherd GM (2003) Olfactory signal transduction in the mouse septal organ. The Journal of neuroscience : the official journal of the Society for Neuroscience 23:317-324.
Madisen L, Zwingman TA, Sunkin SM, Oh SW, Zariwala HA, Gu H, Ng LL, Palmiter RD, Hawrylycz MJ, Jones AR, Lein ES, Zeng H (2010) A robust and high-throughput Cre reporting and characterization system for the whole mouse brain. Nature neuroscience 13:133-140.
Madisen L et al. (2012) A toolbox of Cre-dependent optogenetic transgenic mice for light-induced activation and silencing. Nature neuroscience 15:793-802.
Malvaut S, Gribaudo S, Hardy D, David L, Daroles L, Labrecque S, Lebel-Cormier M-A, Chaker Z, Coté D, Koninck P, Holzenberger M, Trembleau A, Caille I, Saghatelyan A (2017) CaMKIIα Expression Defines Two Functionally Distinct Populations of Granule Cells Involved in Different Types of Odor Behavior. Current Biology 27:3315.
Mamasuew K, Hofmann N, Breer H, Fleischer J (2011) Grueneberg ganglion neurons are activated by a defined set of odorants. Chemical senses 36:271-282.
Marking S, Krosnowski K, Ogura T, Lin W (2017) Dichotomous Distribution of Putative Cholinergic Interneurons in Mouse Accessory Olfactory Bulb. Frontiers in neuroanatomy 11:10.
Maruniak JA, Wysocki CJ, Taylor JA (1986) Mediation of male mouse urine marking and aggression by the vomeronasal organ. Physiology & behavior 37:655-657.
Matsuoka M, Yoshida-Matsuoka J, Sugiura H, Yamagata K, Ichikawa M, Norita M (2002a) Mating behavior induces differential Arc expression in the main and accessory olfactory bulbs of adult rats. Neurosci Lett 335:111-114.
Matsuoka M, Yamagata K, Sugiura H, Yoshida-Matsuoka J, Norita M, Ichikawa M (2002b) Expression and regulation of the immediate-early gene product Arc in the accessory olfactory bulb after mating in male rat. Neuroscience 111:251-258.
Matsuoka M, Yoshida-Matsuoka J, Yamagata K, Sugiura H, Ichikawa M, Norita M (2003) Rapid induction of Arc is observed in the granule cell dendrites in the accessory olfactory bulb after mating. Brain Res 975:189-195.
Matsuoka M, Kaba H, Moriya K, Yoshida-Matsuoka J, Costanzo RM, Norita M, Ichikawa M (2004) Remodeling of reciprocal synapses associated with persistence of long-term memory. The European journal of neuroscience 19:1668-1672.

Matsutani S, Yamamoto N (2008) Centrifugal innervation of the mammalian olfactory bulb. Anatomical Science International 83:218-227.
Mattis J, Tye KM, Ferenczi EA, Ramakrishnan C, O'Shea DJ, Prakash R, Gunaydin LA, Hyun M, Fenno LE, Gradinaru V, Yizhar O, Deisseroth K (2011) Principles for applying optogenetic tools derived from direct comparative analysis of microbial opsins. Nature methods 9:159-172.
McCurry CL, Shepherd JD, Tropea D, Wang KH, Bear MF, Sur M (2010) Loss of Arc renders the visual cortex impervious to the effects of sensory experience or deprivation. Nature neuroscience 13:450-457.
McLean JH, Shipley MT, Nickell WT, Aston-Jones G, Reyher CKH (1989) Chemoanatomical organization of the noradrenergic input from locus coeruleus to the olfactory bulb of the adult rat. Journal of Comparative Neurology 285:339-349.
Meeks JP, Jiang X, Mennerick S (2005) Action potential fidelity during normal and epileptiform activity in paired soma-axon recordings from rat hippocampus. J Physiol 566:425-441.
Meeks JP, Arnson HA, Holy TE (2010) Representation and transformation of sensory information in the mouse accessory olfactory system. Nature neuroscience 13:723-730.
Meredith M (1994) Chronic recording of vomeronasal pump activation in awake behaving hamsters. Physiology & behavior 56:345-354.
Messaoudi E, Kanhema T, Soule J, Tiron A, Dagyte G, da Silva B, Bramham CR (2007) Sustained Arc/Arg3.1 synthesis controls long-term potentiation consolidation through regulation of local actin polymerization in the dentate gyrus in vivo. The Journal of neuroscience : the official journal of the Society for Neuroscience 27:10445-10455.
Mikuni T, Uesaka N, Okuno H, Hirai H, Deisseroth K, Bito H, Kano M (2013) Arc/Arg3.1 Is a Postsynaptic Mediator of Activity-Dependent Synapse Elimination in the Developing Cerebellum. Neuron 78:1024-1035.
Munger SD, Leinders-Zufall T, Zufall F (2009) Subsystem Organization of the Mammalian Sense of Smell. Annual review of physiology 71:115-140.
Munger SD, Leinders-Zufall T, McDougall LM, Cockerham RE, Schmid A, Wandernoth P, Wennemuth G, Biel M, Zufall F, Kelliher KR (2010) An Olfactory Subsystem that Detects Carbon Disulfide and Mediates Food-Related Social Learning. Current Biology 20:1438-1444.
Nakayama D, Hashikawa-Yamasaki Y, Ikegaya Y, Matsuki N, Nomura H (2016) Late Arc/Arg3.1 expression in the basolateral amygdala is essential for persistence of newly-acquired and reactivated contextual fear memories. Scientific Reports 6:21007.
Newman SW (1999) The medial extended amygdala in male reproductive behavior. A node in the mammalian social behavior network. Annals of the New York Academy of Sciences 877:242-257.

Nodari F, Hsu FF, Fu X, of … HTF (2008) Sulfated steroids as natural ligands of mouse pheromone-sensing neurons. Sulfated steroids as natural ligands of mouse pheromone-sensing neurons.

Nunez-Parra A, Maurer RK, Krahe K, Smith RS, Araneda RC (2013) Disruption of centrifugal inhibition to olfactory bulb granule cells impairs olfactory discrimination. Proceedings of the National Academy of Sciences of the United States of America 110:14777-14782.

Oettl L-L, Ravi N, Schneider M, Scheller MF, Schneider P, Mitre M, da Silva Gouveia M, Froemke RC, Chao MV, Young SW, Meyer-Lindenberg A, Grinevich V, Shusterman R, Kelsch W (2016) Oxytocin Enhances Social Recognition by Modulating Cortical Control of Early Olfactory Processing. Neuron 90:609-621.

Omura M, Mombaerts P (2014) Trpc2-expressing sensory neurons in the main olfactory epithelium of the mouse. Cell reports 8:583-595.

Papes F, Logan DW, Stowers L (2010) The vomeronasal organ mediates interspecies defensive behaviors through detection of protein pheromone homologs. Cell 141:692-703.

Park S, Park JM, Kim S, Kim J-AA, Shepherd JD, Smith-Hicks CL, Chowdhury S, Kaufmann W, Kuhl D, Ryazanov AG, Huganir RL, Linden DJ, Worley PF (2008) Elongation factor 2 and fragile X mental retardation protein control the dynamic translation of Arc/Arg3.1 essential for mGluR-LTD. Neuron 59:70-83.

Peele P, Salazar I, Mimmack M, Keverne EB, Brennan PA (2003) Low molecular weight constituents of male mouse urine mediate the pregnancy block effect and convey information about the identity of the mating male. European Journal of Neuroscience 18:622-628.

Plath N et al. (2006) Arc/Arg3.1 is essential for the consolidation of synaptic plasticity and memories. Neuron 52:437-444.

Ploski JE, Pierre VJ, Smucny J, Park K, Monsey MS, Overeem KA, Schafe GE (2008) The activity-regulated cytoskeletal-associated protein (Arc/Arg3.1) is required for memory consolidation of pavlovian fear conditioning in the lateral amygdala. The Journal of neuroscience : the official journal of the Society for Neuroscience 28:12383-12395.

Poolos NP, Migliore M, Johnston D (2002) Pharmacological upregulation of h-channels reduces the excitability of pyramidal neuron dendrites. Nature neuroscience 5:767-774.

Prince JE, Brignall AC, Cutforth T, Shen K, Cloutier JF (2013) Kirrel3 is required for the coalescence of vomeronasal sensory neuron axons into glomeruli and for male-male aggression. Development 140:2398-2408.

Qiu J, Dunbar DR, Noble J, Cairns C, Carter R, Kelly V, Chapman KE, Seckl JR, Yau JLW (2016) Decreased Npas4 and Arc mRNA Levels in the Hippocampus of Aged Memory-Impaired Wild-Type But Not Memory Preserved 11β-HSD1 Deficient Mice. Journal of Neuroendocrinology 28.

Ramirez-Amaya V, Vazdarjanova A, Mikhael D, Rosi S, Worley PF, Barnes CA (2005) Spatial exploration-induced Arc mRNA and protein expression: evidence for

selective, network-specific reactivation. The Journal of neuroscience : the official journal of the Society for Neuroscience 25:1761-1768.
Ren M, Cao V, Ye Y, Manji HK, Wang KH (2014) Arc regulates experience-dependent persistent firing patterns in frontal cortex. The Journal of neuroscience : the official journal of the Society for Neuroscience 34:6583-6595.
Reynolds J, Keverne EB (1979) The accessory olfactory system and its role in the pheromonally mediated suppression of oestrus in grouped mice. Journal of reproduction and fertility 57:31-35.
Robertson DH, Hurst JL, Bolgar MS, Gaskell SJ, Beynon RJ (1997) Molecular heterogeneity of urinary proteins in wild house mouse populations. Rapid communications in mass spectrometry : RCM 11:786-790.
Robinson RB, Siegelbaum SA (2003) Hyperpolarization-activated cation currents: from molecules to physiological function. Annual review of physiology 65:453-480.
Rodriguez I, Feinstein P, Mombaerts P (1999) Variable patterns of axonal projections of sensory neurons in the mouse vomeronasal system. Cell 97:199-208.
Rosser AE, Keverne EB (1985) The importance of central noradrenergic neurones in the formation of an olfactory memory in the prevention of pregnancy block. Neuroscience 15:1141-1147.
Rothermel M, Carey RM, Puche A, Shipley MT, Wachowiak M (2014) Cholinergic inputs from Basal forebrain add an excitatory bias to odor coding in the olfactory bulb. The Journal of neuroscience : the official journal of the Society for Neuroscience 34:4654-4664.
Shah MM (2014) Cortical HCN channels: function, trafficking and plasticity. The Journal of physiology 592:2711-2719.
Shakhawat AM, Gheidi A, Hou Q, Dhillon SK, Marrone DF, Harley CW, Yuan Q (2014) Visualizing the engram: learning stabilizes odor representations in the olfactory network. The Journal of neuroscience : the official journal of the Society for Neuroscience 34:15394-15401.
Shepherd JD, Bear MF (2011) New views of Arc, a master regulator of synaptic plasticity. Nature neuroscience 14:279-284.
Shepherd JD, Rumbaugh G, Wu J, Chowdhury S, Plath N, Kuhl D, Huganir RL, Worley PF (2006) Arc/Arg3.1 mediates homeostatic synaptic scaling of AMPA receptors. Neuron 52:475-484.
Shipley MT, Halloran FJ, de la Torre J (1985) Surprisingly rich projection from locus coeruleus to the olfactory bulb in the rat. Brain research 329:294-299.
Smith GB, Heynen AJ, Bear MF (2009a) Bidirectional synaptic mechanisms of ocular dominance plasticity in visual cortex. Philosophical Transactions of the Royal Society B: Biological Sciences 364:357-367.
Smith RS, Weitz CJ, Araneda RC (2009b) Excitatory actions of noradrenaline and metabotropic glutamate receptor activation in granule cells of the accessory olfactory bulb. Journal of neurophysiology 102:1103-1114.
Smith RS, Hu R, DeSouza A, Eberly CL, Krahe K, Chan W, Araneda RC (2015) Differential Muscarinic Modulation in the Olfactory Bulb. The Journal of

neuroscience : the official journal of the Society for Neuroscience 35:10773-10785.

Smith-Hicks C, Xiao B, Deng R, Ji Y, Zhao X, Shepherd JD, Posern G, Kuhl D, Huganir RL, Ginty DD, Worley PF, Linden DJ (2010) SRF binding to SRE 6.9 in the Arc promoter is essential for LTD in cultured Purkinje cells. Nature neuroscience 13:1082-1089.

Steward O, Wallace CS, Lyford GL, Worley PF (1998) Synaptic activation causes the mRNA for the IEG Arc to localize selectively near activated postsynaptic sites on dendrites. Neuron 21:741-751.

Storan MJ, Key B (2006) Septal organ of Grüneberg is part of the olfactory system. The Journal of comparative neurology 494:834-844.

Stowers L, Holy TE, Meister M, Dulac C, Koentges G (2002) Loss of sex discrimination and male-male aggression in mice deficient for TRP2. Science 295:1493-1500.

Takami S, Fernandez GD, Graziadei PP (1992) The morphology of GABA-immunoreactive neurons in the accessory olfactory bulb of rats. Brain research 588:317-323.

Taniguchi H, He M, Wu P, Kim S, Paik R, Sugino K, Kvitsiani D, Kvitsani D, Fu Y, Lu J, Lin Y, Miyoshi G, Shima Y, Fishell G, Nelson SB, Huang ZJ (2011) A resource of Cre driver lines for genetic targeting of GABAergic neurons in cerebral cortex. Neuron 71:995-1013.

Taniguchi M, Kaba H (2001) Properties of reciprocal synapses in the mouse accessory olfactory bulb. Neuroscience 108:365-370.

Taniguchi M, Yokoi M, Shinohara Y, Okutani F, Murata Y, Nakanishi S, Kaba H (2013) Regulation of synaptic currents by mGluR2 at reciprocal synapses in the mouse accessory olfactory bulb. The European journal of neuroscience 37:351-358.

Tian H, Ma M (2004) Molecular organization of the olfactory septal organ. The Journal of neuroscience : the official journal of the Society for Neuroscience 24:8383-8390.

Turrigiano GG (2008) The Self-Tuning Neuron: Synaptic Scaling of Excitatory Synapses. Cell 135:422-435.

Vazdarjanova A, Ramirez-Amaya V, Insel N, Plummer TK, Rosi S, Chowdhury S, Mikhael D, Worley PF, Guzowski JF, Barnes CA (2006) Spatial exploration induces ARC, a plasticity-related immediate-early gene, only in calcium/calmodulin-dependent protein kinase II-positive principal excitatory and inhibitory neurons of the rat forebrain. The Journal of comparative neurology 498:317-329.

Vousden DA, Epp J, Okuno H, Nieman BJ, van Eede M, Dazai J, Ragan T, Bito H, Frankland PW, Lerch JP, Henkelman RM (2015) Whole-brain mapping of behaviourally induced neural activation in mice. Brain Struct Funct 220:2043-2057.

Wagner S, Gresser AL, Torello TA, Dulac C (2006) A Multireceptor Genetic Approach Uncovers an Ordered Integration of VNO Sensory Inputs in the Accessory Olfactory Bulb. Neuron 50:697-709.

Waltereit R, Dammermann B, Wulff P, Scafidi J, Staubli U, Kauselmann G, Bundman M, Kuhl D (2001) Arg3.1/Arc mRNA induction by Ca2+ and cAMP requires protein kinase A and mitogen-activated protein kinase/extracellular regulated kinase activation. The Journal of neuroscience : the official journal of the Society for Neuroscience 21:5484-5493.

Wang H, Ardiles AO, Yang S, Tran T, Posada-Duque R, Valdivia G, Baek M, Chuang Y-AA, Palacios AG, Gallagher M, Worley P, Kirkwood A (2016) Metabotropic Glutamate Receptors Induce a Form of LTP Controlled by Translation and Arc Signaling in the Hippocampus. The Journal of neuroscience : the official journal of the Society for Neuroscience 36:1723-1729.

Wang K, Majewska A, Schummers J, Farley B, Hu C, Sur M, Tonegawa S (2006) In Vivo Two-Photon Imaging Reveals a Role of Arc in Enhancing Orientation Specificity in Visual Cortex. Cell 126:389-402.

Waung MW, Pfeiffer BE, Nosyreva ED, Ronesi JA, Huber KM (2008) Rapid translation of Arc/Arg3.1 selectively mediates mGluR-dependent LTD through persistent increases in AMPAR endocytosis rate. Neuron 59:84-97.

Wilkerson JR, Albanesi JP, Huber KM (2017) Roles for Arc in metabotropic glutamate receptor-dependent LTD and synapse elimination: Implications in health and disease. Seminars in Cell & Developmental Biology.

Wysocki CJ, Lepri JJ (1991) Consequences of removing the vomeronasal organ. The Journal of steroid biochemistry and molecular biology 39:661-669.

Yi F, Danko T, Botelho SC, Patzke C, Pak C, Wernig M, Südhof TC (2016) Autism-associated SHANK3 haploinsufficiency causes Ih channelopathy in human neurons. Science (New York, NY) 352.

Zhang W, Wu J, Ward MD, Yang S, Chuang Y-A, Xiao M, Li R, Leahy DJ, Worley PF (2015) Structural Basis of Arc Binding to Synaptic Proteins: Implications for Cognitive Disease. Neuron 86:490-500.